

Offshore Windfarm

Eneco Luchterduinen

Ecological monitoring of seabirds

T1 report



September 2016

This report has been prepared under the DHI Business Management System certified by DNV to comply with ISO 9001 (Quality Management)



DNV Business Assurance, Danmark A/S

Offshore Windfarm

Eneco Luchterduinen

Ecological monitoring of seabirds

T1 report

Prepared for ENECO
 Represented by Ms. Sytske van den Akker



Photo by Thomas W Johansen

Project manager	Henrik Skov
Author	Henrik Skov Stefan Heinänen Martin Lazcny Magda Chudzinska
Quality supervisor	Ramunas Zydelis
Project number	11813060
Approval date	13 September 2016
Revision	Final
Classification	Confidential

CONTENTS

1	Abbreviations	3
2	Executive summary	4
3	Introduction	5
4	Materials and methods	6
4.1	Monitoring approach	6
4.2	Survey design and available data	6
4.3	Seabird counting techniques	8
4.4	Quality control and post-processing of survey data	10
4.5	Distance analysis	10
4.6	Distribution models	11
4.7	Analysis of displacement and number of included surveys	13
4.8	Presentation of data	15
5	Results	15
5.1	Effort and sample sizes	15
5.2	Distance analysis	17
5.3	Species accounts	18
5.3.1	<i>Divers: Red-throated Gavia stellata and Black-throated Divers Gavia arctica</i>	18
5.3.2	<i>Great Crested Grebe Podiceps cristatus</i>	21
5.3.3	<i>Northern Gannet Morus bassanus</i>	24
5.3.4	<i>Great Cormorant Phalacrocorax carbo</i>	31
5.3.5	<i>Little Gull Hydrocoloeus minutus</i>	34
5.3.6	<i>Black-headed Gull Chroicocephalus ridibundus</i>	37
5.3.7	<i>Common Gull Larus canus</i>	40
5.3.8	<i>Lesser Black-backed Gull Larus fuscus</i>	43
5.3.9	<i>Herring Gull Larus argentatus</i>	46
5.3.10	<i>Great Black-backed Gull Larus marinus</i>	49
5.3.11	<i>Black-legged Kittiwake Rissa tridactyla</i>	52
5.3.12	<i>Common Guillemot Uria aalge</i>	55
5.3.13	<i>Razorbill Alca torda</i>	62
5.3.14	<i>Marine mammal observations</i>	65
6	Discussion	67
7	References	69
	APPENDIX A – Detailed results of species distribution models for the T-1 surveys	70
	APPENDIX B – Overview of the environmental variables in the “greater” study area during surveys between February 2012 and March 2016	98
	APPENDIX C – Example of simulation for “power” calculation of significant impact of LUD	105

1 Abbreviations

AIC	Akaike Information Criterion
AUC	Area Under Curve. Probability of correctly predicting presence of species
EEZ	Dutch Exclusive Economic Zone
EIA	Environmental Impact Assessment
ESW	Effective Strip Width
GAM	Generalized Additive Model
LUD	Offshore Windfarm Eneco Luchterduinen
LAT	Lowest Astronomical Tide
MEP	Monitoring and Evaluation Program
OWEZ	Offshore Windfarm Egmond aan Zee
OWF	Offshore Windfarm
PAWP	Prinses Amalia windfarm
TOR	Terms of Reference
UTM	Universal Transverse Mercator
WTG	Wind Turbine Generator

2 Executive summary

The T1 report provides the first results from the Offshore Windfarm Eneco Luchterduinen (LUD) seabird monitoring program regarding displacement of seabirds from LUD as well as updated results from PAWP and OWEZ. The four LUD-T1 surveys generated knowledge about the distribution and abundance of seabirds during the first post-construction season. The abundance of the different species of seabirds largely followed the patterns from the LUD baseline and T-Constr periods with the overall impression that the waters around LUD are mainly characterised by high densities of Common Guillemot and low to moderate densities of other species of seabirds. However, during the December 2015 survey, high abundance of Northern Gannet was also recorded.

The T-1 results should be seen as the first step in the collection of evidence regarding potential displacement impacts of LUD on seabirds. Predicted changes in densities between LUD baseline and T-1 surveys were compared using the dynamic habitat modelling framework established during T-0 and using all available surveys from 2007 (see Table 1) to present. The analyses are reported in two ways, an assessment of significance of the three “distance to windfarm variables” (indicating a statistically significant displacement/attraction) and the difference in mapped predicted densities pre- and post-construction. Two power tests were conducted to assess the models ability to detect a displacement, an empirical test and a simulation based power test. The empirical power tests assessed the influence of the number of surveys on the ability to detect displacement of Common Guillemots and Northern Gannets from OWEZ and PAWP. These results were supplemented by simulations of the statistical power of the monitoring data to detect seabird displacement at LUD.

In line with the results of the monitoring program related to OWEZ and PAWP, the LUD-T1 data indicated negative responses of Northern Gannets (2 km avoidance) and Common Guillemot (2-4 km avoidance) to all three windfarms, yet only the displacement at PAWP and OWEZ was significant. This was the case, even if displacement of Gannets and Guillemots was not complete, and both species were observed in the windfarms. Due to the short scale of the displacement no cumulative displacement effects due to OWEZ and PAWP were found. In addition, a positive response (attraction) of Great Cormorants to LUD, PAWP and OWEZ was recorded. The empirical analyses of the power of OWEZ and PAWP data to detect displacement effects on Northern Gannet and Common Guillemot indicated that displacement of both species could be determined following four surveys post-construction (one survey at PAWP for the Common Guillemot). However, simulations based on the existing post-construction survey conditions indicated, that following four surveys a reasonable power (>80%) for both species could only be achieved in situations with at least 75% displacement from LUD. If a displacement buffer of 4 km was added (the displacement is then assumed to occur within a larger area, not only within the WF but also in an area surrounding the windfarm) a power above 80% could be achieved with 50% displacement. Simulating the power to detect 25% and 50% displacement from LUD without a 4 km buffer and following eight surveys indicated that high power would not be achieved under these conditions for Northern Gannet within this number of surveys. Yet, high power would be achievable for Common Guillemot for detecting a displacement of 50%. Based on these simulations it seems unlikely given the oceanographic variability and mobile behaviour and hence variability of abundance of Northern Gannet at LUD that it will be possible to detect reductions of 50% of this species from this windfarm after T2. It is therefore recommended to finalise all surveys as planned under T2, and re-assess the power of the collected data as scheduled before deciding on execution of T3.

As documented by the available surveys included in the models, the abundance of both species in the studied region off the Dutch coast varies between years and within years. This is especially the case with respect to Northern Gannet, which is closely associated with the North Sea water mass. As the distribution models have been specifically designed to account for the oceanographic variability it is reasonable to judge the results of the empirical and simulation based power tests as relatively reliable.

3 Introduction

Construction of the Offshore Windfarm Eneco Luchterduinen (LUD) started in 2014, and the 129 MW (43 turbines) were fully operational by summer 2015. The windfarm covers an area of 16 km². The location for the LUD is 17 km south of the existing Prinses Amaliawindpark (PAWP), roughly 23km off the coast of IJmuiden in block Q10 of the Netherlands Continental Shelf (NCS) in the Dutch Exclusive Economic Zone (EEZ). The water depth at this location ranges between 19 m and 24 m relative to LAT. The water depth and composition of the sediment underground allow for steel mono-piles to be used in conjunction with the preferred wind turbine generator (WTG) type which, under these circumstances, is the most cost effective solution. At a water depth of 25 m the WTGs require mono-piles of 51.5 m in length, with a diameter between 4.2 and 4.6 m and a transition piece of 19.1 m in length with a diameter of 4.5 m. Pile penetration in the seabed is approximately 23 m. An offshore high voltage station (OHVS) collects the generated energy at all WTGs and transforms the voltage from MV level to HV level, suited for export to shore. The windfarm is connected to the 150 kV onshore substation in Sassenheim.

OWEZ was constructed between April and August 2006, while PAWP was constructed between October 2006 and June 2008. The two windfarms have very different designs; PAWP has a much higher turbine density than OWEZ (60/17km² [3.5 WTG·km⁻²] and 36/24 km² [1.5 WTG·km⁻²] resp.) and has been built in slightly deeper waters (19-24 m versus 18-20 m) and further offshore (ca 23 km versus ca 15 km) than OWEZ.

As part of the Wbr-permit application an ‘Environmental Impact Assessment’ (EIA) and an ‘Appropriate Assessment’ were carried out. The outcome of these studies resulted in the requirement by the Competent Authority for a ‘Monitoring and Evaluation Program’ (MEP). The MEP is undertaken in conjunction with and for approval by the Competent Authority. Currently the MEP consists of eleven monitoring topics, of which seabirds is one topic. LUD is obliged to carry out a 3-5 year monitoring program on seabirds. According to the license permit the objective of the Luchterduinen seabird monitoring program is to conduct the seabird monitoring program in a way that location specific and cumulative avoidance behaviour can be measured in LUD and the two existing offshore windfarms (OWEZ and PAWP). For this purpose, a ship-based line transect monitoring program of seabirds focusing on the winter season has been proposed by Clusius CV and approved by the Competent Authority. The program covers pre-construction (baseline), construction and post-construction phases. This report covers the results of the first year of post-construction monitoring with ship-based surveys (T-1) undertaken October and December 2015, January and early March 2016. The main aim of the report is to present the results of the T1 surveys and assess to what extent displacement (including cumulative displacements) of seabirds can be detected and whether there are any differences between LUD, PAWP and OWEZ with respect to the displacement of seabirds. The assessments of the T1 results should include tests, which will indicate the value of additional monitoring (T2/T3).

Pelagic seabirds such as gannets, divers and alcids flying in the vicinity of offshore windfarms consistently show strong avoidance behaviour, with only a few exceptions (Krijgsveld 2014). Evaluations of the habitat displacement of seabirds from OWEZ and PAWP indicated strong avoidance of Northern Gannet and Common Guillemot (although they not fully avoided the windfarms). Other species showing significant avoidance behaviour were divers, Great Crested Grebe, Little Gull, Lesser Black-backed Gull, Black-legged Kittiwake and Razorbill (Leopold et al. 2013). The lay-out of the windfarms seemed to be an important factor, as the widely distributed birds avoided PAWP to a larger degree than the more widely spaced OWEZ (Leopold et al. 2013), which also partly could be due to distance from coast.

4 Materials and methods

4.1 Monitoring approach

The TORs for the seabird monitoring are to study the distribution and abundance of seabirds in the region of the three windfarms before, during and after construction of the LUD windfarm. After the post-construction surveys, the results will be evaluated (once or twice) to determine to what extent the behavioural responses of species of seabirds have been determined, and whether the ship-based surveys can be curtailed. The collected data should be used to assess the avoidance behaviour of seabirds both in relation to the LUD windfarm and as a secondary priority cumulatively to the LUD, OWEZ and PAWP windfarms. The study should be undertaken using three sets of four NE-SW oriented transects traversing the three windfarms. Each of the proposed transects measures approximately 20 km. Results of the monitoring of habitat displacement of seabirds and waterbirds at other offshore windfarms have strongly indicated displacements to a distance of 1-2 kilometers (Petersen et al. 2006, Skov et al. 2012). Hence, the use of relatively short transect lines in the three windfarms is suitable for detecting gradients in abundance (densities) within a relatively well-defined area around each of the windfarms. Thus, the design allows to detect changes in densities between pre- and post-construction periods which can be attributed to ecological habitats (by integration of hydrodynamic data), shipping activity (by integration of AIS data) and the presence of the windfarms (Skov et al. 2015). This means that the degree of habitat displacement from all three windfarms can be tested statistically by gradient analysis.

In addition to the three series of four 20 km long primary transects through each of the LUD, OWEZ and PAWP windfarms, the monitoring approach includes a number of 30-40 km long secondary transects running east-west through the entire survey region. As habitat displacement of seabirds from offshore windfarms is typically short-scaled, this survey design provides a good basis for determining to what degree the different species of seabirds are impacted by habitat displacement, which can be determined by testing for changes in densities at increasing distances from the windfarms.

4.2 Survey design and available data

The survey design is given in Figure 1, showing the three series of four dense primary transects through LUD, OWEZ and PAWP designed to detect habitat displacement and the coarse set of secondary transects covering a larger region surrounding the three windfarms designed to describe distributions over a wider region. Between LUD and PAWP-OWEZ the shipping lane to/from IJmuiden is located. Two anchoring sites are associated with the shipping lane. The study area extends from about 52°30'N (Noordwijk) to about 52°45'N (Hondsbosche Zeewering) and from the shore to circa 18 nm out to sea. The size of the study area is circa 725 km². The primary transects are oriented NE-SW to capture the expected density gradient in seabirds, whereas the secondary transects are largely perpendicular to the main physical and ecological parameters, such as distance from the coast, water depth, temperature and salinity.

Four surveys in winter 2015-2016 were undertaken following the construction of the LUD windfarm. Each survey conducted during a period of five days (if permitted by the weather). The survey strategy has been to cover primary transects during all surveys, and as many of the secondary transects as possible. The primary transects were surveyed first, and surveying of the secondary transects was only initiated once the primary transects had been surveyed. The primary transects measure 209 km (+ 11 km transit) which can be covered in 12-14 hours of survey time. The secondary transects measure 660 km (+ 48 km transits). It was the strategy to achieve as much coverage as possible in the coastal and offshore environment surrounding the Luchterduinen survey area. The coverage of the secondary transects was therefore designed to achieve as much survey effort as possible on the secondary transects in the southern part of the survey region.

When crossing the three windfarms a safety distance of 250 m was kept to the turbines. During crossing of the shipping lane a minimum distance of 1000 m was maintained to all vessels in the shipping lane.

Surveys were initiated only on the basis of a forecasted weather window (less than Beaufort 5, good visibility (≥ 2 km), no heavy precipitation) of at least 2 days. Surveys should only be undertaken during sea states less than or equal to 4 and visibility of 2 km or more. Cancellation of a survey would only take place in situations with adverse weather conditions in relation to surveying (sea state above 4, visibility < 2 km) extending beyond the 5 day period of a survey.

By including the T0 and T1 data from OWEZ and PAWP (Leopold et al. 2013) data from a total of 13 surveys could be included in the analyses of habitat displacement at LUD (Table 1). In the analyses the OWEZ and PAWP T0 and T1 survey data were treated as part of the LUD baseline.

Table 1. List of available surveys included in the analyses of seabird displacement from LUD.

Year	Survey dates	Reference
2007	5-6/11 and 20-24/11	PAWP/OWEZ T1
2008	14-18/1 and 3-7/11	PAWP/OWEZ T1
2009	19-22/1, 5-9/10 and 2-6/11	PAWP/OWEZ T1
2010	18-22/1 and 22-26/2	PAWP/OWEZ T1
2011	3-7/10 and 31/10-4/11	PAWP/OWEZ T1
2012	9-13/1 and 20-23/2	PAWP/OWEZ T1
2013	18-22/10	LUD T0
2014	10-14/1 and 19-23/1	LUD T0
2015	19-23/10 and 13-17/12	LUD T1
2016	11-16/2 and 4-8/3	LUD T1

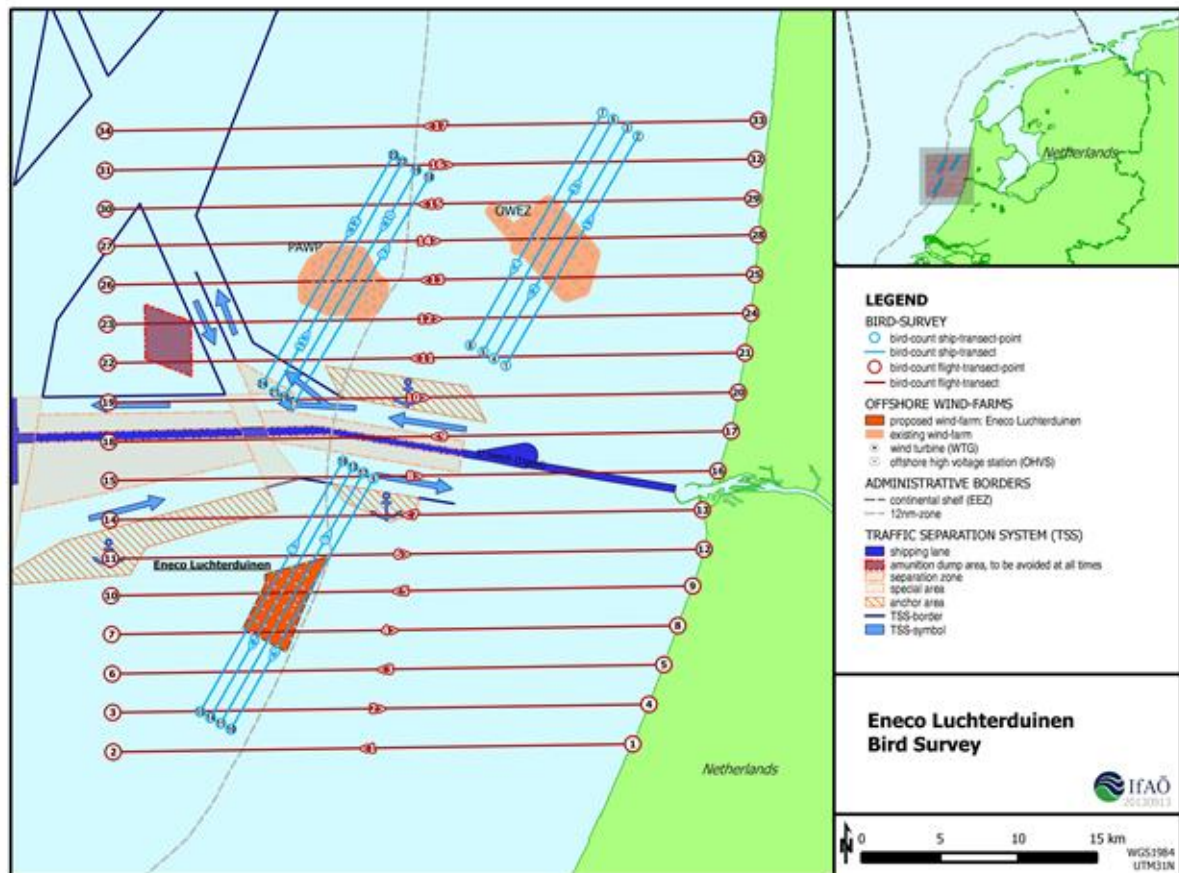


Figure 1. Primary (blue) and secondary (red) transects with indications of Luchterduinen, Prinses Amalia and Egmond aan Zee windfarms indicated.

4.3 Seabird counting techniques

Seabirds were recorded according to the method for surveying seabirds from ship by means of the strip-transect method as suggested by Tasker et al. 1984, Camphuysen & Garthe 2004, Camphuysen et al. 2004 and Leopold et al. 2004, and implemented as a standard by the European Seabirds at Sea Database (ESASD). As the search mode used during previous surveys for OWEZ and PAWP was ‘naked-eye’ (Leopold et al. 2013) this mode was also used during the monitoring of seabirds for LUD. The observation height was between 6.5 and 10 m above sea level. The method is a modified strip transect with a width of 300 meter, and five perpendicular distance sub-bands:

- 0-50 m;
- 50-100 m;
- 100-200 m;
- 200 – 300 m;
- ≥ 300 m.

Transect lines were broken up into 1 minute (time) stretches and birds seen “in transect” in each individual 1 minute count were pooled (from t=0 to t=1 mins and for portside and starboard). At t=1 mins, the next count commenced, from t=1 mins to t=2 mins, etc. Densities were calculated as numbers seen in transect, divided by area surveyed. Area surveyed is the segment length covered in that particular 1 minute period, depending on sailing speed (average 9 knots) and strip width (300 m), which were both continuously monitored, corrected for the proportion of birds that were missed by the observers (see next section: distance sampling). The location of each count was taken as the mid-position between the positions at t=0 and t=1 mins, for each count, on the ship’s transect line.

Birds were counted from the roof of the survey ship by four bird observers (Table 2), two on each side of the ship (Figure 2). Swimming seabirds were counted on both sides of the ship, and snap-shot counts of flying birds were made whereby every minute all birds were counted within an area of 300 by 300 m transverse and directly in front of the ship (Figure 3).



Figure 1. The ‘Ivero’ used as the survey ship.

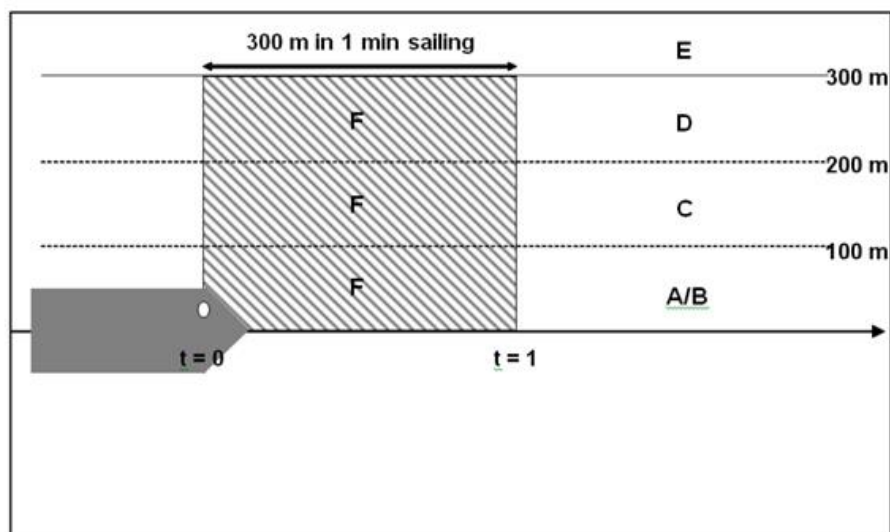


Figure 2. Schematic overview of the seabird survey method (see above for definitions of bands A-E).

Table 2. List of observers engaged in the LUD-T0 seabird surveys.

Survey	Observers
LUD-1-01	Jörn Hartje*, Thomas Schubert, Thomas W. Johansen, Ernst Eric Schrijver
LUD-1-02	Jörn Hartje*, Thomas Schubert, Thomas W. Johansen, Lars Maltha Rasmussen
LUD-1-03	Jörn Hartje*, Thomas Schubert, Troels Ortvad, Ernst Eric Schrijver

4.4 Quality control and post-processing of survey data

General quality assurance and management were conducted and documented in accordance with internationally accepted principles for quality and environmental management as described in the DS/EN ISO 9001 standard. Post-processing of the survey data followed Leopold et al. (2013).

Before and after every survey an equipment check was carried out following an approved checklist. On the ship all routines followed strictly briefing rules with the party chief as outlined in the Work Method Statement. All observations of seabirds, marine mammals and ships were recorded on sheets and the ship's position and speed in a GPS. After each survey the GPS-track was downloaded to a computer and checked for completeness. As soon as possible after the survey the sheets were transcribed by one of the observers directly into a special developed database. Unusual data were marked and commented and the observers were asked for clarification or confirmation if needed. This procedure is very important to get rid of erroneous data as soon as possible. Later on, the data sets were run through different automated routines to detect mistyping and other errors.

All observations and GPS positions were stored in a special SQL geo-database (FULMAR) held by IfaÖ for aerial and ship-based surveys, which is linked to ArcGIS, and which exports the results to a Microsoft Access® database. The post-processing chain starts by transcribing the general survey metadata (e.g. date, observer, observation height etc.) from the observation sheets into the database. The next step is to import the GPS-track into the database by using a special extension for ArcGIS, which is started by the database. In ArcGIS the whole track is shown. The start and end points of each transect line are marked and then the track points with their position and time are imported into the database. The user of the database can now view track points, time and the columns for the sightings. Every observation will be sorted by time to the nearest 1 minute count period. Also the weather conditions which are monitored continuously during the survey are stored into the database during this step.

After finishing the data input, different tools are used to visualize the observed seabirds along the transect lines. The next step was the validation of the data by a senior biologist, who also checked the weather conditions along all the transect lines on each side of the ship according to sea state, glare and visibility. If the observations of parts of the lines are affected by strong glare, sea state over Bft 4 or poor visibility, he marks that period as "invalid". After the evaluation, and if necessary by additional confirmation of the observer, the data will be exported to a report-file, which is a Microsoft Access® database file. Here, all common types of results are generated by queries. Two tools are generating the export files for ArcGIS and population estimation in Distance.

4.5 Distance analysis

The term 'Distance analysis' used in this report refers to analyses following standard distance sampling techniques (Buckland et al. 2001) conducted using the Distance package in R (<https://cran.r-project.org/web/packages/Distance>). These analyses were conducted to calculate distance detection functions for swimming seabirds. Sitting seabirds like auks or divers may be difficult to detect in the outer distance bands (farther away from the ship) and may also respond to the approaching survey vessel, and hence the collected densities of sitting seabirds are biased. As flying seabirds are comparatively easy to detect the collected densities of flying seabirds have been treated as unbiased, and no distance correction was applied. Flying birds were included (uncorrected) for Gannets, large gulls and small gulls. In the distance analysis all birds are assumed to be detected in the distance band closest to the ship, further away detectability decreases with increasing distance from the ship. A set of different detection function models were fitted. Half normal and hazard rate detection functions were fitted and Cosine adjustment terms were added to the models as well as Hermite polynomials (for Half-normal detection function) and simple polynomial (for the hazard rate detection function). Bird abundance and sea state were available as

covariates in the models. Finally the best fitting function was chosen on the basis of the smallest Akaike Information Criterion (AIC) values (Burnham and Anderson 2002).

Detection functions were calculated for the entire dataset (dedicated project surveys) for each species with sufficient number of observations, assuming that detectability of bird species was similar among surveys, as two of four observers were the same during both surveys. Estimated detection functions were used to estimate species-specific effective strip widths (ESW), which represent the width within which the expected number of detected seabirds would be the same as the numbers actually detected within the full width of 300 m (Buckland et al. 2001). Correction factors were then calculated by $1/(ESW/300)$. In line with Leopold et al. (2013), seabird species were pooled into species groups before Distance analysis (Table 3). The abundance of each species in each segment was thereafter corrected using the correction factor. The corrected abundance was merged with the effort data and species-specific densities (birds/km²) was calculated. The data was finally re-segmented (mean density) into approximately 1 km segments, to resemble the historic data resolution. Distance correction of the historic data was done using the corrections factors (and method) reported by Leopold et al. (2013). The historic and dedicated survey data was finally merged and used in species distribution modelling.

Table 3. Grouping of species for distance analysis. Some individuals were only identified to species group level, but could be used in distance analyses for groups: small divers (G stellata/G arctica), ‘commic’ terns (S hirundo/S paradisaea) and large auks (U aalga/A torda).

Group	Species
Divers	Red-throated Diver (<i>Gavia stellata</i>)
Divers	Black-throated Diver (<i>Gavia arctica</i>)
Gannets	Northern Gannet (<i>Morus bassanus</i>)
Cormorants	Great Cormorant (<i>Phalacrocorax carbo</i>)
Small gulls	Little Gull (<i>Hydrocoloeus minutus</i>)
Small gulls	Black-headed Gull (<i>Chroicocephalus ridibundus</i>)
Small gulls	Common Gull (<i>Larus canus</i>)
Small gulls	Black-legged Kittiwake (<i>Rissa tridactyla</i>)
Large gulls	Herring Gull (<i>Larus argentatus</i>)
Large gulls	Lesser Black-backed Gull (<i>Larus fuscus</i>)
Large gulls	Great Black-backed Gull (<i>Larus marinus</i>)
Auks	Common Guillemot (<i>Uria aalge</i>)
Auks	Razorbill (<i>Alca torda</i>)

4.6 Distribution models

For the assessment of potential displacement from LUD and cumulative and in-combination displacement with PAWP and OWEZ, fine-scale distribution models capable of describing the distribution during the LUD post-construction period were developed in line with the baseline models (Skov et al. 2015). In this study a cumulative effect is defined as a displacement from one windfarm affecting the occurrence of the displaced species at another windfarm. The in-combination effect is defined as the combined detection of displacement, i.e. is a bird species displaced from all windfarms or only one or two?. For the purpose of this LUD T-1 report the distribution models were mainly developed with the aim to assess the “power” of

detecting a significant displacement of seabirds (see chapter 4.7). To enhance the power of detecting a displacement in a highly variable environment it is important to include the factors causing the large variability and account for any unexplained spatial autocorrelation (Perez-Lapena 2010). In one survey seabirds might be in a specific location due to suitable oceanographic conditions which enhance the availability of prey fish. In another survey the condition might be unsuitable and the seabirds therefore absent. If this location happens to be the windfarm it can be difficult to assess a displacement effect if the important factors driving the distribution are not included. In order to assess the impact of LUD (significance) and map the survey-specific distribution of seabirds during the LUD-T1 winter of 2015-2016, prediction models were therefore applied taking both static (depth) and dynamic habitat conditions (salinity, current speed, eddy potential, current gradient and water depth) as well as pressures (distance to the windfarms truncated at 4 km and shipping intensity AIS) into account. A factor variable with each survey as a level was also included as a fixed factor, enabling survey specific predictions.

The hydrodynamic dynamic variables (fixed factors) salinity, current speed, eddy potential (vorticity) and current gradient were extracted to the survey data as mean values during each survey period (whole days), together with water depth and distance to each windfarm truncated at 4 km. Distance further away than 4 km from each specific windfarm was set to 4.001. The distance in pre-construction data was all set to 4.001 km. The environmental variables are mapped in Appendix B, the dynamic variables are mapped for surveys done from 2012-2016 (Appendix B). Data from 2007 until 2016 were included and the two surveys conducted during construction (October 2014 and December 2014) were excluded from the species-specific models, so in total 19 surveys were included. Surveys with no-records of the model species were also dropped, if any. Generalized additive mixed models (GAMMs) were used as these are capable of fitting different family distributions and nonlinear responses (Hastie & Tibshirani 1990), which are expected between seabirds and habitat variables. The mixed models can also account for potential temporal and spatial autocorrelation in model residuals. To account for zero inflation a two-step model (hurdle model) was fitted consisting of a presence-absence model and a positive model part (densities) where all zeroes were excluded.

The autocorrelation was accounted for by either adding a correlation structure (corAR1 or corARMA) or a random term, grouped by survey hour (in accordance with Leopold et al. 2013), to account for the temporal and spatial autocorrelation. If the preferred autocorrelation structure failed to converge, a random term was used instead. The “`gamm`” function in “`mgcv`” R package was used for fitting the models as it is possible to include both autocorrelation structures and random terms. The species-specific models were fitted in a stepwise manner, an initial full model was first fitted including all environmental variables and further simplified by dropping uninfluential variables in a stepwise manner. Variables displaying ecologically unrealistic shapes (for example if divers would show a preference of high shipping intensity, or grebes would prefer very deep water response that we know from experience is wrong) were also dropped. The distance to windfarm variables (truncated at 4 km) were always retained in the model, being significant or not. The final model was chosen based on AIC and the ability to account for autocorrelation in model residuals. The model residuals were checked for autocorrelation using a correlogram. The models were evaluated for predictive accuracy by fitting the model on 70% of the data (randomly selected) and predicted on the 30% withheld data. The presence-absence model part was tested using AUC and the combined density predictions using Spearman’s correlation coefficient.

The species-specific models were finally used for predicting the distribution of mean densities in the whole study area during a range of different surveys. The mean density of the post construction (LUD) surveys were calculated and mapped together with corresponding number of pre-construction surveys. The change in density between these two periods was also mapped to illustrate potential predicted displacement or attraction.

Compared to the model framework described in Skov et al. (2015) a more detailed account of the presence of ships in the study region during LUD baseline (2007-2014) and T-1 surveys was developed. AIS counts of ships were analysed by MARIN www.marin.nl by aggregating the number of ships entering a grid cell of 1000 by 1000 meter over the course of each of the 21 survey periods (see Table 1). The methodology may introduce overestimation of the number of ships crossing a grid cell in anchorage areas and harbours where ships may move back and forth. The effect of this potential bias will be tested during T2.

4.7 Analysis of displacement and number of included surveys

This report includes the first results of the analyses of displacement of seabirds at LUD and updated results for PAWP and OWEZ. The analyses are reported in two ways, an assessment of significance of the three “distance to windfarm variables” (indicating a statistically significant displacement) and the difference in predicted densities pre- and post-construction. The ability of detecting a significant displacement by the models was tested empirically by fitting models on different numbers of surveys (starting with only one survey and adding one more survey at a time), we call it an empirical power test. The power (probability of detecting a change) was further also tested using simulated bird observations on the same environmental conditions as the actual surveys.

Both power tests were conducted on the two species identified by Leopold et al. (2013) as displaying a strong displacement at PAWP and OWEZ; Northern Gannet and Common Guillemot, as both species show similar trends at LUD. To be able to include a pre-construction survey in the empirical power test we also added the survey conducted in February 2004. The survey from 2004 was not included in the main analysis because AIS data was not available. For the empirical power test we assumed the AIS data to be similar to the first survey in 2007, i.e. AIS data from 2007 were extracted to the survey conducted in 2004. As a first model we included the pre-construction survey and the first post-construction survey. We refitted the GAMMs for Common Guillemot and Northern Gannet on the reduced data set (including only two surveys) and we extracted the p-values from the model results. We further step-wise added one survey at a time and refitted the models and for each added survey we extracted the p-values. We finally plotted the extracted values in a graph to assess the influence of number of surveys on the significance of the displacement effect.

We also assessed the power of detecting a significant displacement of Northern Gannet and Common Guillemot from LUD by using a simulation approach. We refitted the GAMMs for these two species as Generalized Linear Mixed Models, GLMMs (with survey hour as a random effect using the R package “lme4” and function “glmer”), without the variable distance to LUD included (i.e. ignoring the windfarm effect and by that simulating a distribution as it would be without the LUD windfarm). The reason for refitting the GAMMs as GLMMs is because there is a readily available function for simulating GLMMs in the package lme4 (function called “simulate”), which allowed us to simulate 100 new bird distributions (based on the modelled relationships) on the actual survey conditions (i.e. the conditions extracted to each real survey). In other words, all 19 surveys included in the modelling were artificially re-surveyed 100 times (for each simulation displacement scenario). During each simulated survey bird distribution were simulated in accordance with the model relationships (which could for example be decreasing shipping intensity in deeper more saline water, see the real species-specific model results below). The variability in the “true” environmental conditions and pressures between surveys and years were therefore included in the simulations. We further artificially and randomly reduced (or displaced) the occurrences and bird density (conditional on occurrences) within the windfarm (or within the windfarm + 4 km buffer) by for example 25%, 50% and 75%. For each simulation, GAMMs were fitted (same as the “original” final models), and the proportion of models that resulted in a significant effect of LUD was calculated. Therefore, if 80 models of 100 models were significant (<0.01) the proportion and power of the data was 80%. The simulation approach taken in this study, is similar to the approach taken by Perez-Lapena et al. (2010), Maclean et al. 2013 and Vanermen et al. 2015 in the sense that statistical model parameters are used as a basis for simulations and artificial reductions are further made for the purpose of assessing the power of detecting a displacement. We have further also included hydrodynamic variables to account for the large variability seen in the dynamic marine environment, which influences the distribution of the birds and should enhance the power of detecting a displacement (Perez-Lapena et al. (2010), Maclean et al. 2013). The modelling and simulation approach is schematically presented in Figure 4). Examples of simulation for “power” calculations of significant impact of LUD are found in Appendix C.

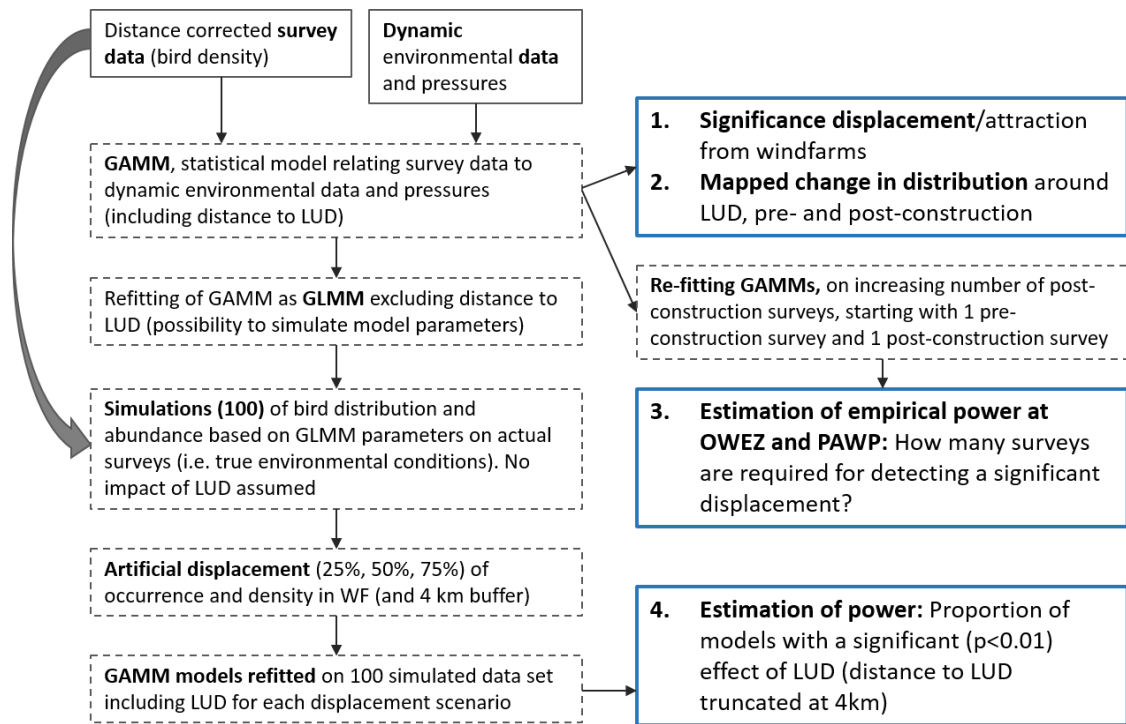


Figure 4. Modelling framework for the simulation based power tests. Input data is indicated by boxes with black outlines, analysis steps are indicated by boxes with dashed outlines and results/outputs by boxes with blue outlines.

4.8 Presentation of data

Maps showing observed densities and (modelled and) predicted mean distributions during the LUD T-1 surveys in the winter 2015-2016 have been produced in UTM 32N WGS84 projection. The observed densities are shown for segments (mid points) of approximately 1 km and the mean predicted density is presented for cells with a resolution of 1 km. The mean of model predictions from four LUD pre-construction surveys are also presented together with a map displaying the change between pre and post construction. Note, that the predictions are based on the statistical models and should be interpreted as model results together with model statistical outputs, see Appendix A. The three disturbance areas (LUD, PAWP, OWEZ) and the 20 m depth contour are indicated.

5 Results

5.1 Effort and sample sizes

Four surveys were undertaken during the 2015-2016 winter using the Ivero. The first survey was conducted from 19th to 23rd of October 2015, the second from 13th to 17rd of December 2015, the third from 11th to 16rd of February 2016 and the fourth from 04th to 08th of March 2016. During the LUD T-1 surveys, the primary transects within PAWP, OWEZ and LUD were completed, and the majority of the secondary transects around LUD were completed. An overview of the survey effort is given in Table 4 and Figure 5. Number of recorded seabirds during the T-1 surveys are listed in Table 5. During the T1-02 survey a Red-necked Grebe was recorded for the first time during the LUD monitoring programme.

Table 4. *Survey effort (km² covered by observation transect) obtained during the four ship-based surveys in the LUD T-1 winter season (2015-2016).*

Period	Survey	Area covered (km ²)
LUD-T1-01	19-23/10 2015	280.56
LUD-T1-02	13-17/12 2015	291.09
LUD-T1-03	11-16/2 2016	289.97
LUD-T1-04	4-8/3 2016	404.45

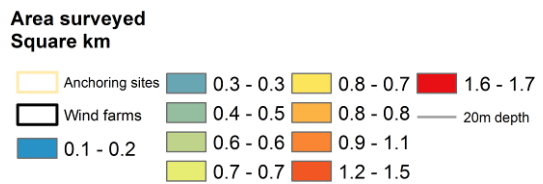
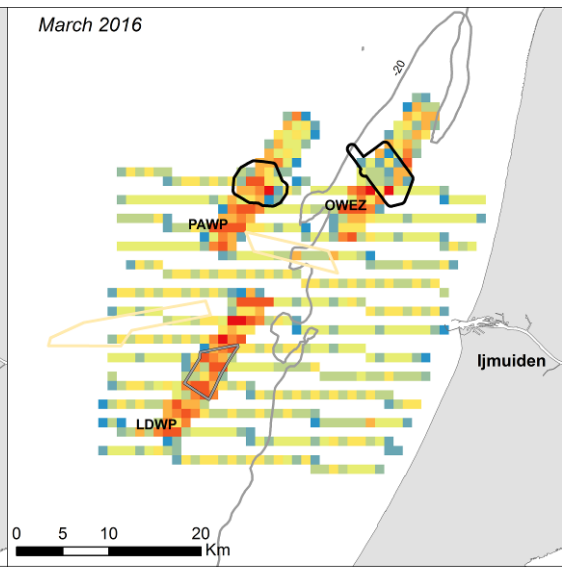
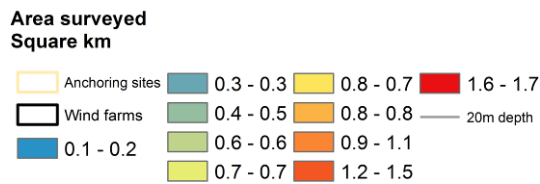
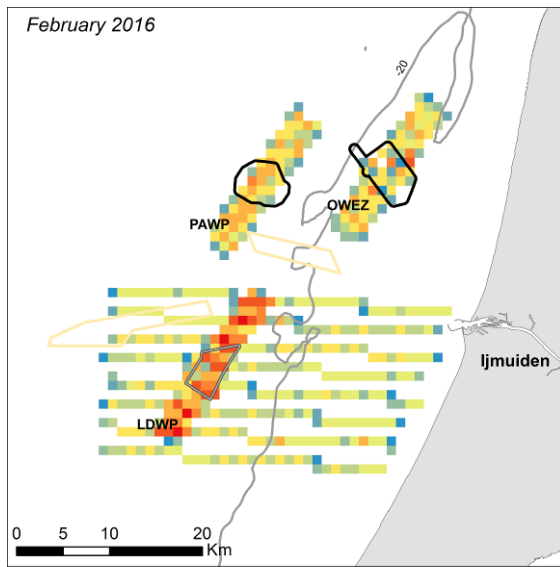
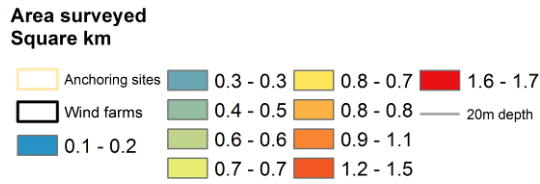
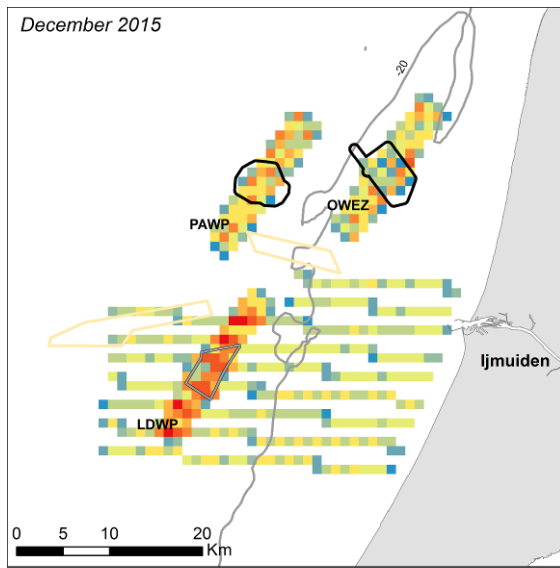


Figure 5. The spatial coverage of survey effort (km²) obtained during the four ship-based surveys in the LUD T-1 season (2015-2016).

Table 5. Numbers of seabirds observed during the two LUD T-1 surveys in winter 2015/2016.

Species	Total Oct 2015	Total Dec 2015	Total Feb 2016	Total Mar 2016
Red-Black-throated Diver	2	74	12	36
Great Crested Grebe	0	57	6	2
Red-necked Grebe	0	1	0	0
Northern Fulmar	0	1	0	0
Northern Gannet	66	356	67	17
Great Cormorant	310	163	140	274
Common Scoter	268	53	18	176
Little Gull	17	10	19	83
Black-headed Gull	34	39	2	17
Common Gull	177	171	170	122
Lesser Black-backed Gull	197	28	39	562
Herring Gull	59	222	24	33
Great Black-backed Gull	108	331	182	96
Black-legged Kittiwake	27	4499	94	79
Common Guillemot	402	2900	493	56
Razorbill	162	137	83	49
Unidentified <i>Alcids</i>	26	10	1	3
Common Eider	0	11	0	4
European Storm Petrel	1	0	0	0
Arctic Skua	1	0	0	0
Great Skua	0	12	0	0
Sandwich Tern	0	0	3	0
Total	1,857	9,075	1,353	1,609

5.2 Distance analysis

Table 6 gives an overview of the selected models used for estimating detection of sitting birds with distance for the different species groups.

Table 6. Distance statistics for sitting birds in each species group.

Species group	Sample size	Key function*	Adjustment term	Effective strip width (ESW)	% CV ESW
Divers	32	HN	Cosine (2)	166	24.7
Grebes	96	HN	Cosine (2)	152	14.9
Gannets	79	HN	Cosine (2)	197	18.9
Cormorants	165	HN	Cosine (2)	245	15.3
Small gulls	445	HN	Cosine (2)	150	6.3
Large gulls	562	HN	Cosine (2)	142	5.5

Auks	4039	HN	Cosine (2,3)	135	2.9
------	------	----	--------------	-----	-----

* HN=Half normal, HR= Hazard rate

5.3 Species accounts

In this chapter an account of the results of the analyses and modelling of the LUD-T1 (together with T0 and the “historic” PAWP and OWEZ data) data is given. For each species the description of the LUD-T1 status starts with a general introduction in which the results of the LUD-T1 surveys during the 2015-2016 winter are summarised. The results of the species-specific distribution models are given in a separate subsection called ‘model results’.

5.3.1 Divers: Red-throated *Gavia stellata* and Black-throated Divers *Gavia arctica*

The LUD-T1 surveys showed similar distribution patterns to LUD baseline surveys with most sightings done in the coastal zone, and only two observations offshore south of PAWP and OWEZ recorded during the March survey (Figure 6). There is a large variability in mean density between surveys as indicated by Figure 7.

Model results

Survey 21 (October 2015) was not included as there were no diver sightings (sitting on water) during that survey. The model did not converge when distance to LUD was included, the two other windfarms were included as parametric terms (not as smooth terms) in the presence-absence model and only distance to OWEZ in the positive model part. Both windfarms were significant in the presence-absence model part, indicating a displacement effect. The probability of presence further increases with lower salinity, lower current speed and intermediate eddy potential (vorticity). All responses indicating a preference for coastal waters, which is also apparent from the predictions (Figure 8). In the positive part only decreasing current speed was significant in addition to the survey factor (Appendix A). The model had a good predictive ability with an AUC value of 0.84, indicating the model is good at distinguishing between presence and absence. The Spearman’s correlation between observed and predicted was also fair with a value of 0.37 (Appendix A). LUD is not overlapping with the general distribution range of diver species in the region, which most likely is one reason for not being important in the model. The predicted distributions indicate a general reduction in the density when the mean of four post-construction surveys were compared against the mean of four LUD pre-construction surveys (Figure 8).

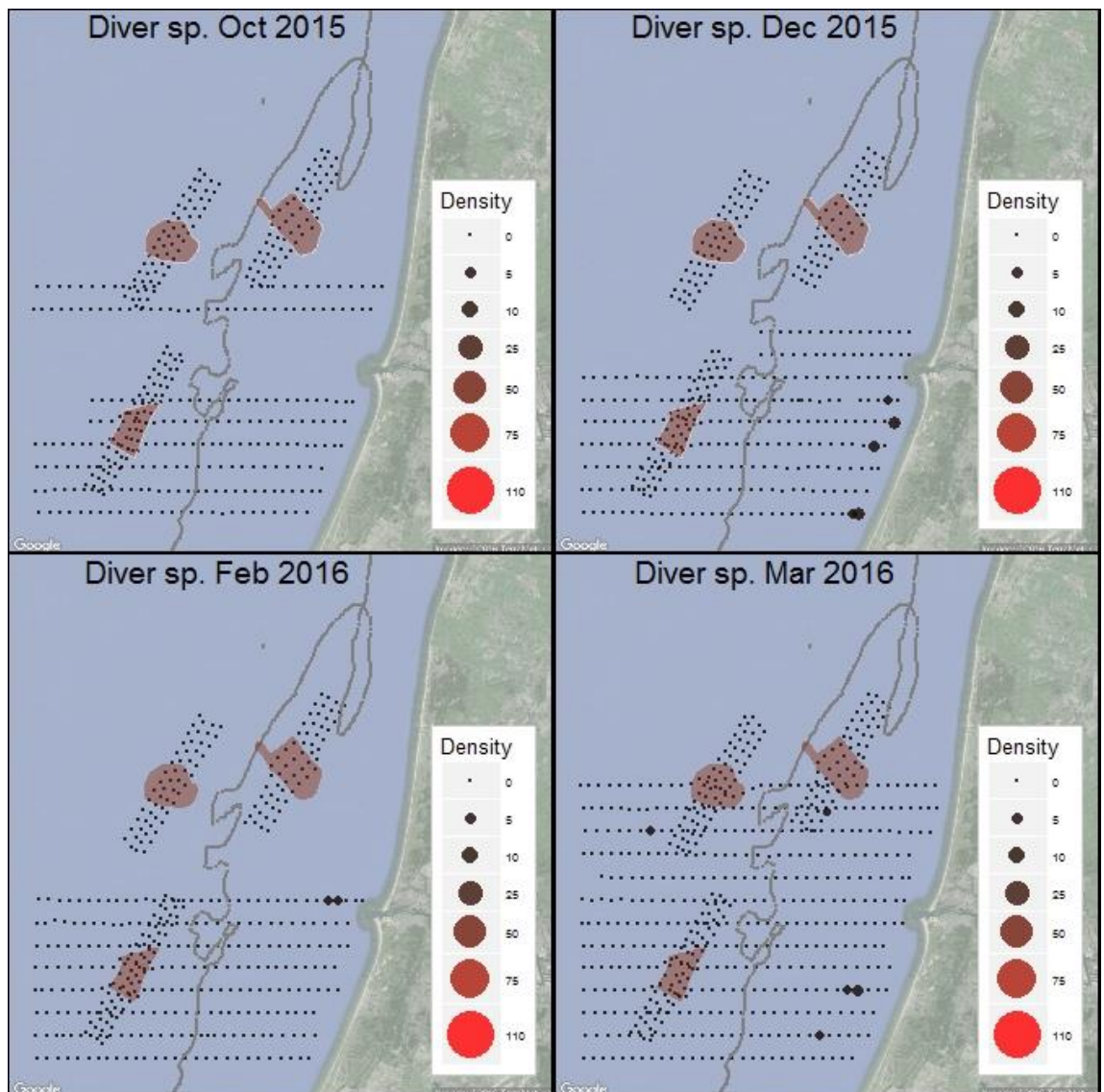


Figure 6. Observed density (birds/km²) of Diver sp. during LUD T-1 surveys 2015-2016. Densities have been corrected for distance bias.

Diver sp, 2002-2016

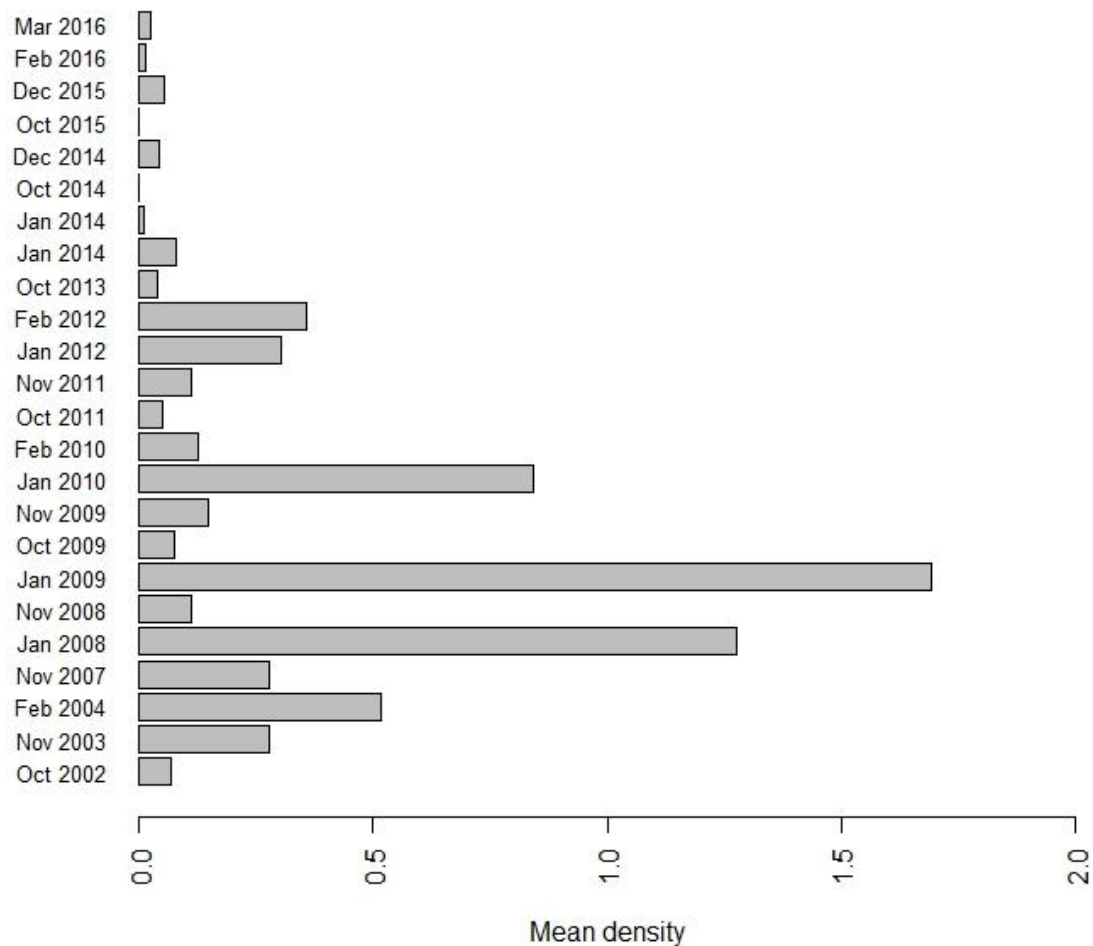


Figure 7. Mean observed density (birds/km²) of Diver sp. during LUD pre- and post-construction surveys. Densities have been corrected for distance bias.

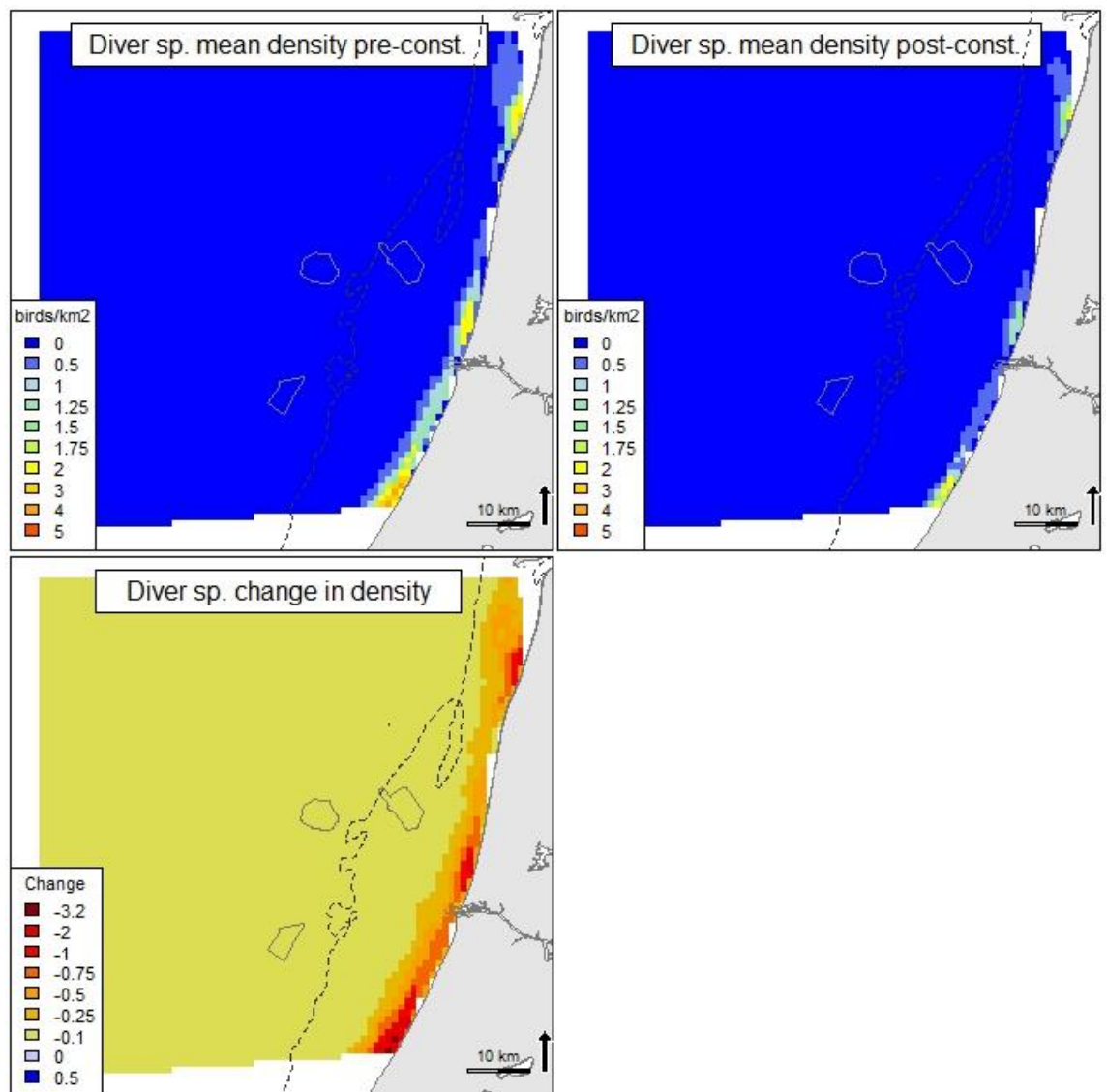


Figure 8. Predicted mean density (birds/km²) and distribution of wintering Diver sp. during three LUD pre- and three LUD post-construction surveys, and the relative change in predicted density between the two periods. Note that all included surveys are OWEZ and PAWP post-construction surveys.

5.3.2 Great Crested Grebe *Podiceps cristatus*

During the T-1 surveys Great Crested were exclusively recorded in the coastal zone (Figure 9) and in low densities (Figure 10).

Model results

Survey 8 (October 2009), 12 (October 2012), 16 (October 2013) and 24 (March 2016) were excluded from the analyses as there were no records of grebes in the model data set. The model did not converge with distance to PAWP and LUD included as predictors. Distance to OWEZ was included as a parametric term and was significant in the presence-absence model part, indicating a displacement effect. Further decreasing depth and salinity was included in both model parts indicating that the Great Crested Grebe mostly occur in higher numbers in coastal waters and the range of the general distribution does therefore not overlap with PAWP or LUD (Figure 11). The model had a good predictive ability when tested on withheld data, an AUC value of 0.93 and a Spearman's correlation of 0.44 (Appendix A). The predicted distributions indicate a general reduction in Great Crested Grebe density when the mean of four post-

(LUD)-construction surveys were compared against the mean of four pre-(LUD)-construction surveys (Figure 11), which is accordance with the mean densities shown in Figure 10.

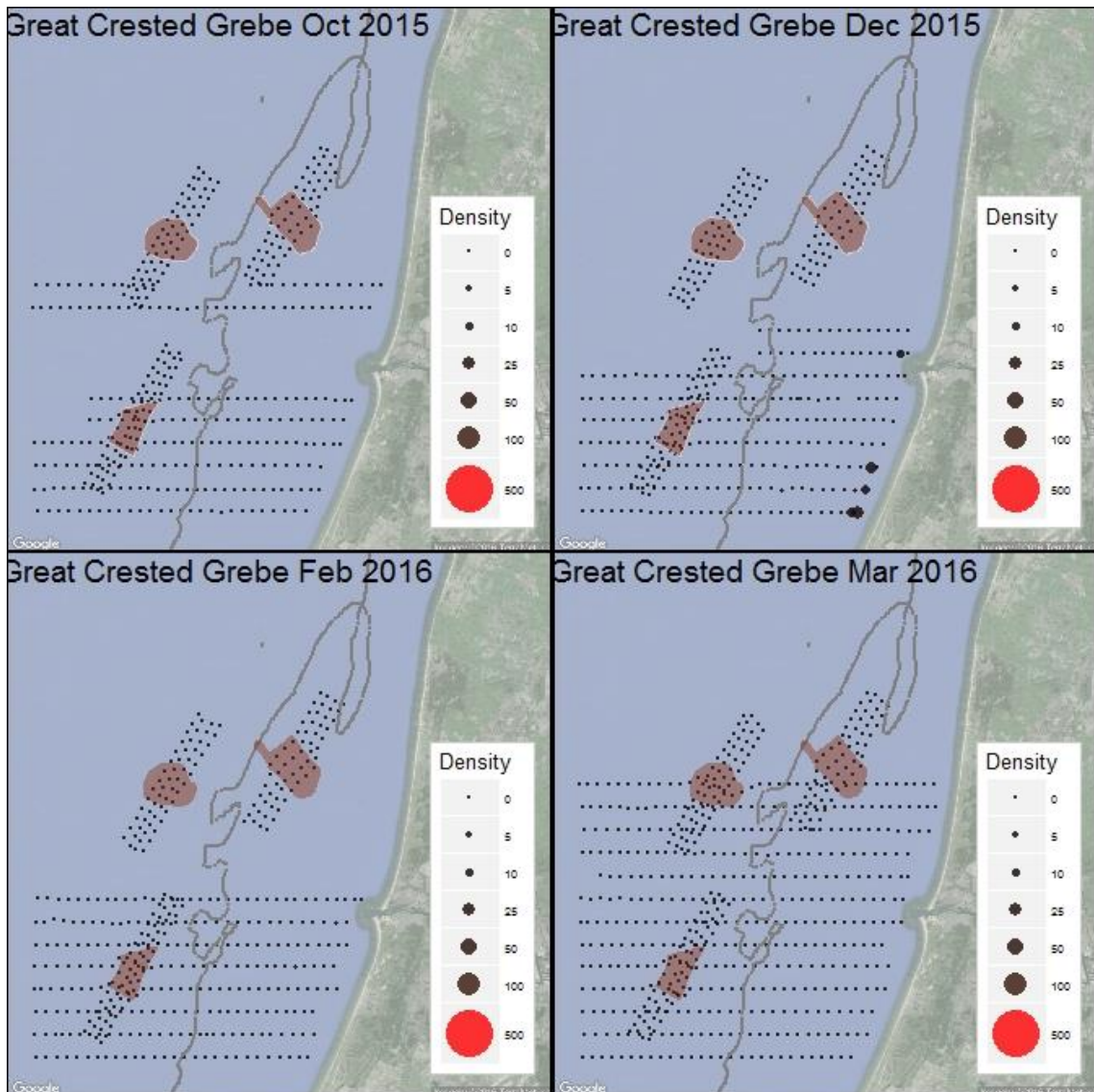


Figure 9. Observed density (birds/km²) of Great Crested Grebe during LUD T-1 surveys 2015-2016. Densities have been corrected for distance bias.

Great Crested Grebe, 2002-2016

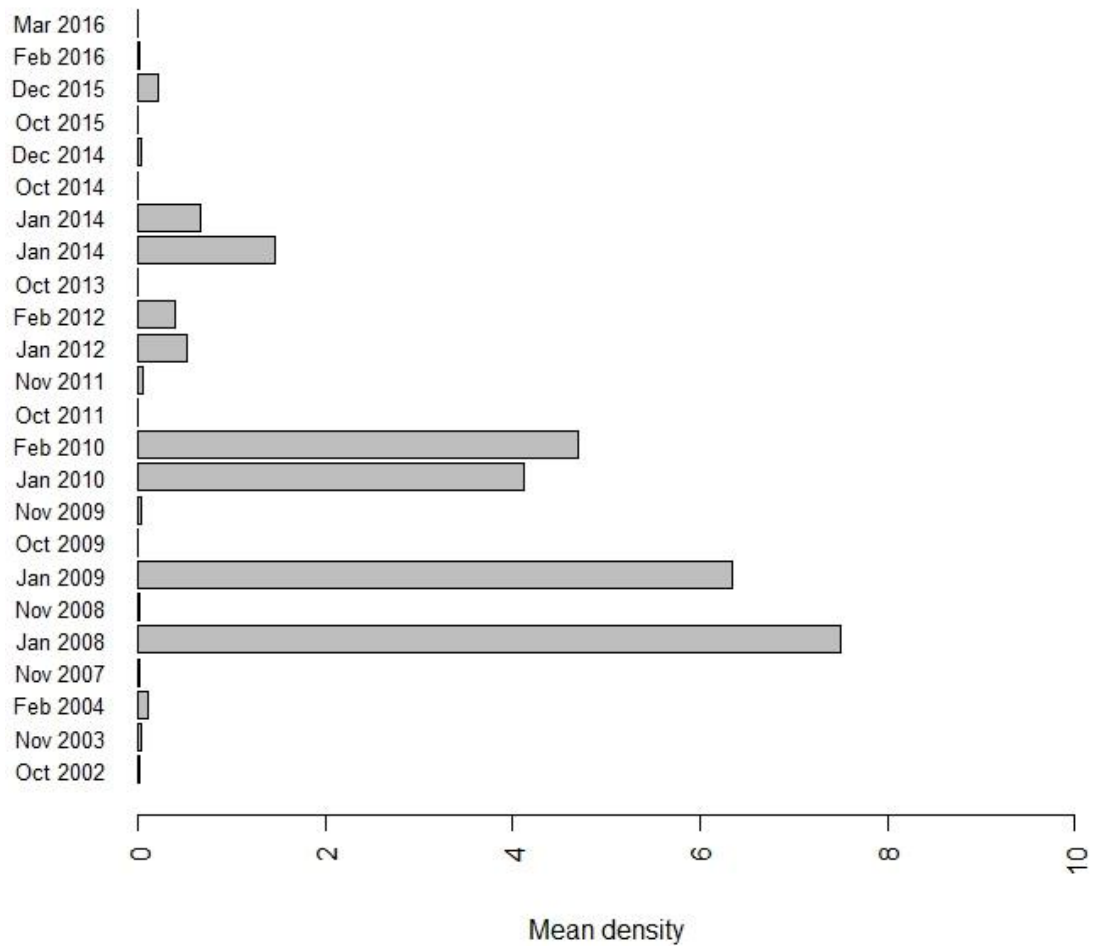


Figure 10. Mean observed density (birds/km²) of Great Crested Grebe during LUD pre- and post-construction surveys. Densities have been corrected for distance bias.

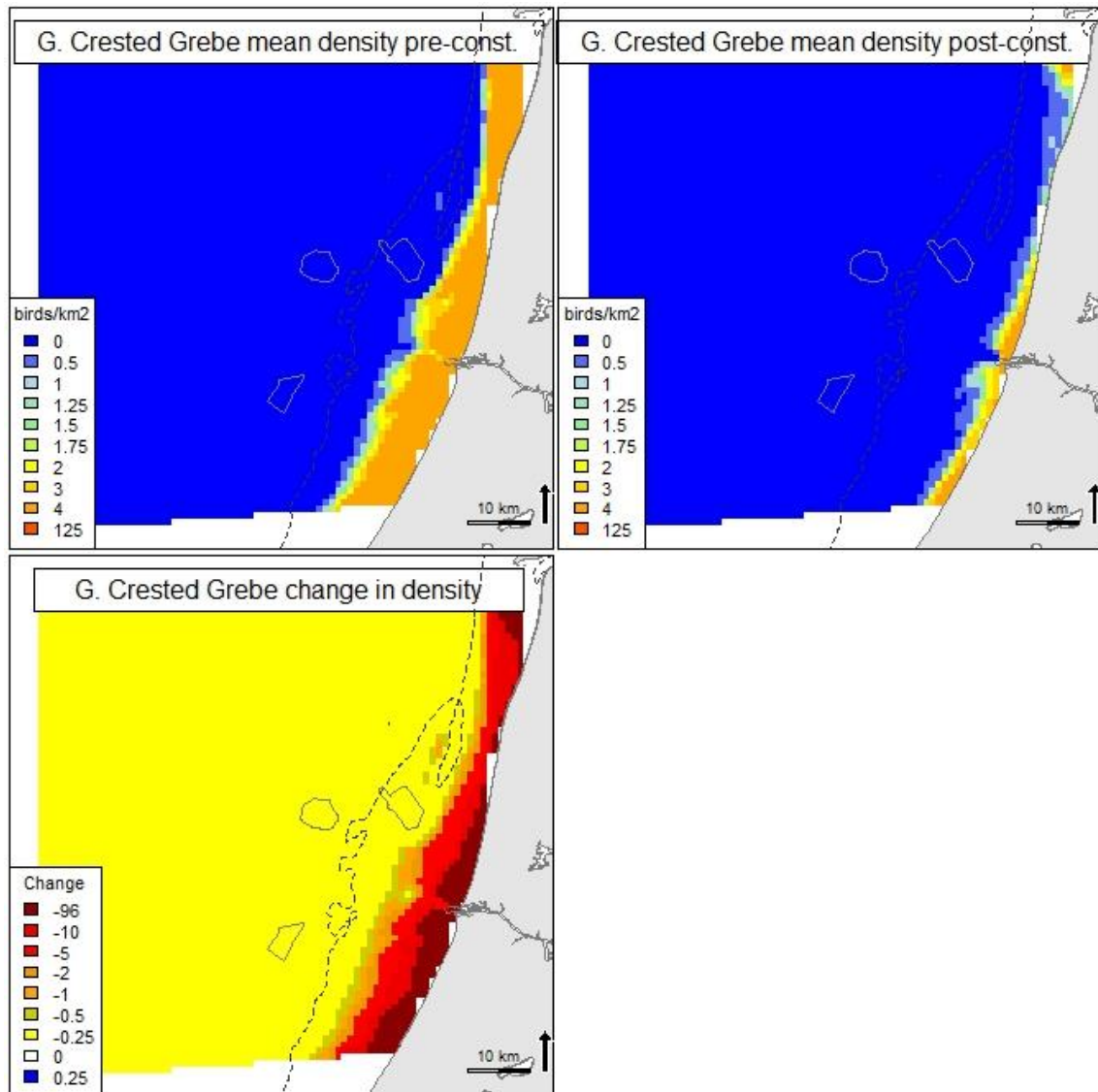


Figure 11. Predicted mean density (birds/km²) and distribution of wintering Great Crested Grebe during two LUD pre- and two LUD post-construction surveys, and the relative change in predicted density between the two periods. Note that all included surveys are OWEZ and PAWP post-construction surveys.

5.3.3 Northern Gannet *Morus bassanus*

During the LUD-T1 surveys the highest numbers of Gannets were recorded around and south of LUD. Similar to what was described for the winter surveys from 2002-2011, Gannets were displaying clear avoidance patterns in relation to OWEZ and PAWP (Leopold et al. 2013), and indications of avoidance was now also recorded in relation to LUD, although Gannets were seen quite close to and inside the windfarm (Figure 12). Highest densities were observed during the December survey. A marked variation is apparent in the recorded densities of Gannet between the 24 surveys conducted (Figure 13) of which 18 were included in the distribution modelling (Appendix A). The Gannet did not seem to prefer the LUD footprint even before construction when comparing mean density within the windfarms with three buffers outside the windfarm. A general large increase in density during post-construction resulted in a higher density within the footprint but a larger increase in the outermost buffer zones in comparison to pre-construction, which could indicate a displacement (Figure 14). Indications of a displacement seem much stronger at PAWP where the highest mean density pre-construction was found within the windfarm, while the densities post-construction was much lower than in the buffer zones (Figure 15). Also at OWEZ there seem to be a displacement, particularly when comparing mean densities of 19 post-construction surveys

(Figure 16). Common to all three windfarms is that there is a very large variability in Gannet density in the different zones as indicated by the standard deviation. The large variation is due to environmental variability and yearly and seasonal variation in bird density.

Model results

The modelling results indicated that the Northern Gannets preferred deeper and saline North Sea water masses with lower current speeds and higher water transparency. There was a highly significant negative relationship to the two existing windfarms up to a distance of about 2 km for PAWP and a linear decrease for OWEZ. The relationship to LUD was negative and linear, yet not significant (Appendix A). The explanation degree of the distribution model for the Northern Gannet was poor for the positive part, whereas the explanation degree was fair for the presence-part of the model (Appendix A). The AUC indicated that the presence-absence model part had a quite good predictive ability while the Spearman's correlation coefficient indicated that predicted densities are not very accurate in terms of predictive ability (Appendix A).

The predicted patterns described a general increasing density gradient from the coast to the offshore and a general increase from four pre-construction to four post construction surveys, however with a smaller increase inside the windfarm areas indicating a displacement from the LUD area (Figure 14, Figure 17). The empirical power analysis indicated that the distance to windfarm effect on Gannets for both PAWP and OWEZ was significant following 4 surveys post-construction (Figure 18).

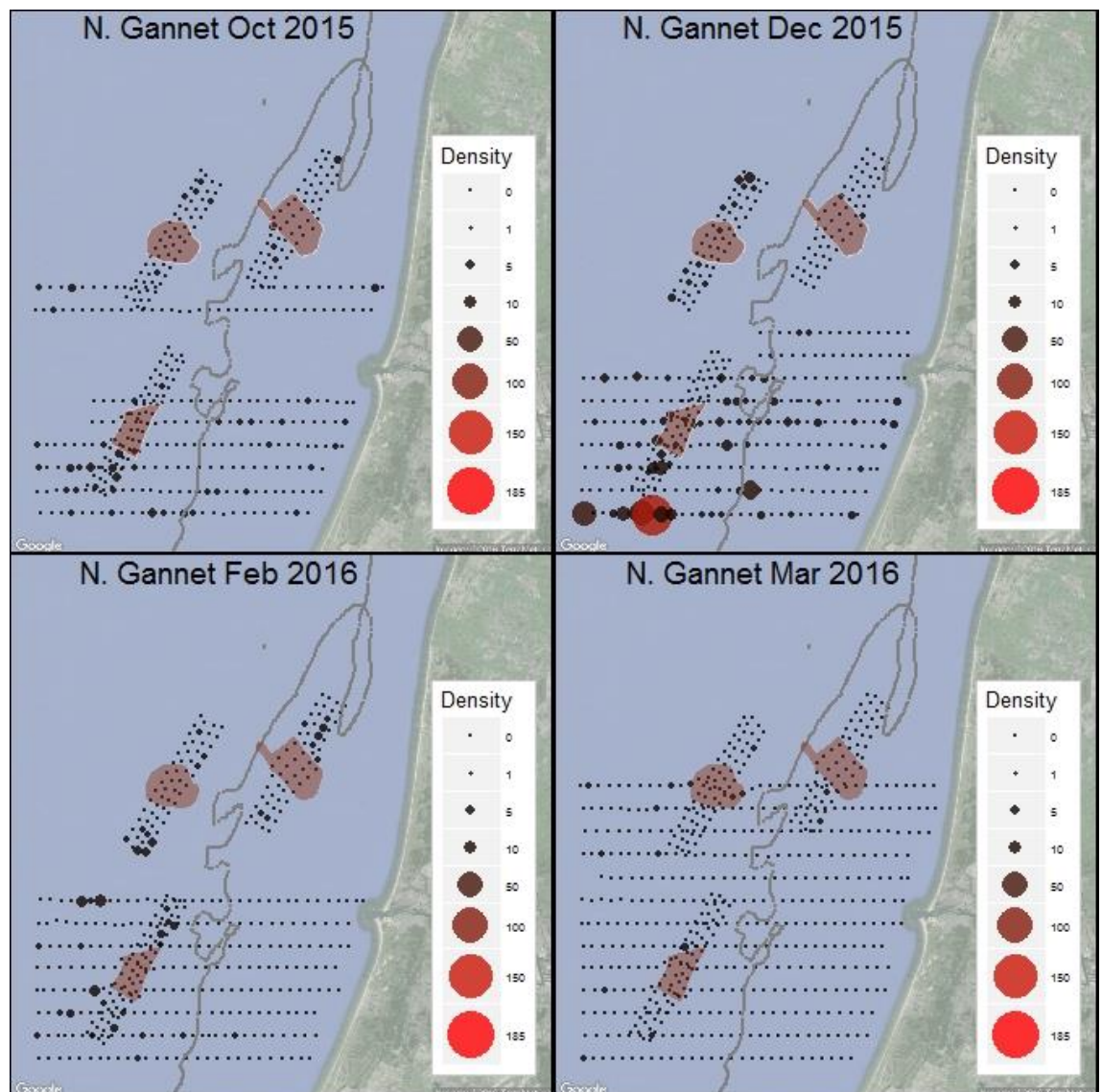


Figure 12 Observed density (birds/km²) of Northern Gannet during LUD T-1 surveys 2015-2016. Densities have been corrected for distance bias.

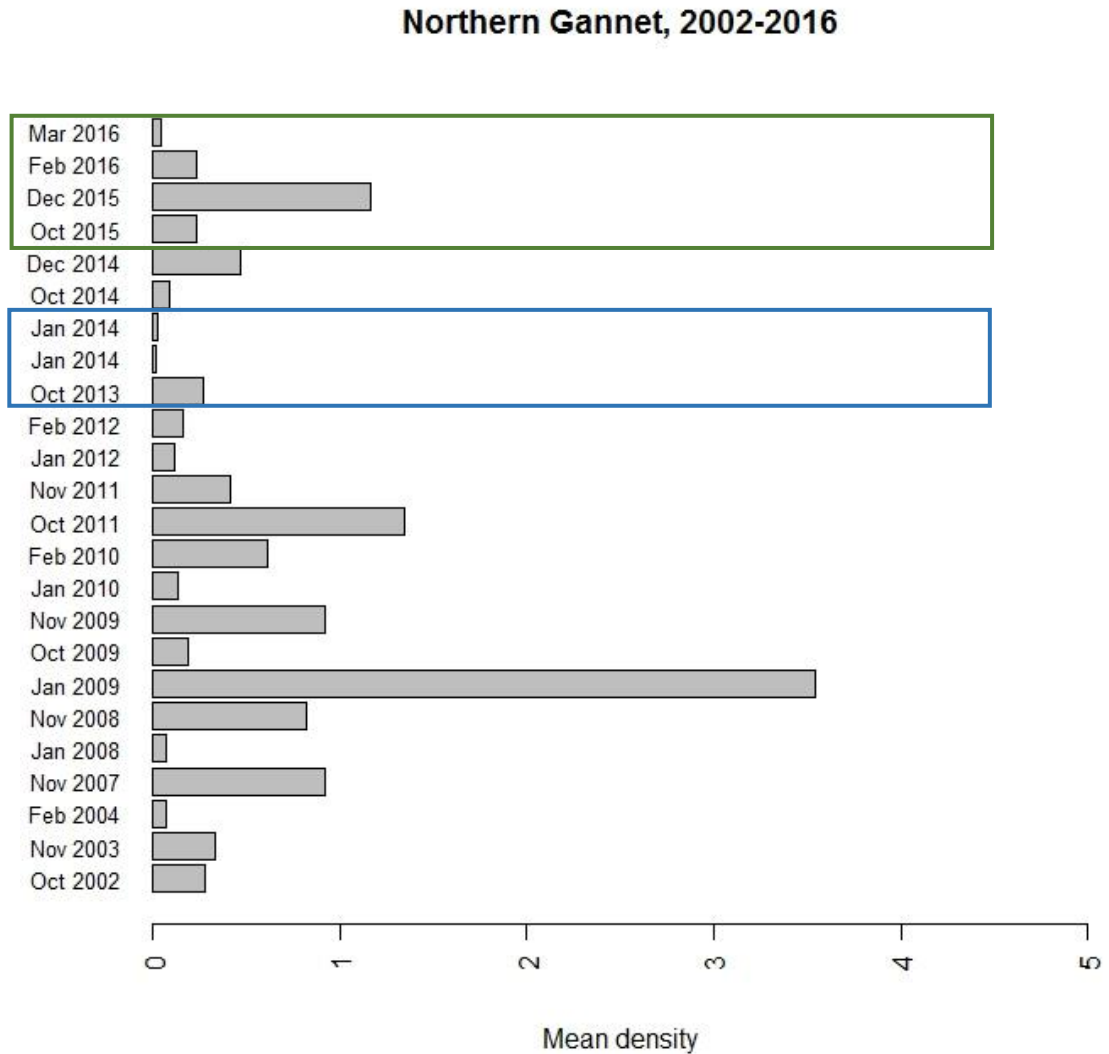


Figure 13 Mean observed density (birds/km²) of Northern Gannet during LUD pre-construction (marked with a blue rectangle) and post-construction surveys (green rectangle). Densities have been corrected for distance bias.

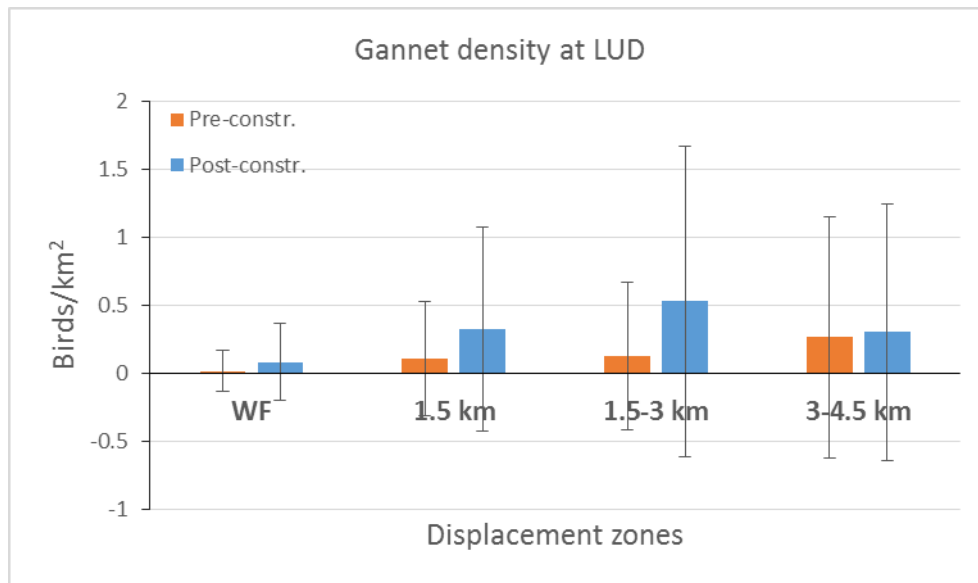


Figure 14. Mean Northern Gannet density pre-construction and post-construction within the LUD windfarm footprint and within three buffer zones around the windfarm, 1.5 km, 1.5 - 3 km and 3 - 4.5 km buffer.

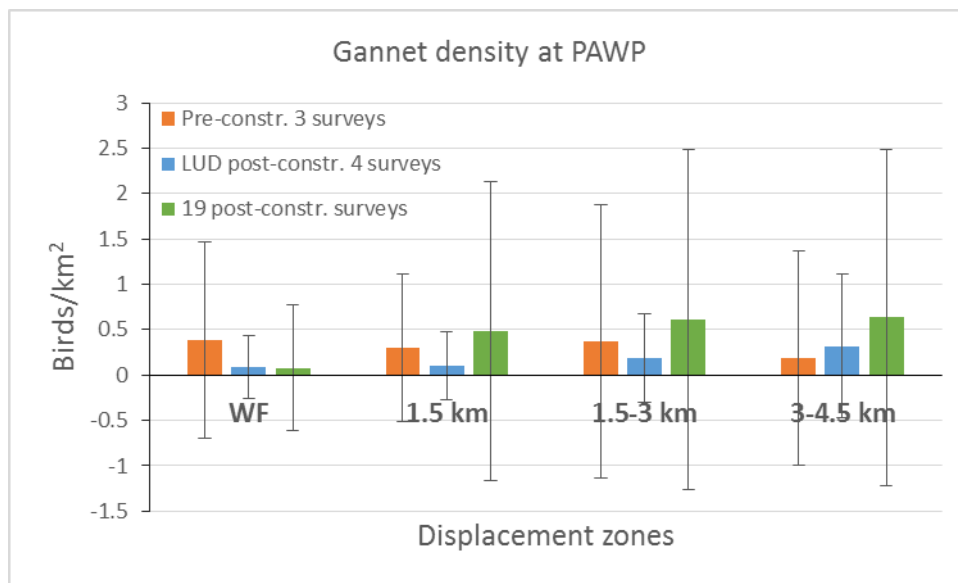


Figure 15. Mean Northern Gannet density pre-construction and post-construction within the PAWP windfarm footprint and within three buffer zones around the windfarm, 1.5 km, 1.5 - 3 km and 3 - 4.5 km buffer.

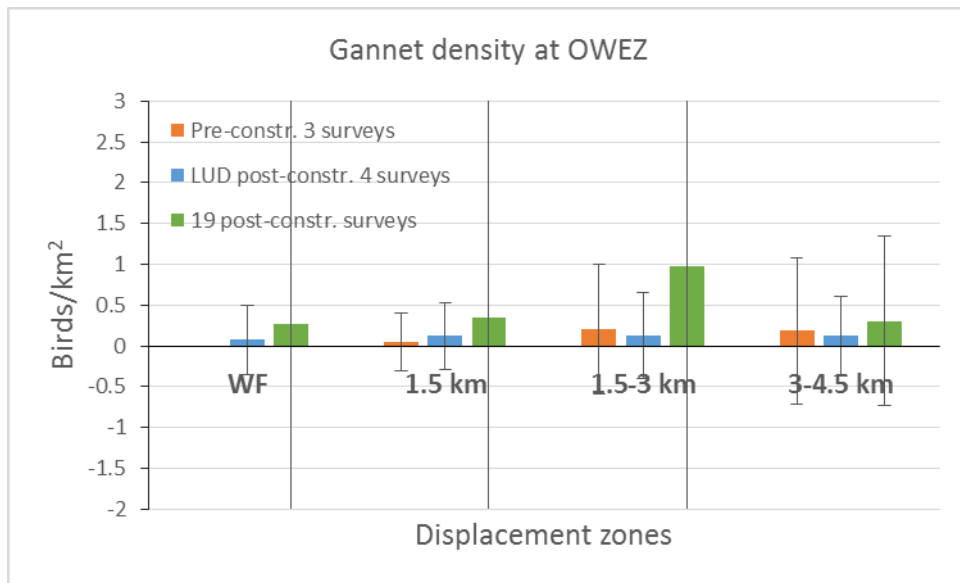


Figure 16. Mean Northern Gannet density pre-construction and post-construction within the OWEZ windfarm footprint and within three buffer zones around the windfarm, 1.5 km, 1.5 - 3 km and 3 - 4.5 km buffer.

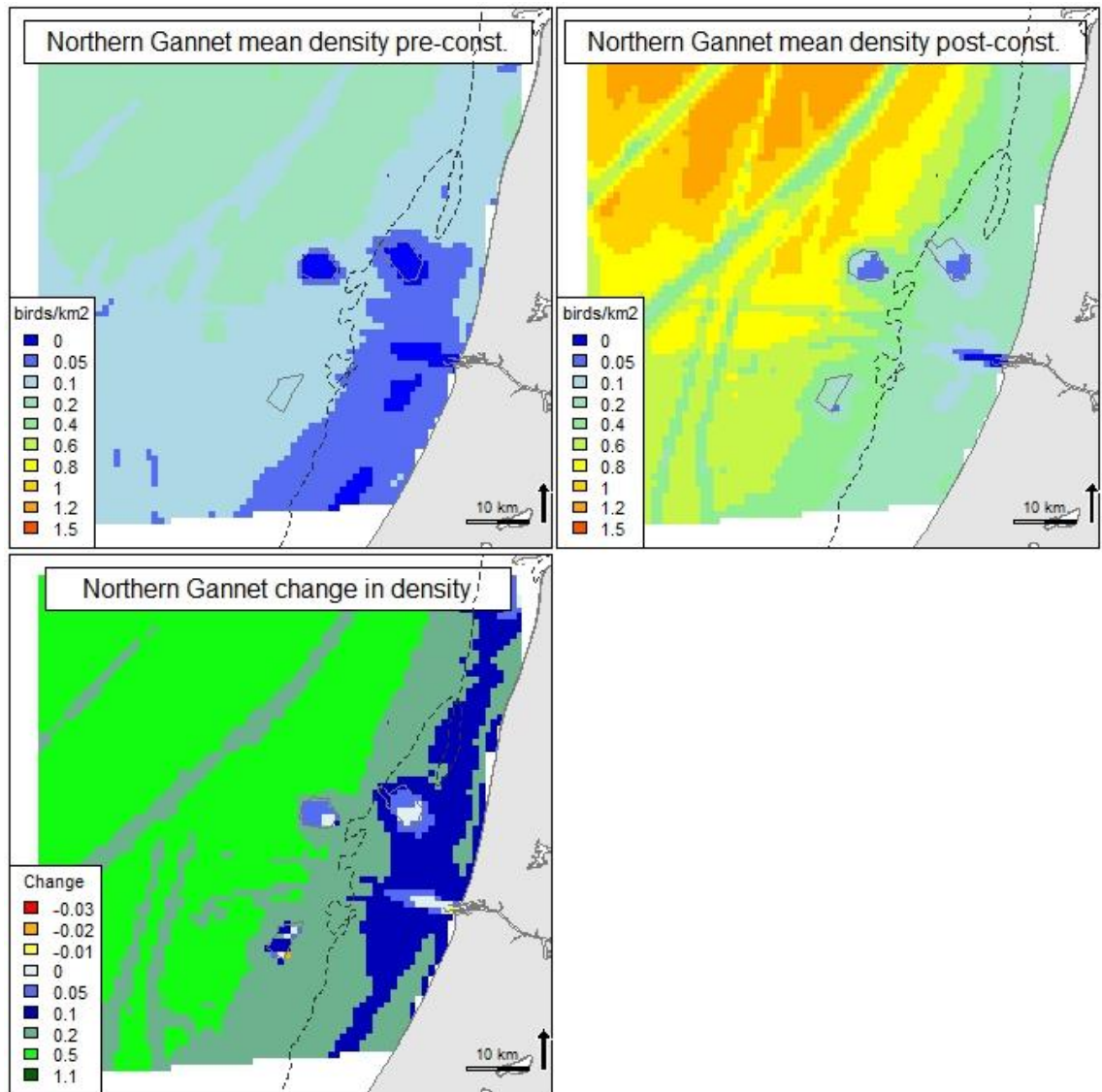


Figure 17. Predicted mean density (birds/km²) and distribution of wintering Northern Gannet during four LUD pre- and four LUD post-construction surveys, and the relative change in predicted density between the two periods. Note that all included surveys are OWEZ and PAWP post-construction surveys.

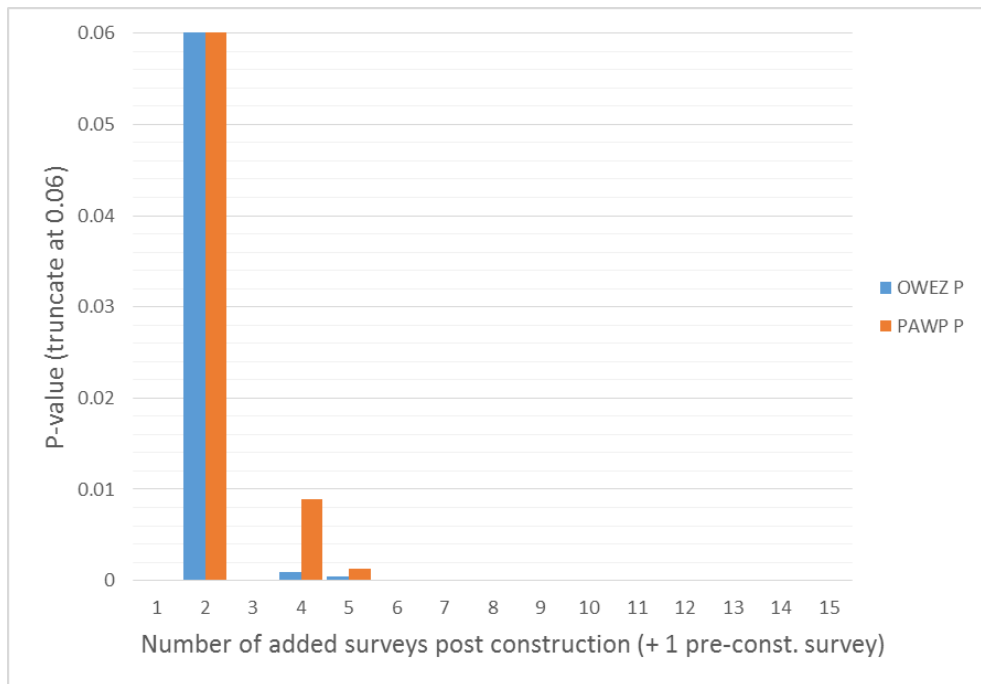


Figure 18. Significance (P-value) of effect parameter (distance from windfarm) for Northern Gannet in relation to the number of post-construction monitoring surveys at OWEZ and PAWP. Models with 1, 3, 6 and 7 additional surveys did not converge. The p-values for 8 and more surveys are so low that they cannot be visualised on this scale.

Simulation “power” analysis

Simulations based on the relationships modelled using GAMM reported above were refitted and simulated on the existing post-construction survey conditions using GLMM (excluding the response from LUD). The power of detecting a decline of 25-90% in LUD was assessed using 100 simulations (of which generally 70-80% converged, Table 7, Table 8). A high power (>80%) was achieved when 75% of both presence and density of Northern Gannets was reduced within windfarm + 4 km buffer (Table 7). When birds were displaced in the same manner only from within the windfarm, a 90% displacement was required to achieve a reasonable power, >80% (Table 8). To further assess whether 8 surveys would be sufficient for detecting a 25% and a 50% reduction with a high power, we used the 3 pre-construction survey and 1 construction survey as fictional post-construction surveys and thus simulated 100 times 8 fictional post-construction surveys with a 25%/50% displacement within the LUD windfarm. The results indicated that the power of detecting a 25% displacement following 8 post-construction surveys was rather low (Table 9). The power clearly increased for detection of a 50% displacement but was still relatively low (Table 9). However, since the Gannets can be assumed to be displaced from a larger area than only the windfarm, the power might to some degree be underestimated.

Table 7. The power of a presence/absence (PA) model part and positive density model part (POS, conditional on PA) including four post-construction surveys, with an artificial displacement of 25%, 50% and 75% from within the windfarm + 4 km buffer. Power larger than 80% is indicated with green.

Displacement from WF + 4 km	PA	POS	N sim.
25%	0.2338	0.1558	77
50%	0.704	0.676	71
75%	1.000	0.973	75
90%	-	-	-

Table 8. The power of a presence/absence (PA) model part and positive density model part (POS, conditional on PA) including four post-construction surveys, with an artificial displacement of 50%, 75% and 90% from within the windfarm perimeter. Power larger than 80% is indicated with green.

Displacement from WF	PA	POS	N sim.
25%	-	-	-
50%	0.080	0.147	75
75%	0.284	0.198	81
90%	0.808	0.077	78

Table 9. The power of a presence/absence (PA) model part and positive density model part (POS, conditional on PA) including eight post-construction surveys, with an artificial displacement of 25%.

Displacement from WF	PA	POS	N sim.
25%	0.074	0.049	81
50%	0.321	0.205	78

5.3.4 Great Cormorant *Phalacrocorax carbo*

The LUD-T1 surveys corroborated the findings of the LUD baseline surveys that the distribution of Cormorants offshore is exclusively associated with PAWP and OWEZ, and now also with LUD (Figure 19).

Model results

The modelling results stressed the importance of PAWP, OWEZ and LUD for the presence of Cormorants, and the effect of distance to all three windfarms was highly significant. The large degree of variation seen in the overall abundance of recorded Cormorants during the 24 surveys is displayed in Figure 20. The predicted patterns of change in density between pre-(LUD) and post-(LUD)-construction periods further underlined the attraction effect of the windfarms on the Cormorants (Figure 21). The explanatory degree of the distribution model for the Great Cormorant was poor for both the presence-absence and the density model parts (Appendix A). However, according to the AUC statistics the model is good at distinguishing between presence and absence, which is due to the clear preference to the windfarm areas and coastal zone (Appendix A).

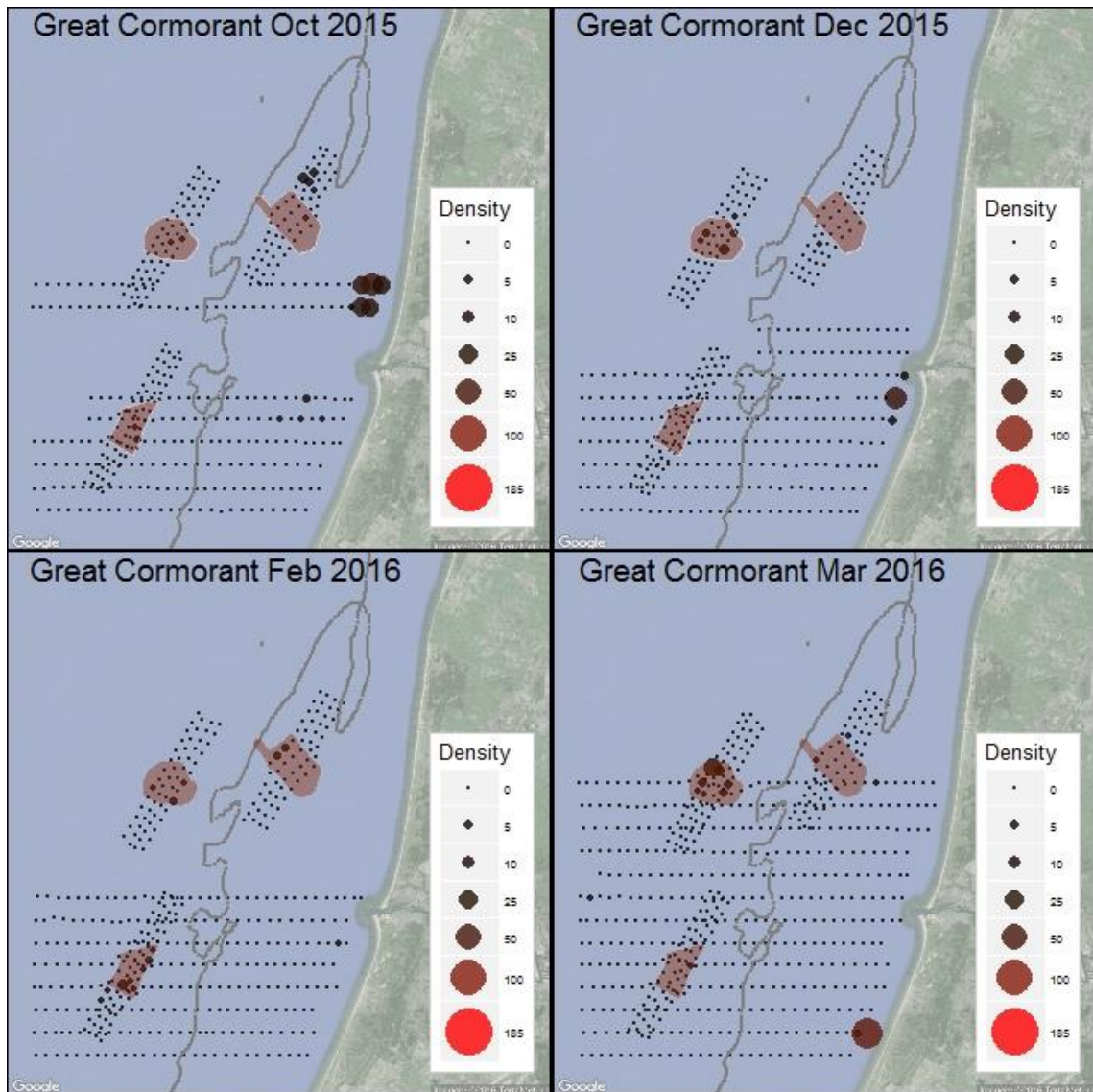


Figure 19. Observed density (birds/km²) of Great Cormorant during LUD T-1 surveys 2015-2016. Densities have been corrected for distance bias.

Great Cormorant, 2002-2016

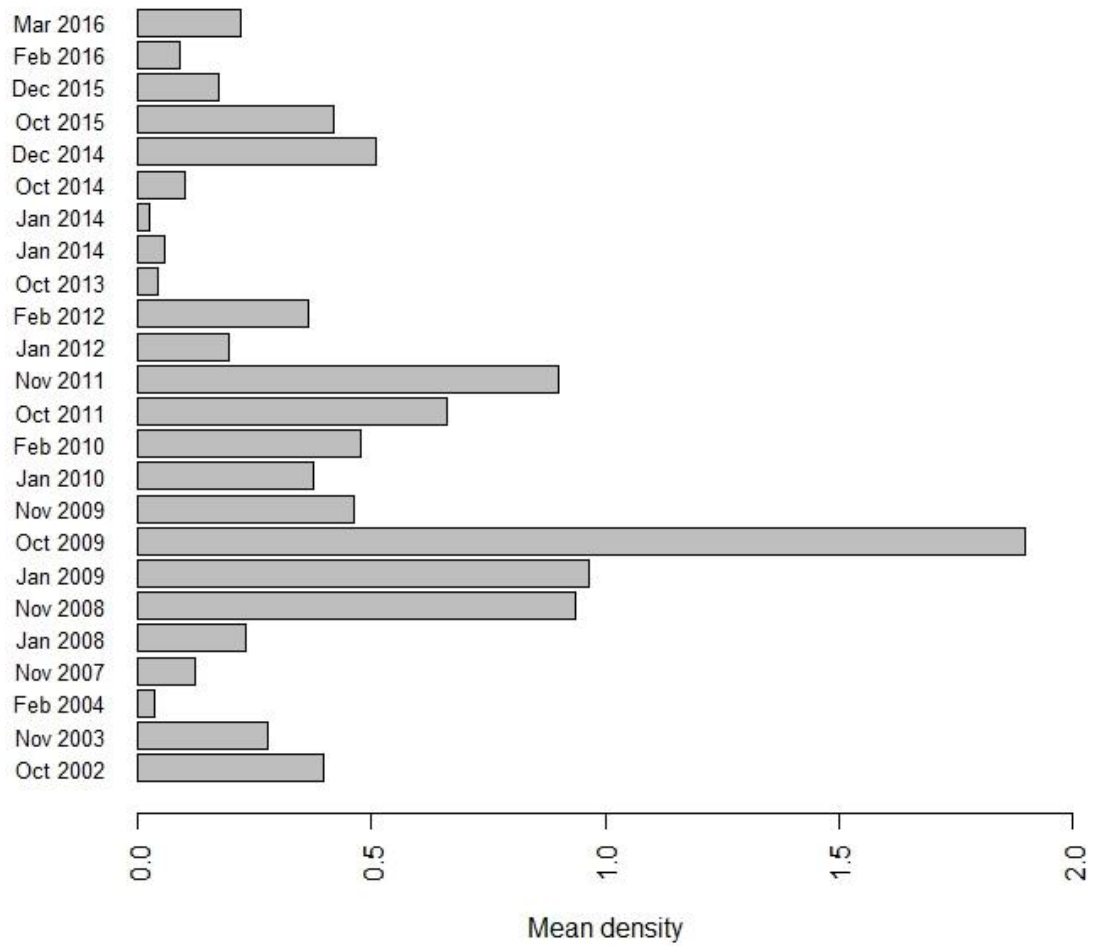


Figure 20. Mean observed density (birds/km²) of Great Cormorant during LUD pre- and post-construction surveys. Densities have been corrected for distance bias.

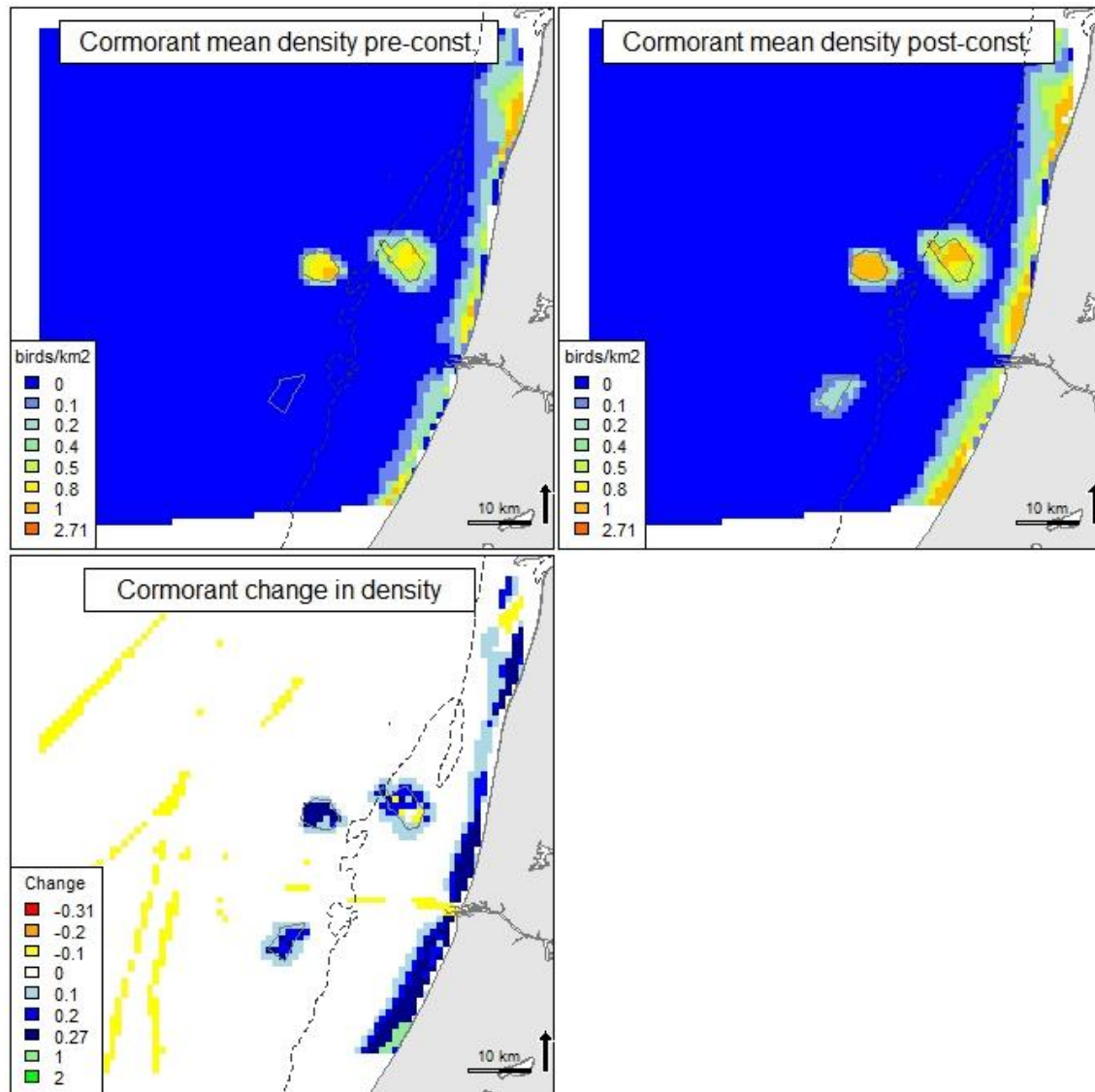


Figure 21. Predicted mean density (birds/km²) and distribution of wintering Great Cormorant during four LUD pre- and four LUD post-construction surveys, and the relative change in predicted density between the two periods. Note that all included surveys are OWEZ and PAWP post-construction surveys.

5.3.5 Little Gull *Hydrocoloeus minutus*

During the three first LUD-T1 surveys scattered observations of Little Gull were made over the surveyed area. During the March 2016 survey, an apparent influx (spring migration?) of birds was recorded in the southern part of the area (Figure 22, Figure 23). Few birds were seen in PAWP but not in the other two windfarms during the four surveys.

Model results

Survey 8 (October 2009) was dropped from the analysis as there were no Little Gulls observed during that survey. The presence-absence model part indicates a significant displacement from LUD ($p < 0.01$) and from PAWP ($p < 0.05$). Other variables retained in the “best” model were water depth (indicating optimal water depth at around 20 m), decreasing salinity and increasing current speed and current gradient. Only salinity was significant, however (Appendix A). The positive model was poor, indicating that the model could not describe differences in density. Overall, the model was poor in terms of predictive ability and explanatory degree. However, still useful for defining a significant effect from LUD (visualised in Figure

24) and PAWP, although the uncertainty is large due to low sample sizes and poor general ability to describe the distribution patterns.

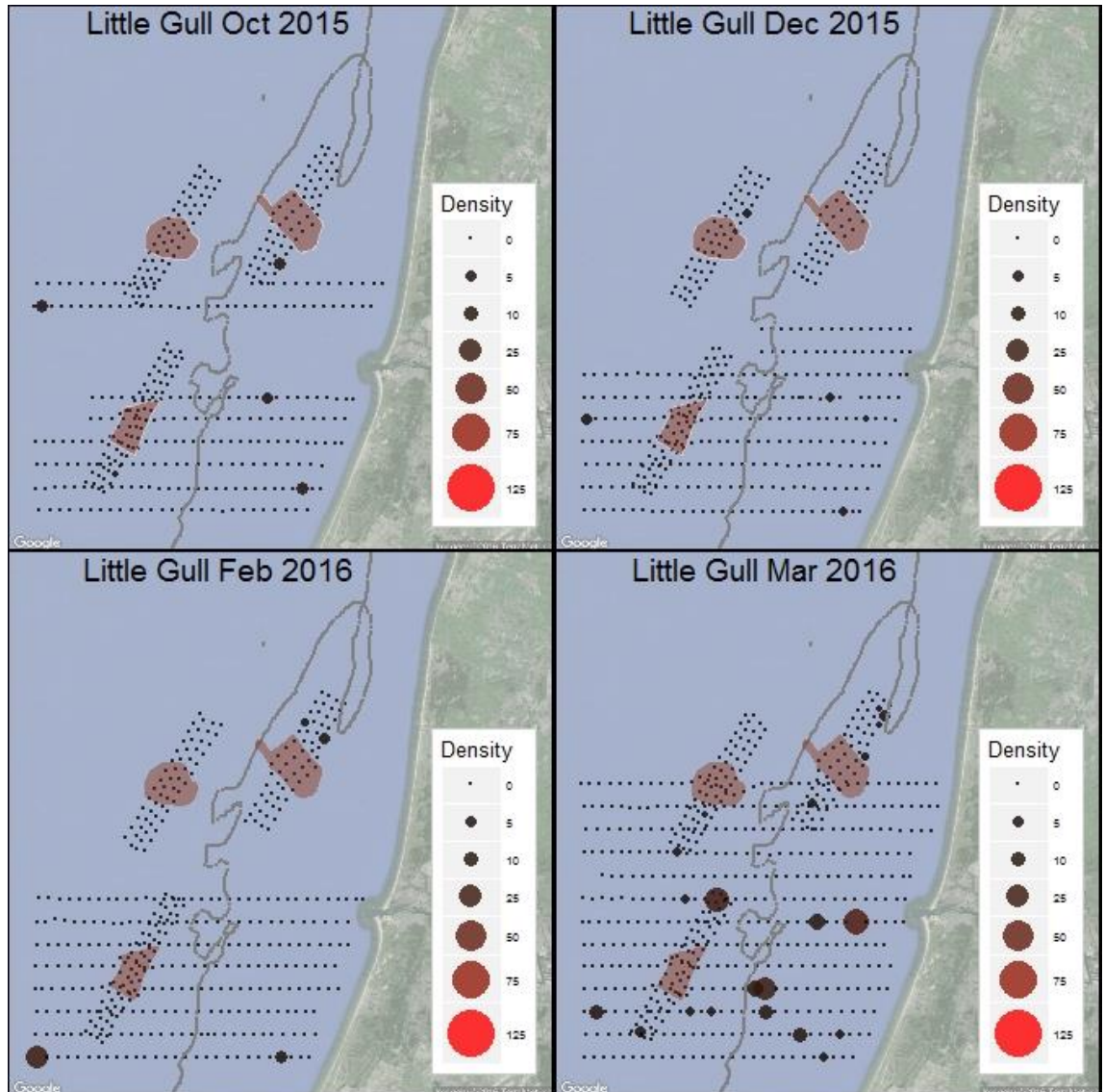


Figure 22. Observed density (birds/km²) of Little Gull during LUD T-1 surveys 2015-2016. Densities have been corrected for distance bias.

Little Gull, 2002-2016

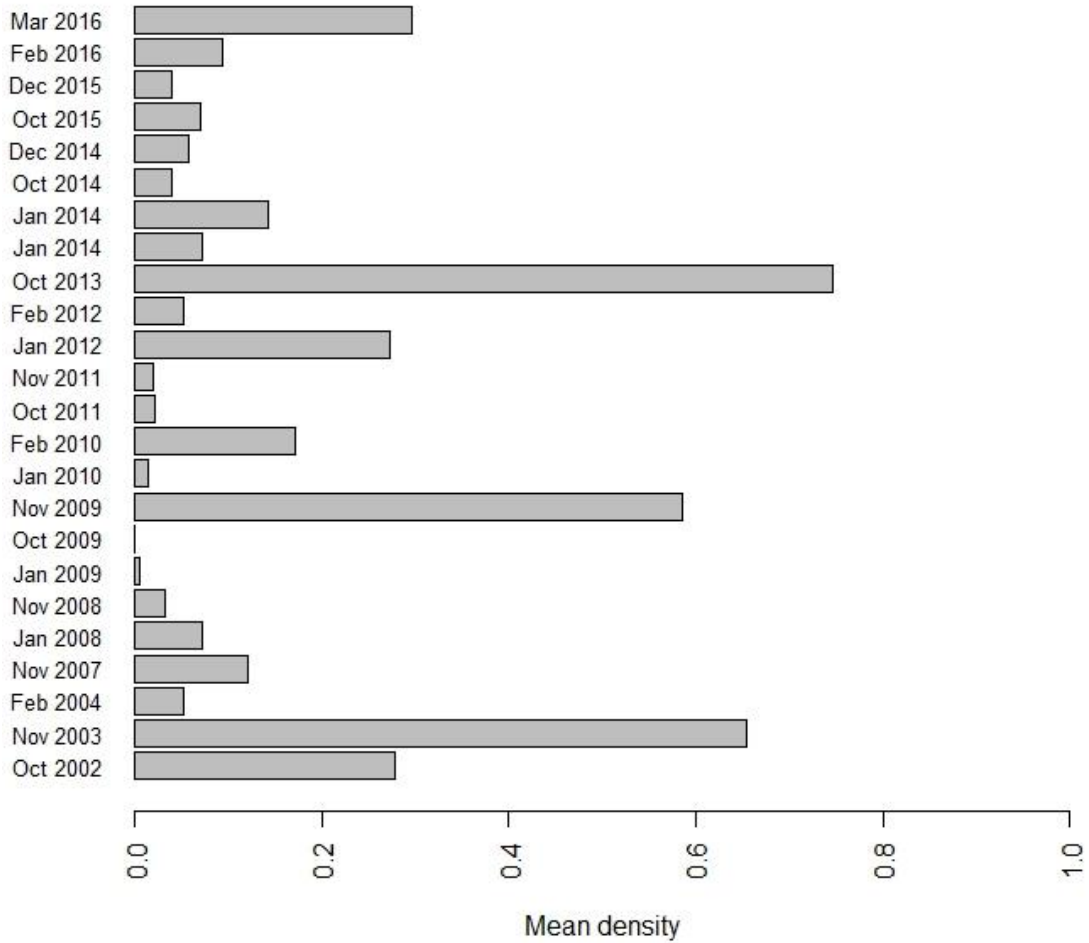


Figure 23. Mean observed density (birds/km²) of Little Gull during LUD pre- and post-construction surveys. Densities have been corrected for distance bias.

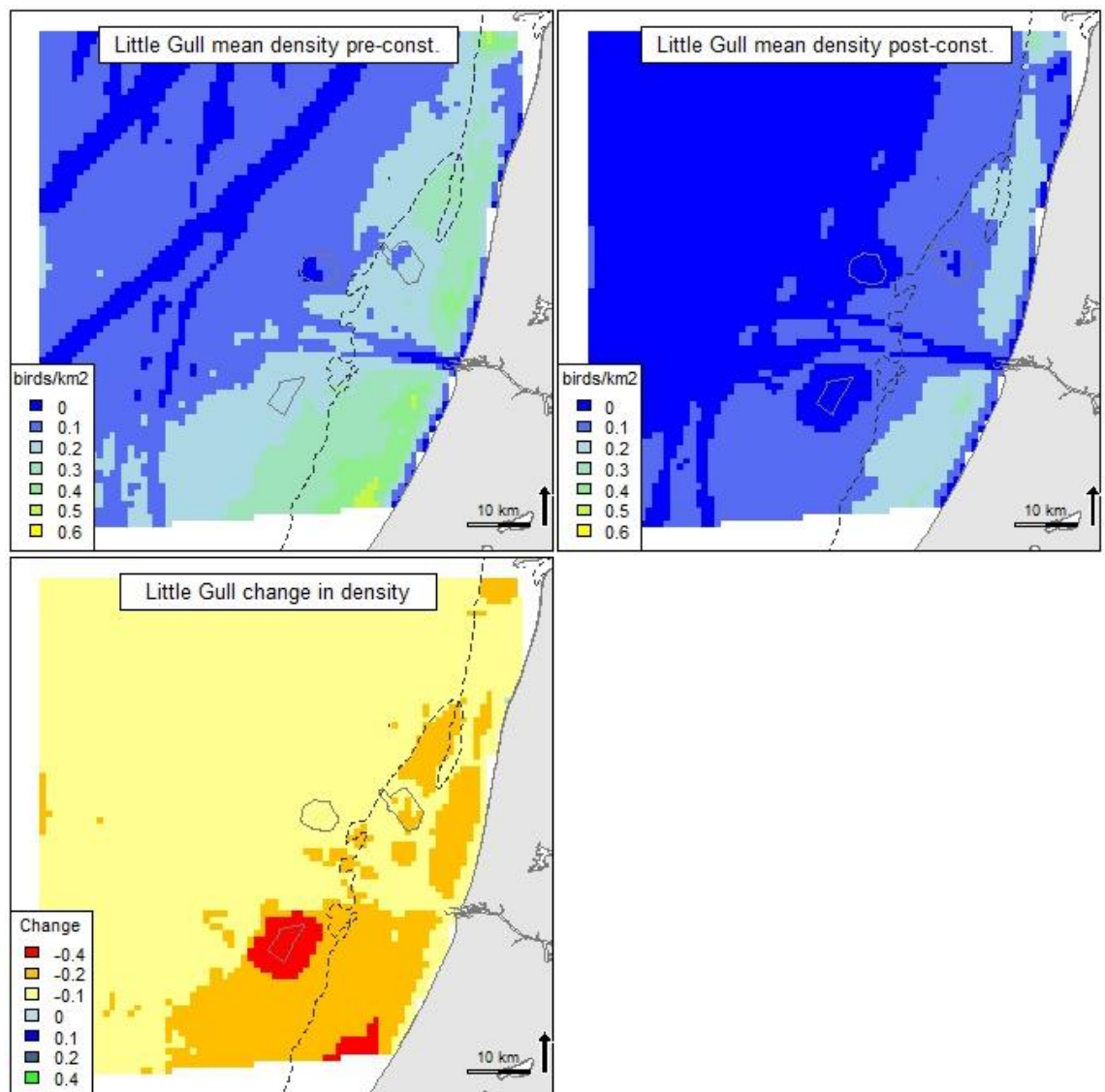


Figure 24. Predicted mean density (birds/km²) and distribution of wintering Little Gull during four LUD pre- and four LUD post-construction surveys, and the relative change in predicted density between the two periods. Note that all included surveys are OWEZ and PAWP post-construction surveys.

5.3.6 Black-headed Gull *Chroicocephalus ridibundus*

During the LUD-T1 surveys most Black-headed Gulls were recorded in the coastal waters, however with few observations of lower densities offshore (Figure 25, Figure 26). Single birds were recorded in PAWP and OWEZ, yet none in LUD.

Model results

The model indicated no significant effect of the windfarms on Black-headed Gull. Only water depth was significant in the presence-absence model part, indicating that the Black-headed Gulls prefer shallow (coastal) waters (Appendix A). This is also illustrated when the model predictions are mapped (Figure 27). The positive model part indicated that the model was not capable of predicting the varying densities in the study area in space and time. Nevertheless, the model was useful for assessing the effect of distance to the windfarms.

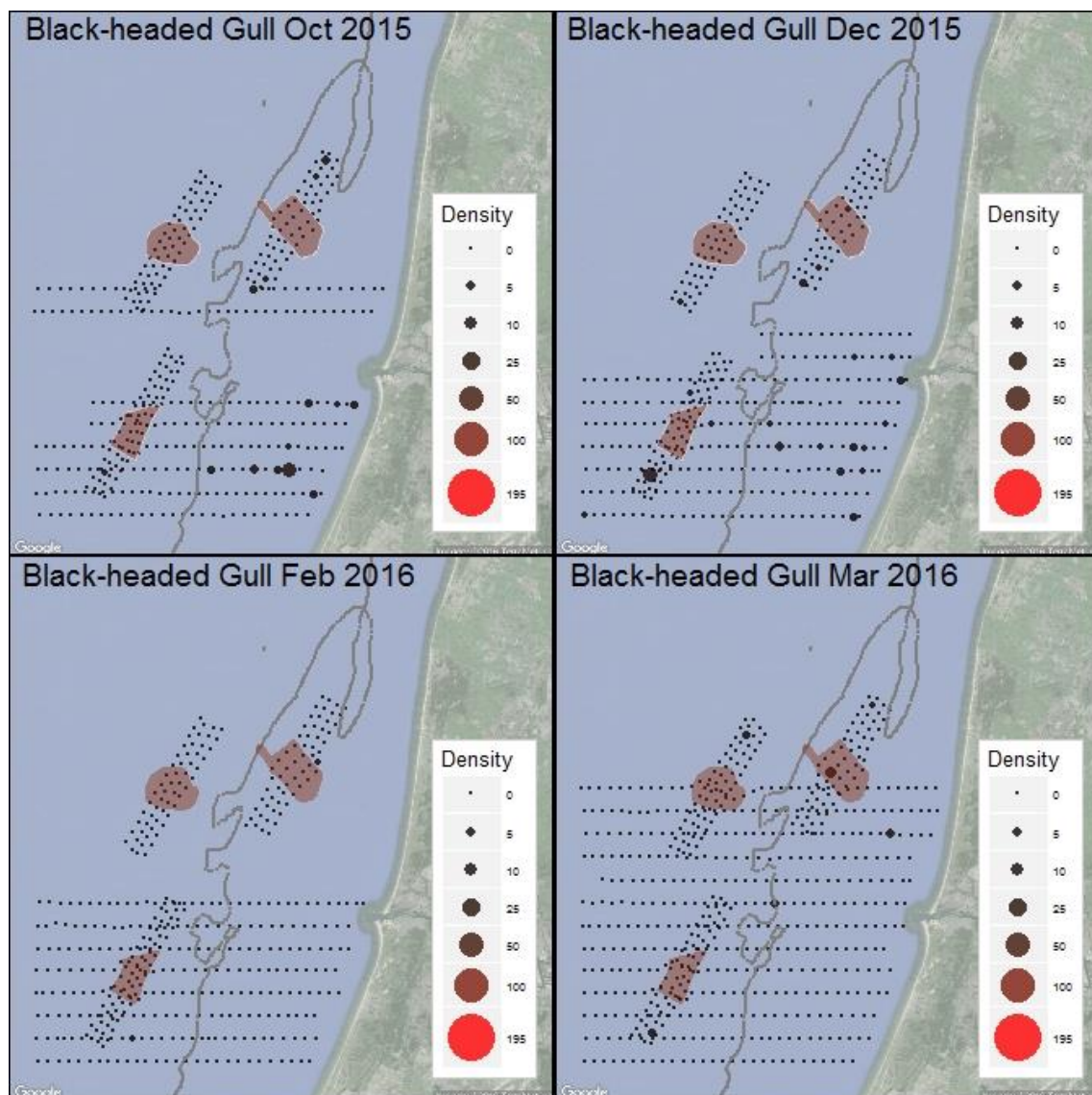


Figure 25. Observed density (birds/km²) of Black-headed Gull during LUD T-1 surveys 2015-2016. Densities have been corrected for distance bias.

Black-headed Gull, 2002-2016

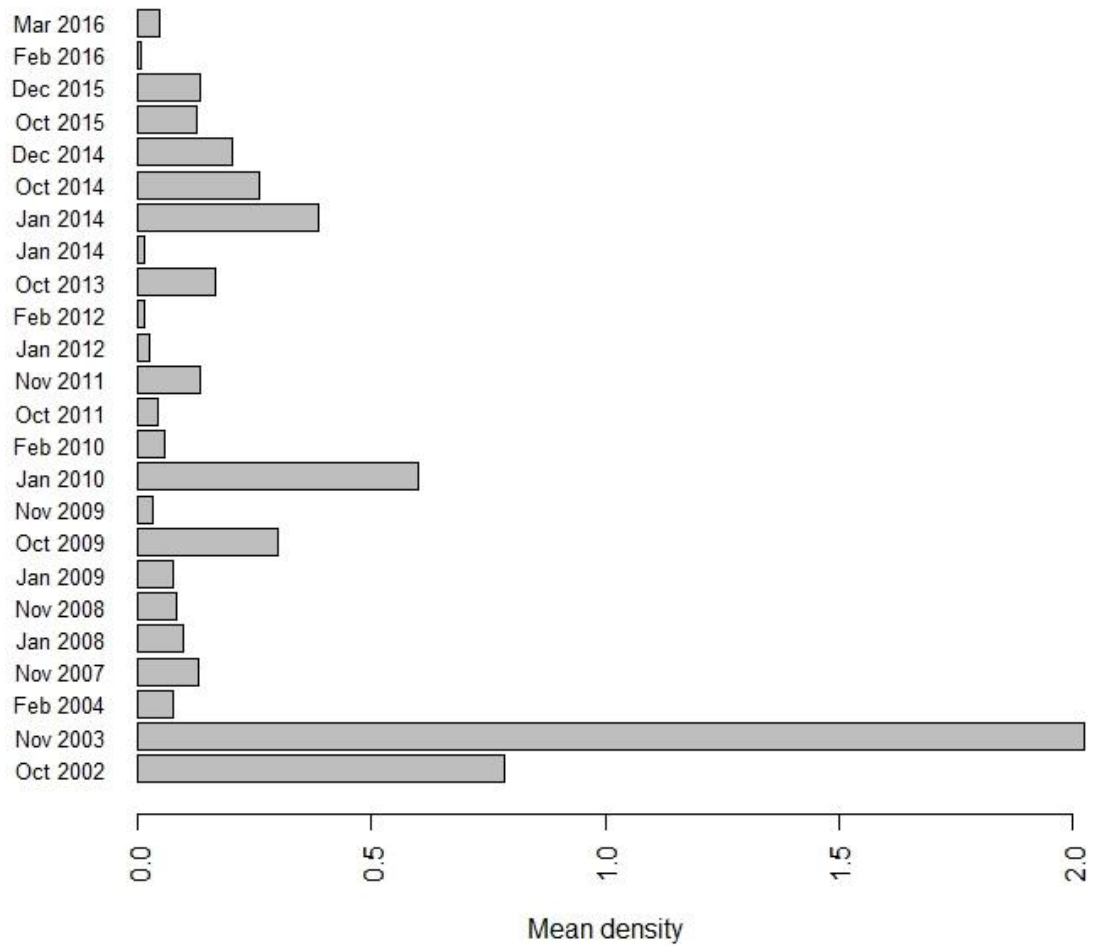


Figure 26. Mean observed density (birds/km²) of Black-headed Gull during LUD pre- and post-construction surveys. Densities have been corrected for distance bias.

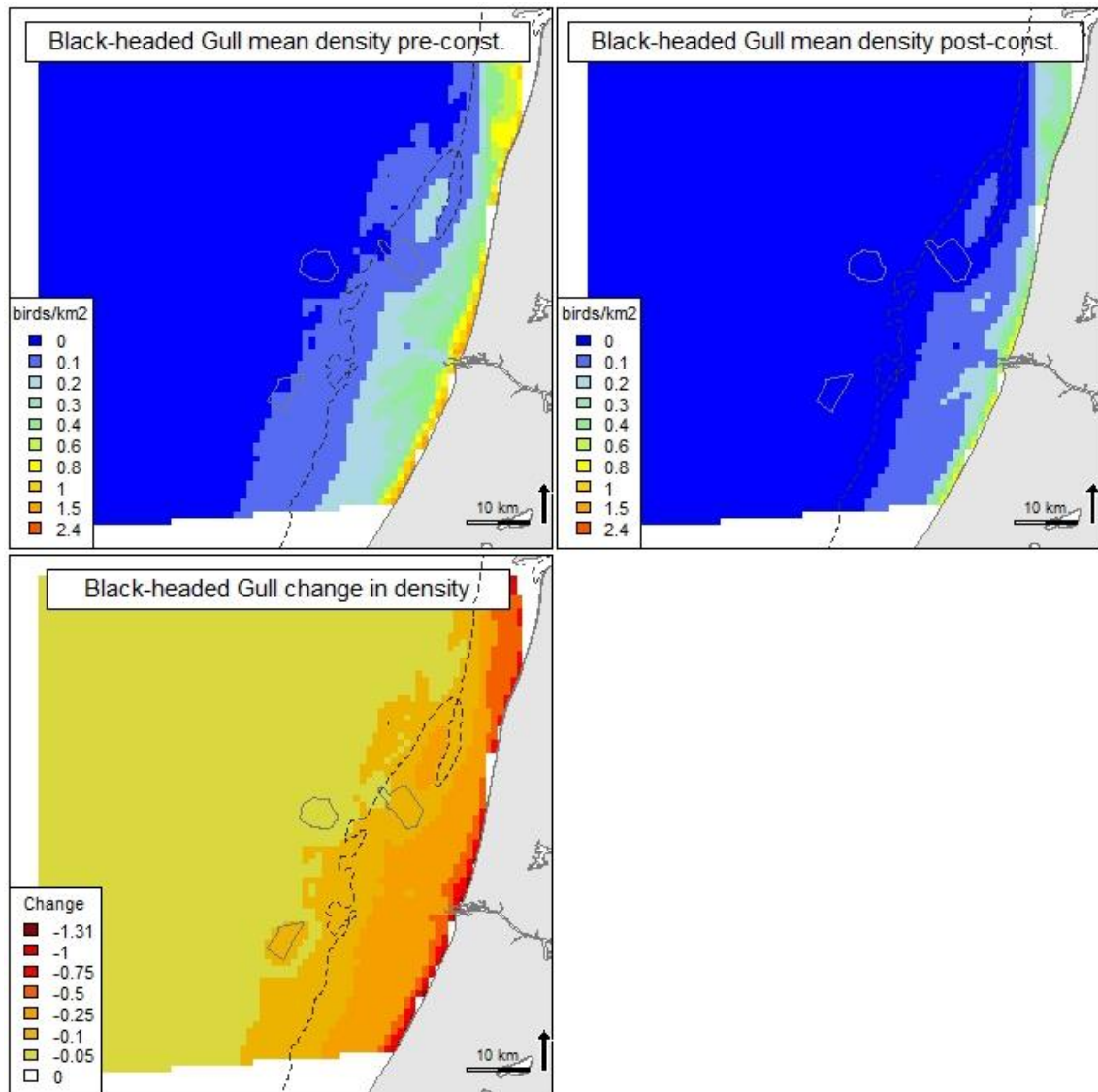


Figure 27. Predicted mean density (birds/km²) and distribution of wintering Black-headed Gull during four LUD pre- and four LUD post-construction surveys, and the relative change in predicted density between the two periods. Note that all included surveys are OWEZ and PAWP post-construction surveys.

5.3.7 Common Gull *Larus canus*

During the LUD-T1 surveys the distribution of Common Gulls was similar to the one found during the earlier surveys with densities being highest in mid winter and birds concentrated within the 20 m depth contour (Figure 28). Birds were seen both in OWEZ and PAWP, and in LUD a small aggregation was recorded during the December 2015 survey. The variability in the sampled mean density of Common Gulls between the 23 surveys included in the analyses is shown in Figure 29.

Model results

The model indicated that the probability of presence of Common Gulls is higher in shallow water, about two km from OWEZ and PAWP and with decreasing distance from LUD and low shipping intensity (Appendix A). The predicted patterns of mean densities showed higher densities in shallower waters, less than 20 m water depth (Figure 30). No obvious changes in modelled densities were identified at OWEZ and PAWP (both periods post-construction), yet slightly more birds were seen in LUD post-construction (Figure 30).

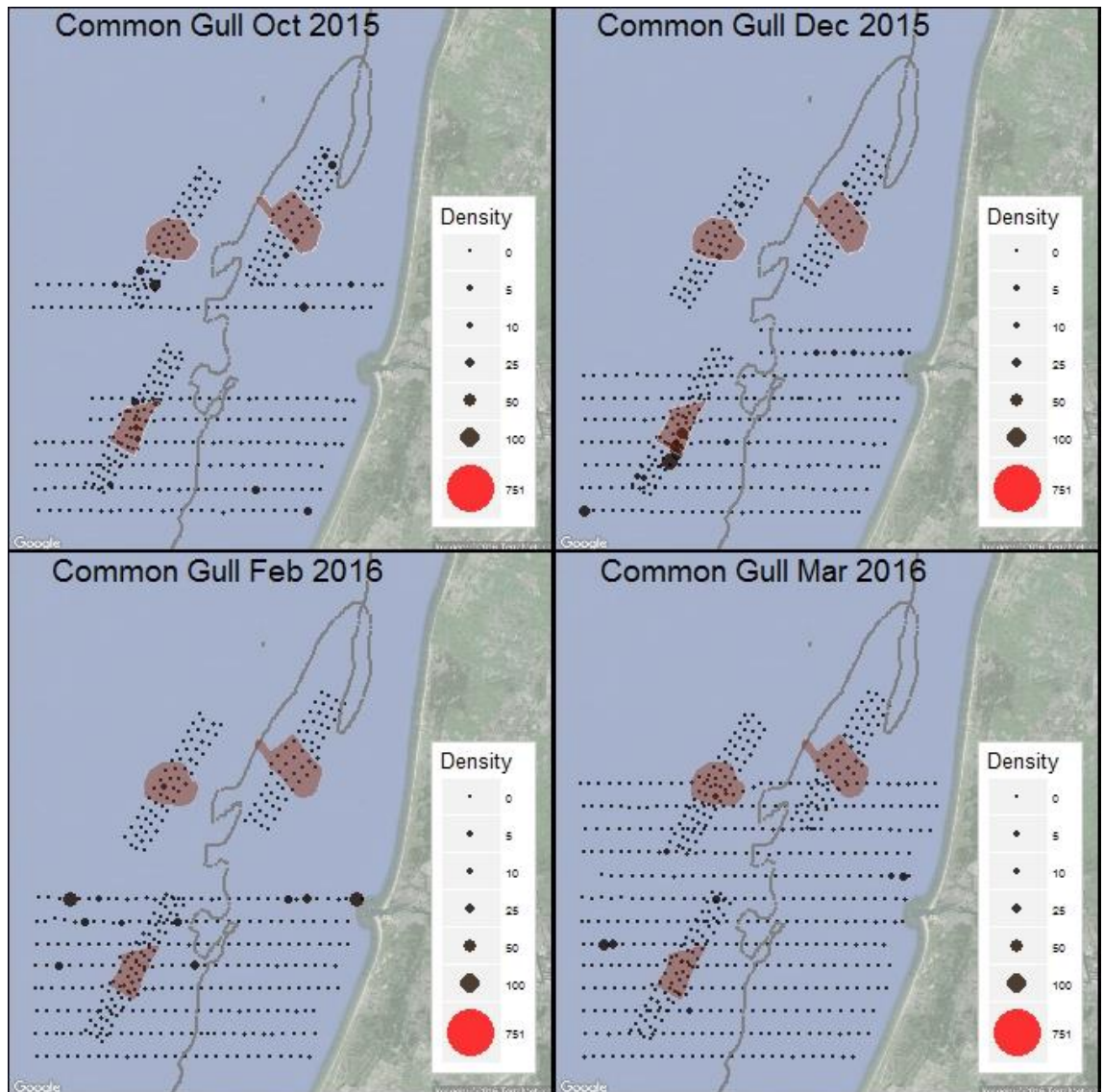


Figure 28. Observed density (birds/km²) of Common Gull during LUD T-1 surveys 2015-2016. Densities have been corrected for distance bias.

Common Gull, 2002-2016

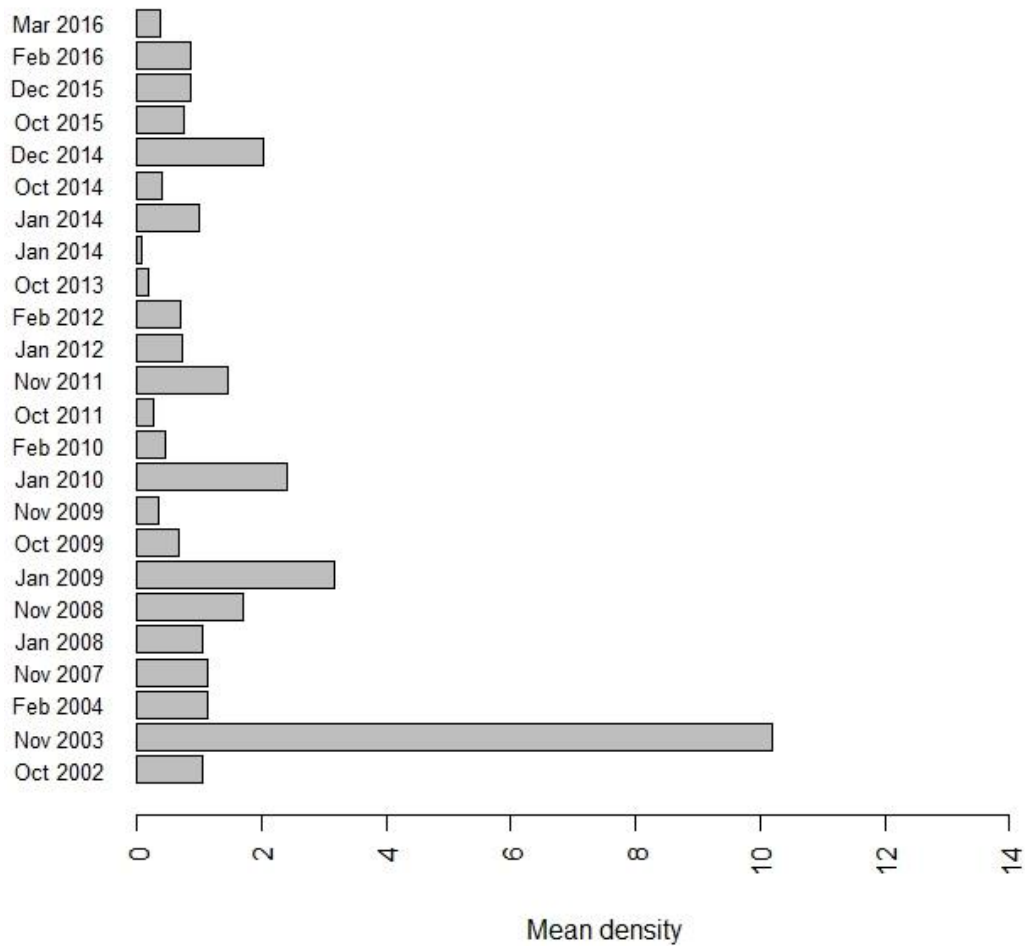


Figure 29. Mean observed density (birds/km²) of Common Gull during LUD pre- and post-construction surveys. Densities have been corrected for distance bias.

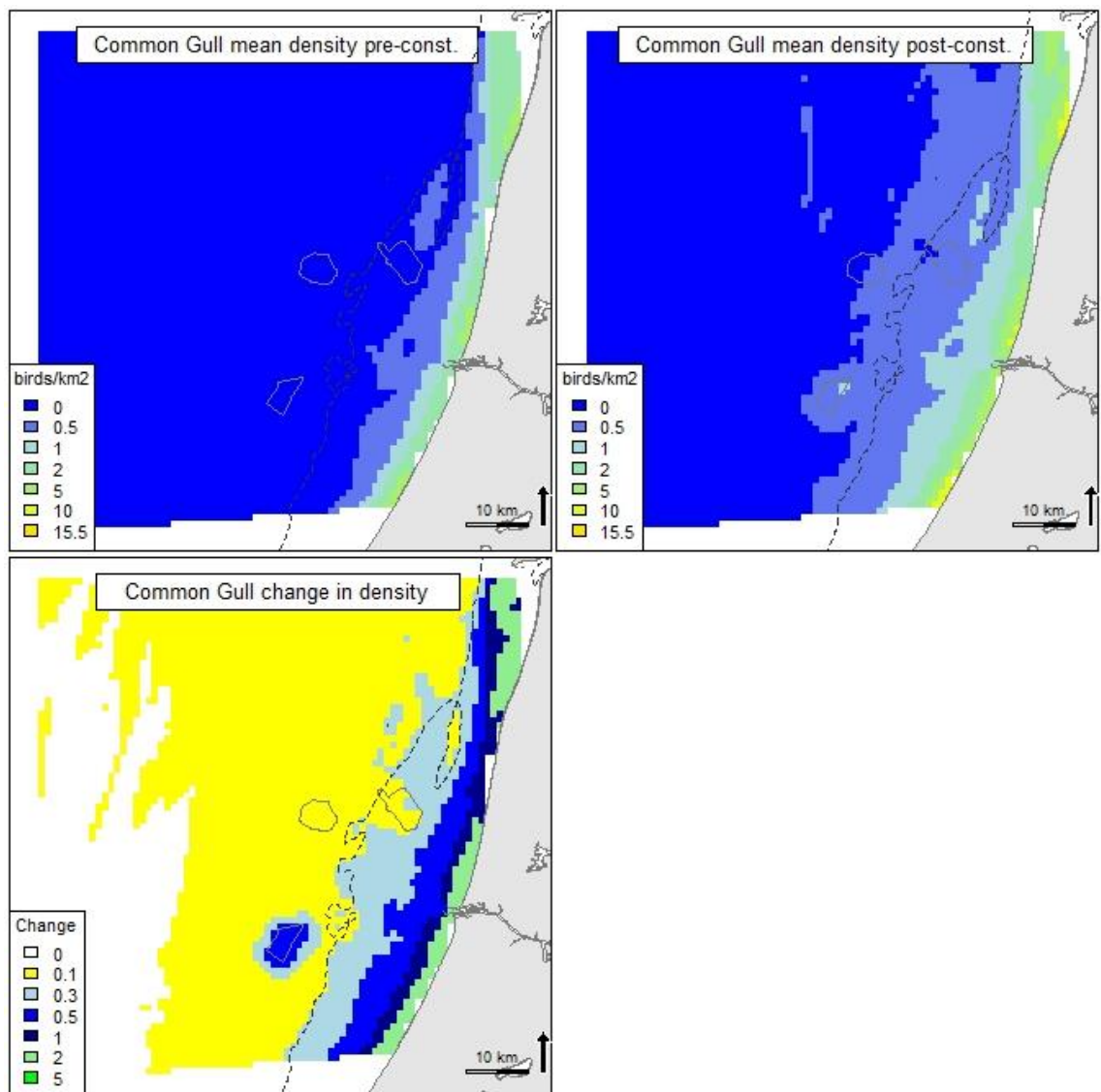


Figure 30. Predicted mean density (birds/km²) and distribution of wintering Common Gull during four LUD pre- and four LUD post-construction surveys, and the relative change in predicted density between the two periods. Note that all included surveys are OWEZ and PAWP post-construction surveys.

5.3.8 Lesser Black-backed Gull *Larus fuscus*

During the LUD-T1 surveys the distribution of Lesser Black-backed gulls appears to be “bi-modal” with birds either close to the coast or far offshore (Figure 31). Highest mean densities were observed in March and October, which could be influx of migrating birds (Figure 32).

Model results

According to the model the probability of presence increased with decreasing water depth and current speed and with increasing salinity. None of the windfarms had a significant displacement or attraction effect, OWEZ was “closest” with a p-value of 0.09 and a displacement effect. Only water depth was significant in the positive model part, indicating higher densities both in shallow and in deeper waters, in accordance with the mapped observations (Figure 33, Appendix A), which is also apparent from the mapped predictions in Figure 33. Overall the model was poor for describing the general distribution in the whole study area, particularly the positive part, however, useful for assessing the impact of the windfarms.

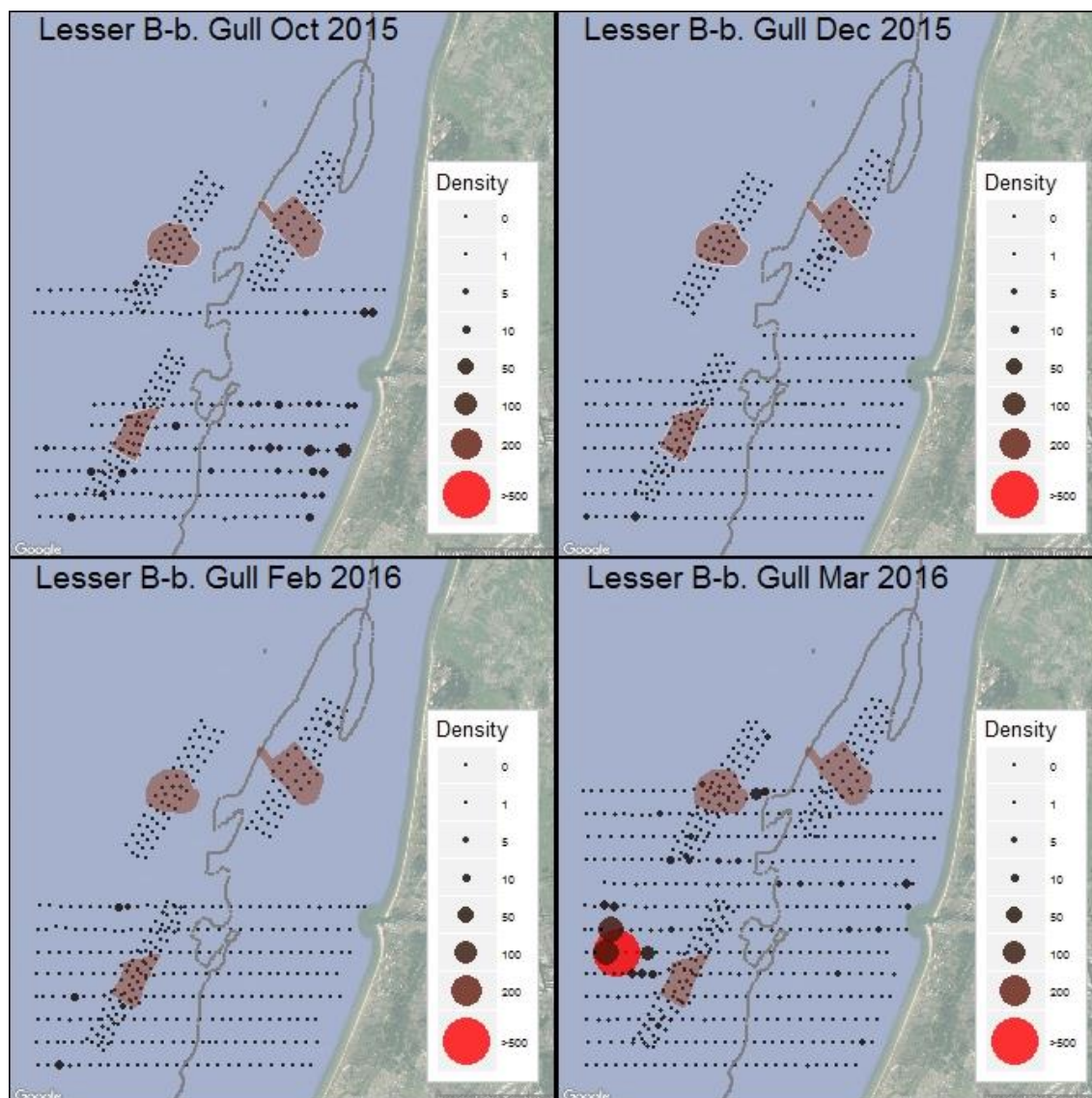


Figure 31. Observed density (birds/km²) of Lesser Black-backed Gull during LUD T-1 surveys 2015-2016. Densities have been corrected for distance bias.

Lesser Black-backed Gull, 2002-2016

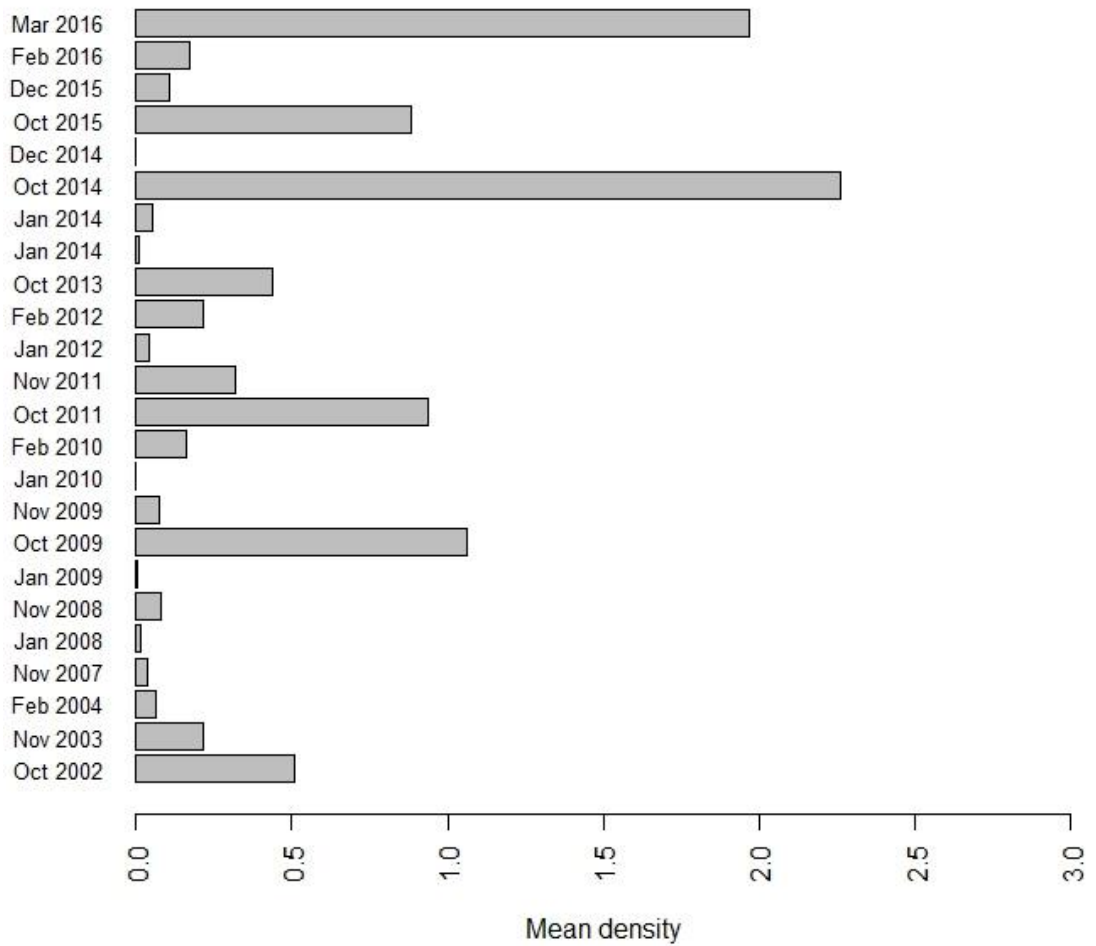


Figure 32. Mean observed density (birds/km²) of Lesser Black-backed Gull during LUD pre- and post-construction surveys. Densities have been corrected for distance bias.

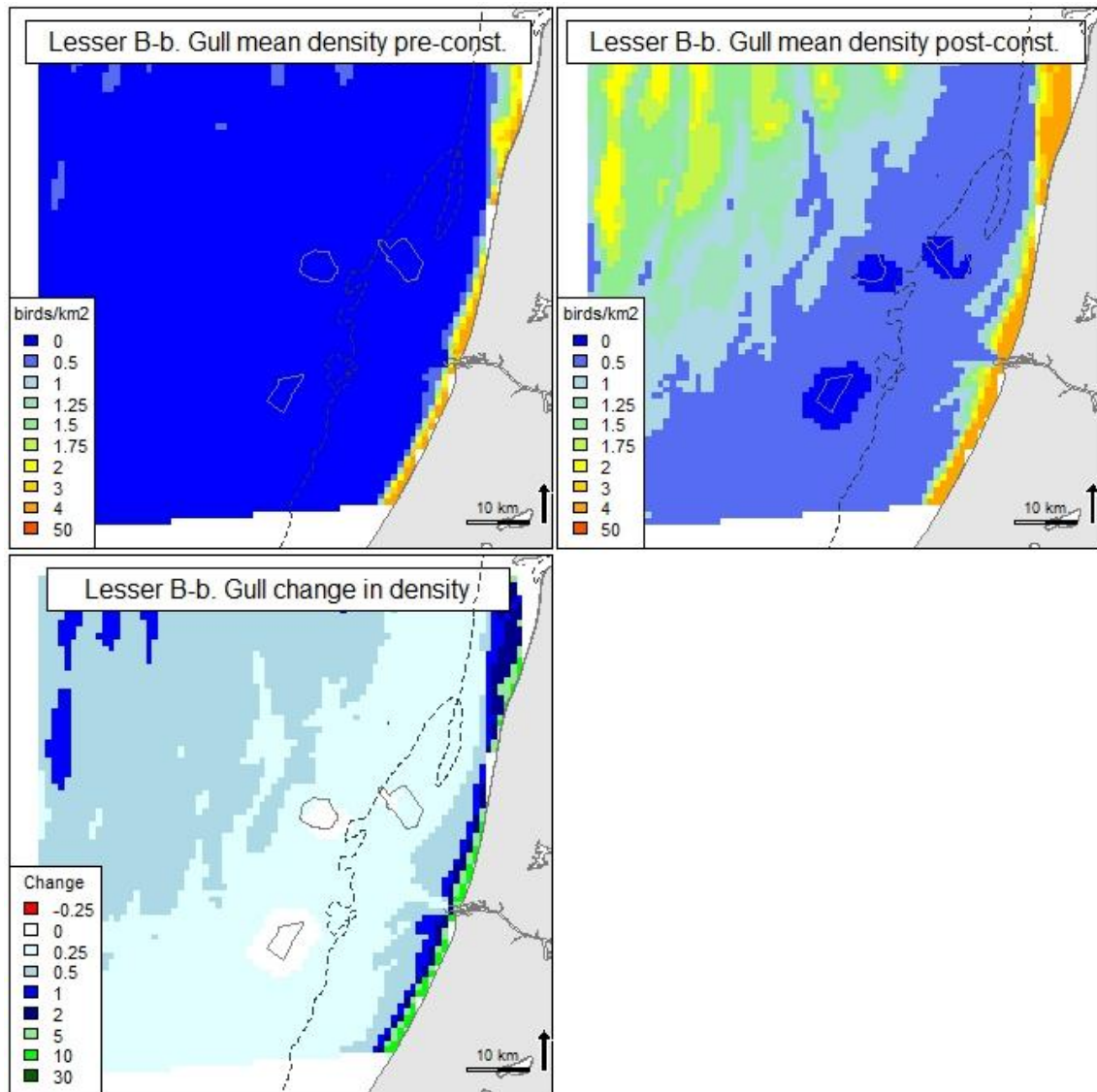


Figure 33. Predicted mean density (birds/km²) and distribution of wintering Lesser Black-backed Gull during four LUD pre- and four LUD post-construction surveys, and the relative change in predicted density between the two periods. Note that all included surveys are OWEZ and PAWP post-construction surveys.

5.3.9 Herring Gull *Larus argentatus*

During the LUD-T1 surveys quite low densities of Herring Gulls were observed without a clear spatial pattern (Figure 34, Figure 35). Highest mean density was observed during the survey in December 2015 (Figure 35).

Model results

According to the model the probability of presence increased within decreasing water depth and increasing current gradient, none of the windfarms had a significant displacement or attraction effect. The positive model part further indicated that higher densities are related to increasing salinity, decreasing current speed and intermediate current gradient. Overall the predictive ability was fair according to the evaluation statistics, with a rather low explanatory degree (Appendix A). The mapped predictions indicate that the coastal waters are preferred by the Herring Gull (Figure 36).

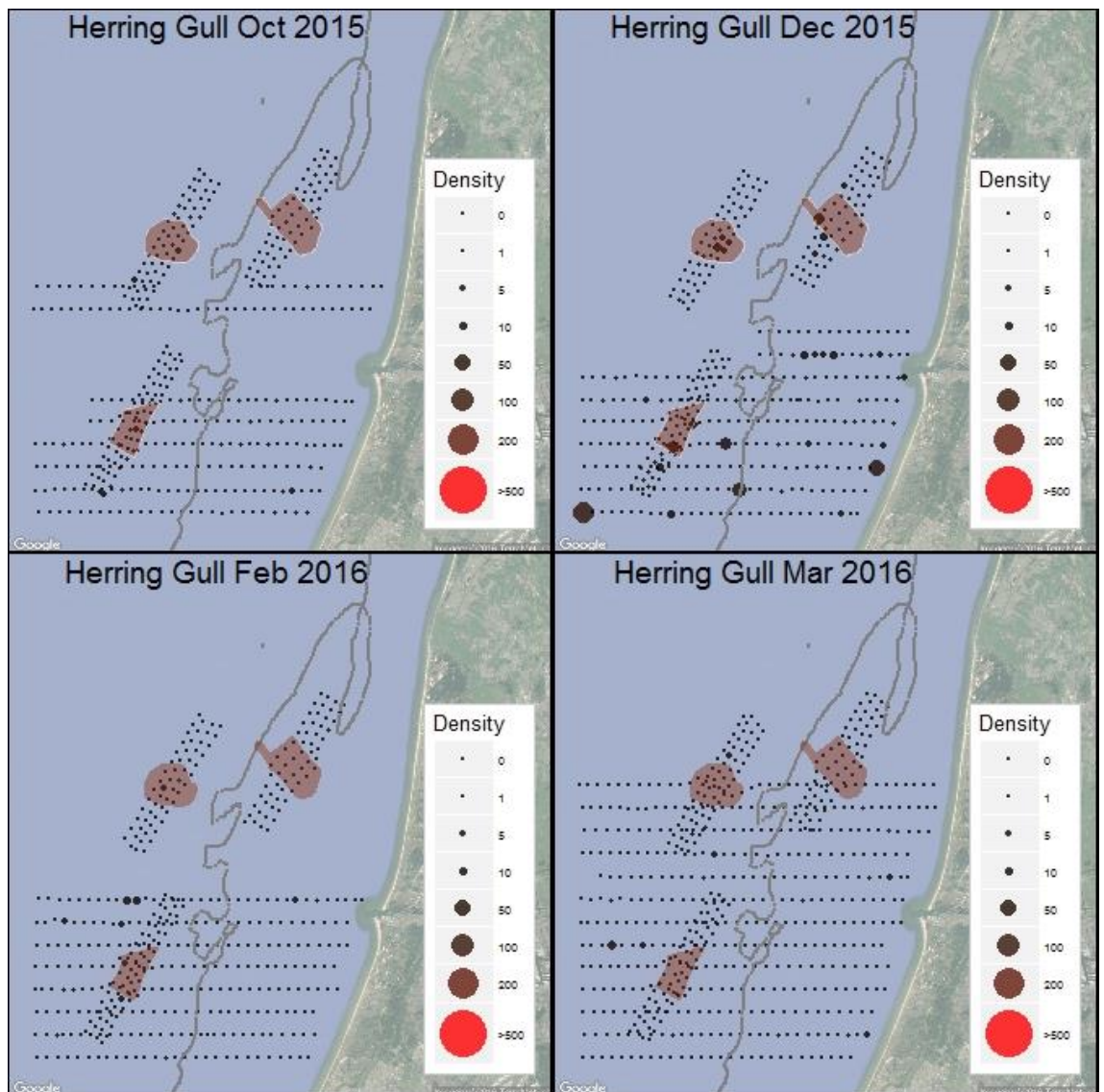


Figure 34. Observed density (birds/km²) of Herring Gull during LUD T-1 surveys 2015-2016. Densities have been corrected for distance bias.

Herring Gull, 2002-2016

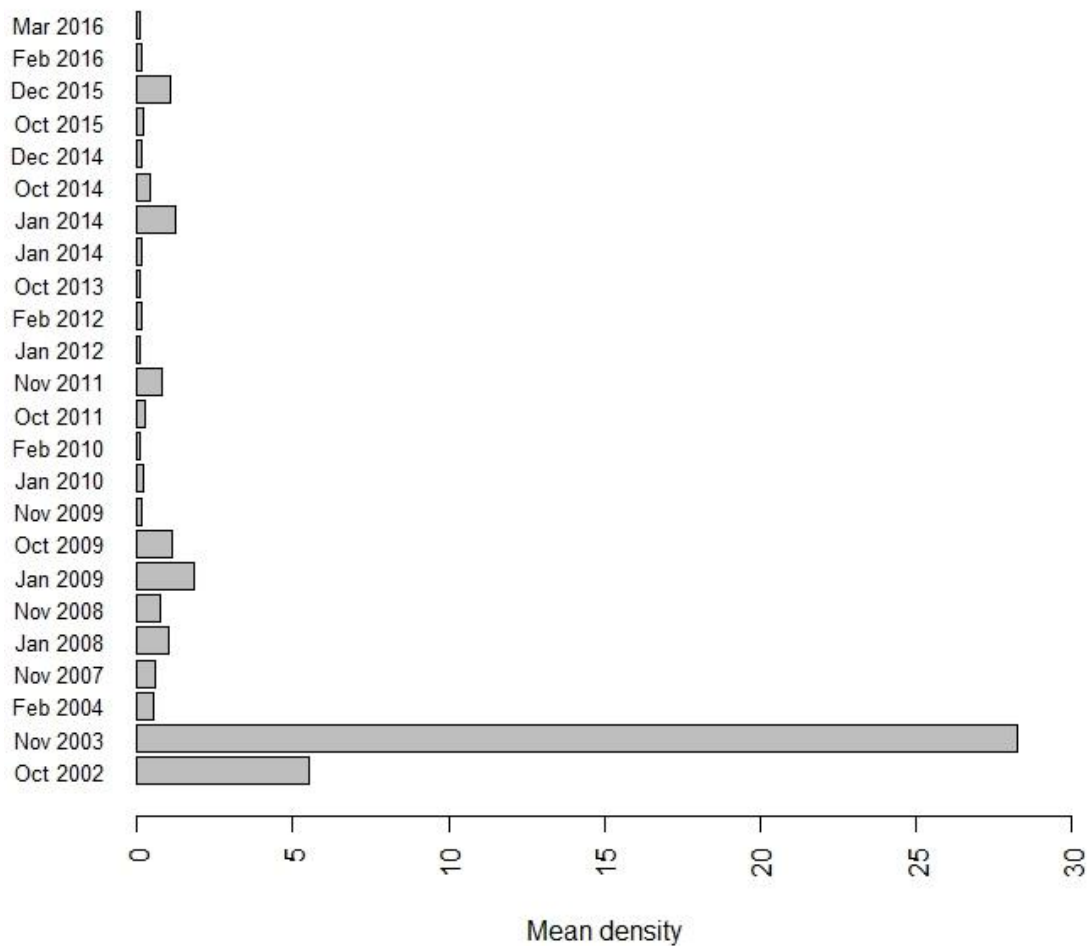


Figure 35. Mean observed density (birds/km²) of Herring Gull during LUD pre- and post-construction surveys. Densities have been corrected for distance bias.

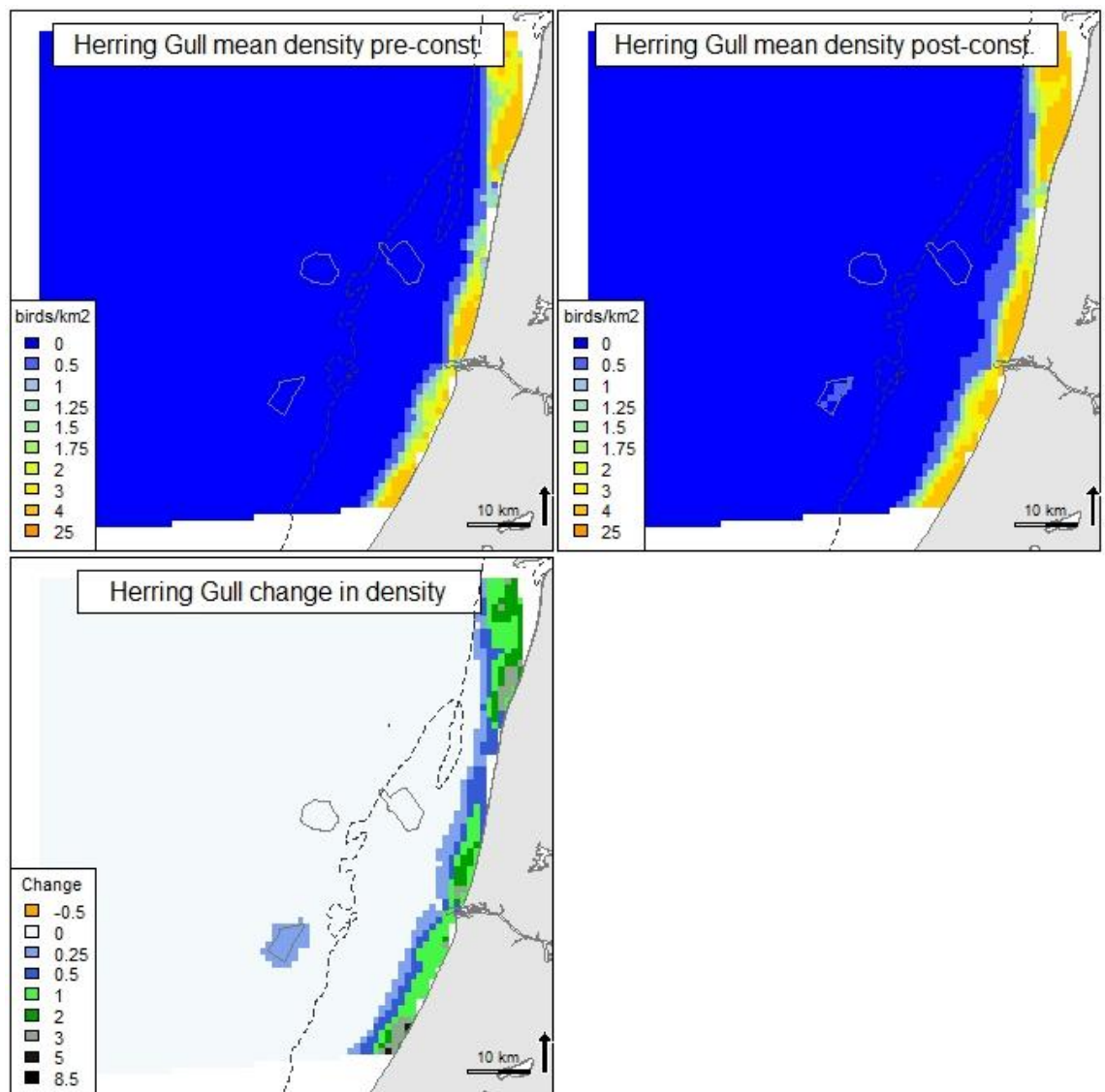


Figure 36. Predicted mean density (birds/km²) and distribution of wintering Herring Gull during four LUD pre- and four LUD post-construction surveys, and the relative change in predicted density between the two periods. Note that all included surveys are OWEZ and PAWP post-construction surveys.

5.3.10 Great Black-backed Gull *Larus marinus*

During the LUD-T1 surveys the highest mean density was observed in December 2015 (Figure 38). It is difficult to identify any clear distribution patterns but rather high densities were observed in the vicinity of LUD (Figure 37).

Model results

According to the presence-absence model the probability of presence increased with lower distance to the windfarm, indicating an attraction to both PAWP ($p < 0.01$) and OWEZ ($p < 0.05$). The probability of presence further increased with decreasing water depth and increasing salinity and current gradient. According to the positive model part higher densities were present at approximately 1.5 km from OWEZ ($p < 0.01$), which can be distinguished from the mapped model predictions in Figure 39. Water depth, salinity and current gradient were also influential in the positive model part. The predictive ability of the model was fair according to the evaluation statistics, the explanatory degree rather low (Appendix A).

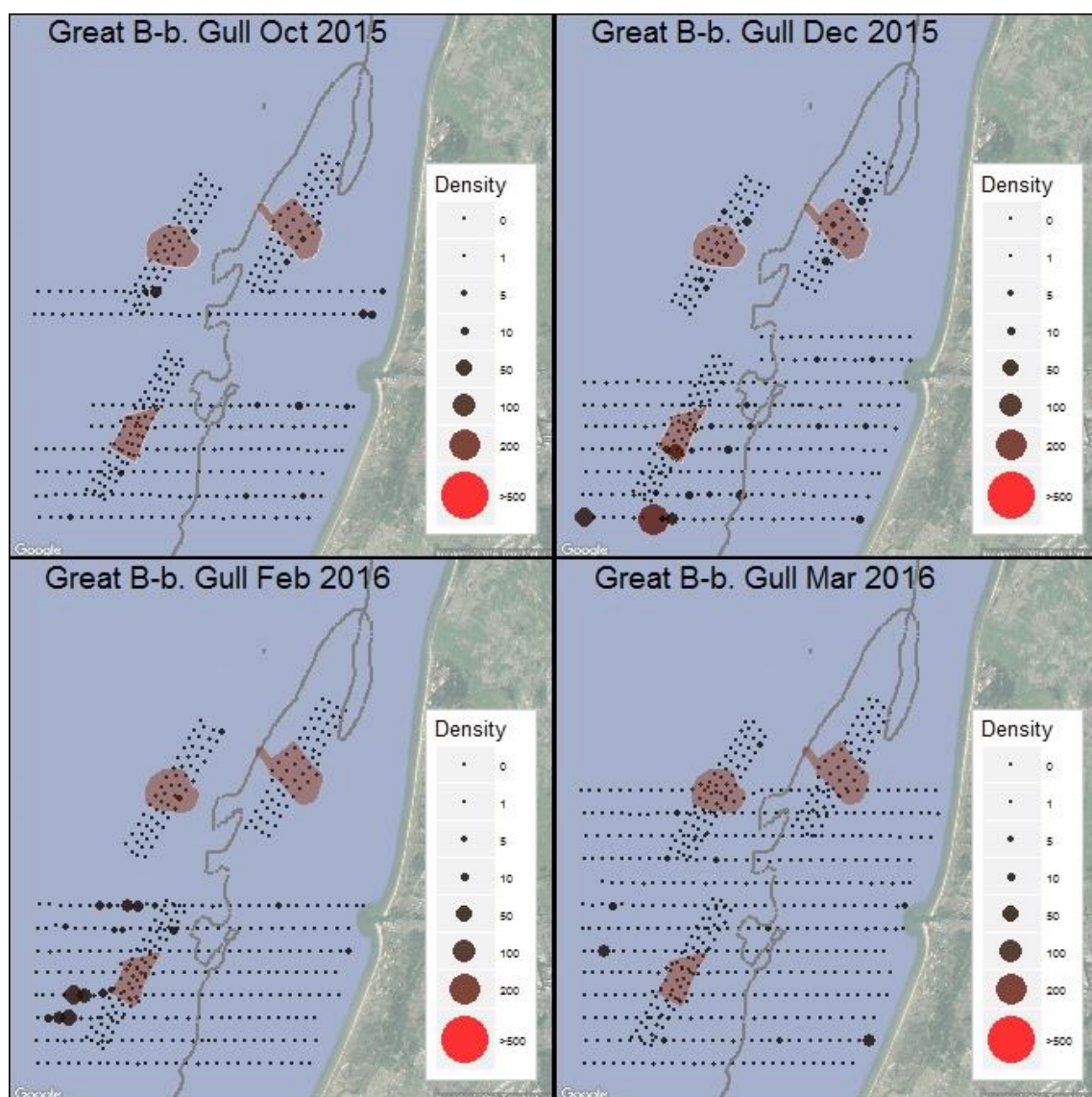


Figure 37. Observed density (birds/km²) of Great Black-backed Gull during LUD T-1 surveys 2015-2016. Densities have been corrected for distance bias.

Great Black-backed Gull, 2002-2016

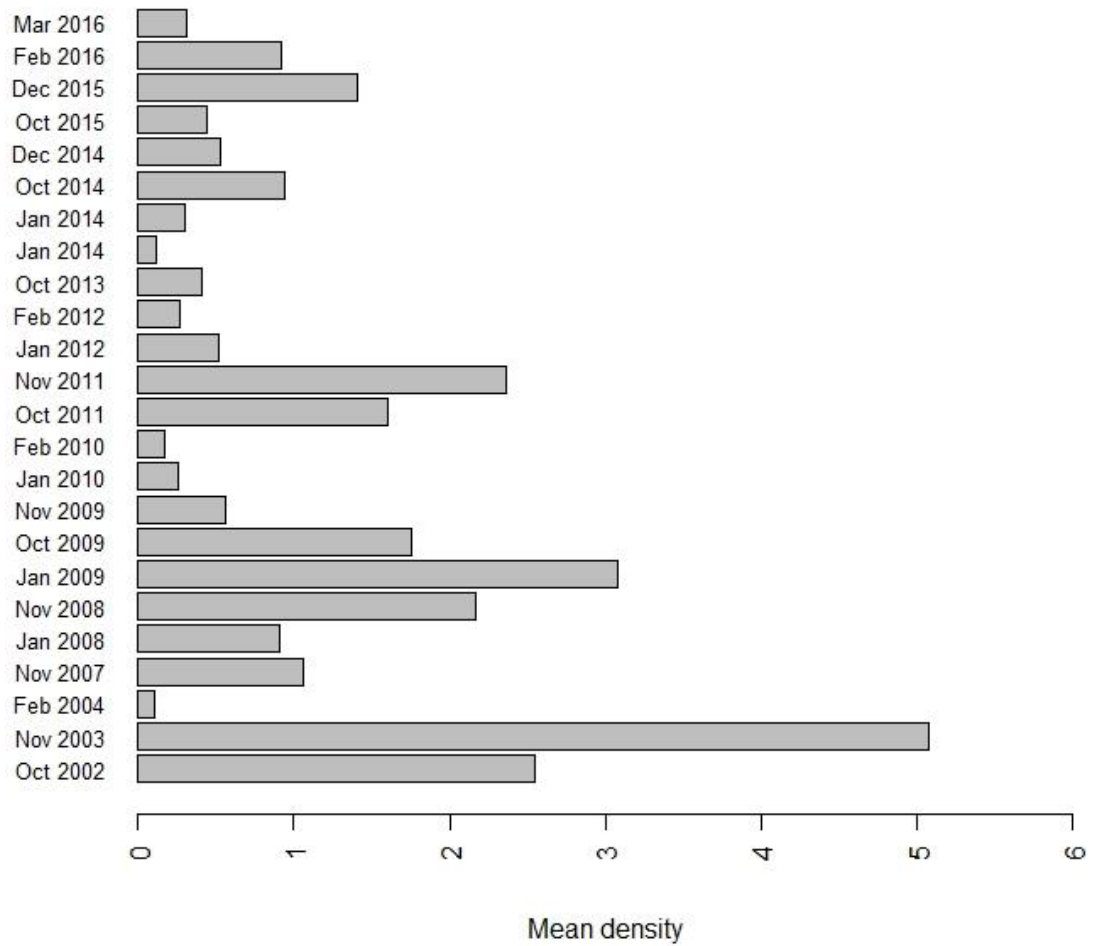


Figure 38. Mean observed density (birds/km²) of Great Black-backed Gull during LUD pre- and post-construction surveys. Densities have been corrected for distance bias.

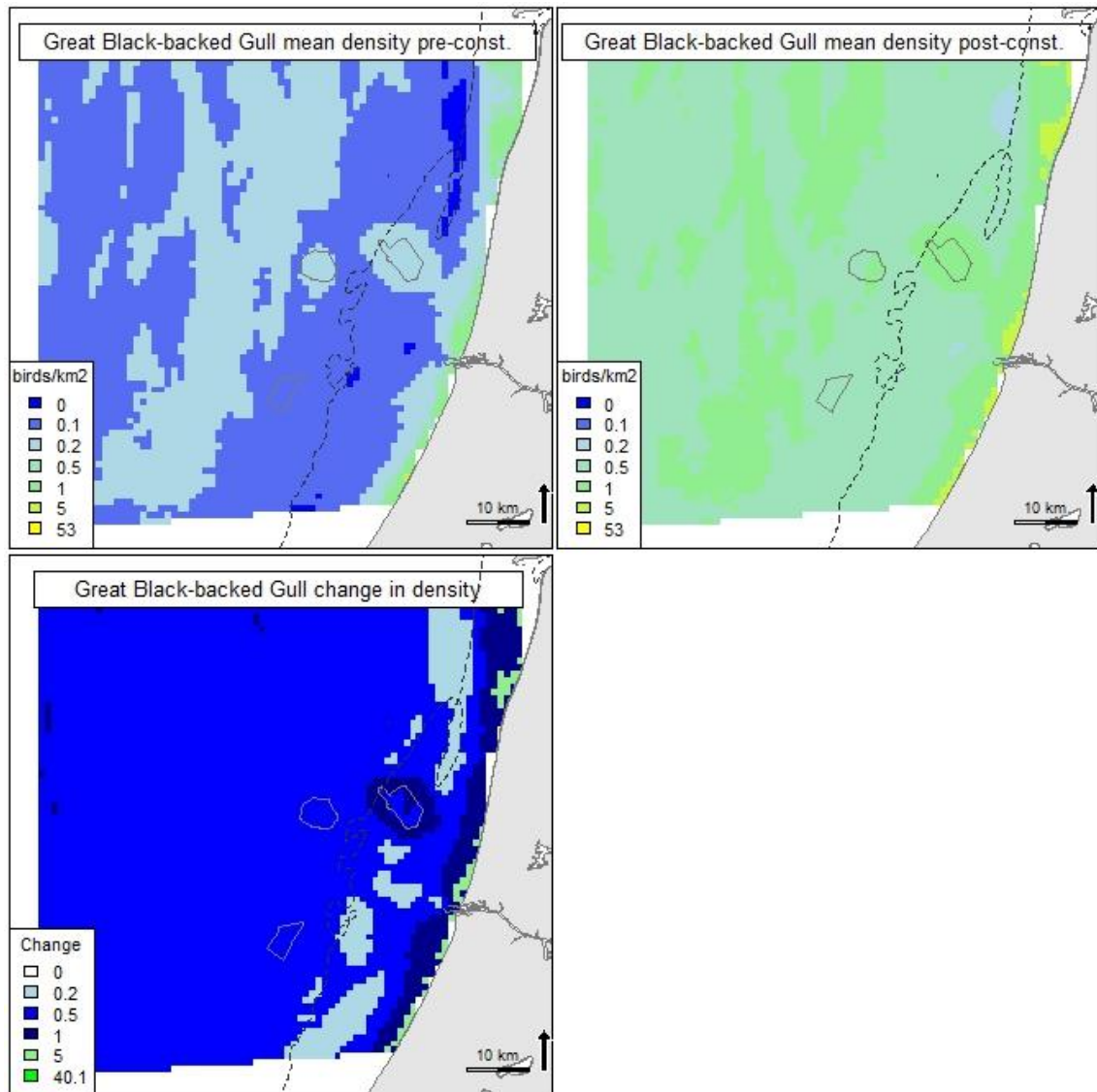


Figure 39. Predicted mean density (birds/km²) and distribution of wintering Great Black-backed Gull during four LUD pre- and four LUD post-construction surveys, and the relative change in predicted density between the two periods. Note that all included surveys are OWEZ and PAWP post-construction surveys.

5.3.11 Black-legged Kittiwake *Rissa tridactyla*

During the four LUD-T1 surveys in 2015-2016 the abundance of Black-legged Kittiwakes was low in three surveys, and very high in December 2015 (Figure 40, Figure 41). During this survey large numbers of Kittiwakes were seen relatively close to the windfarm and also some within all three windfarms. Lower densities were observed close to the coast. During the other surveys the Kittiwake was rather scarce and no clear distribution patterns could be distinguished (Figure 41). The variability of observed densities of Kittiwakes in the 24 surveys of which 19 were included in the distribution analyses is shown in Figure 41.

Model results

According to the model higher probability of presence was related to increasing eddy potential (vorticity). Other variables included, but not significant, were AIS (shipping intensity) as a parametric term (decreasing), water depth (deeper) and current speed (higher). None of the windfarms in the presence-absence model part had a significant effect on the Kittiwake distribution.

In the positive model, distance to LUD indicated that higher densities were recorded approximately 2 km from the windfarm ($p < 0.05$). Increasing current gradient was also significant in the model Appendix A. This effect is also apparent when applying the model for predictions on the whole study area (Figure 42). However, overall, the model is poor and the patterns are therefore not very reliable. It can be concluded that based on the surveys included no displacement effect can be determined for Black-legged Kittiwakes, yet a significant attraction of birds to the (outside of the) windfarm (highest densities within 2 km from the windfarm) was indicated at LUD. The explanatory degree of the distribution model for the Black-legged Kittiwake was fair for the presence-absence part, but low for the positive part of the model (Appendix A).

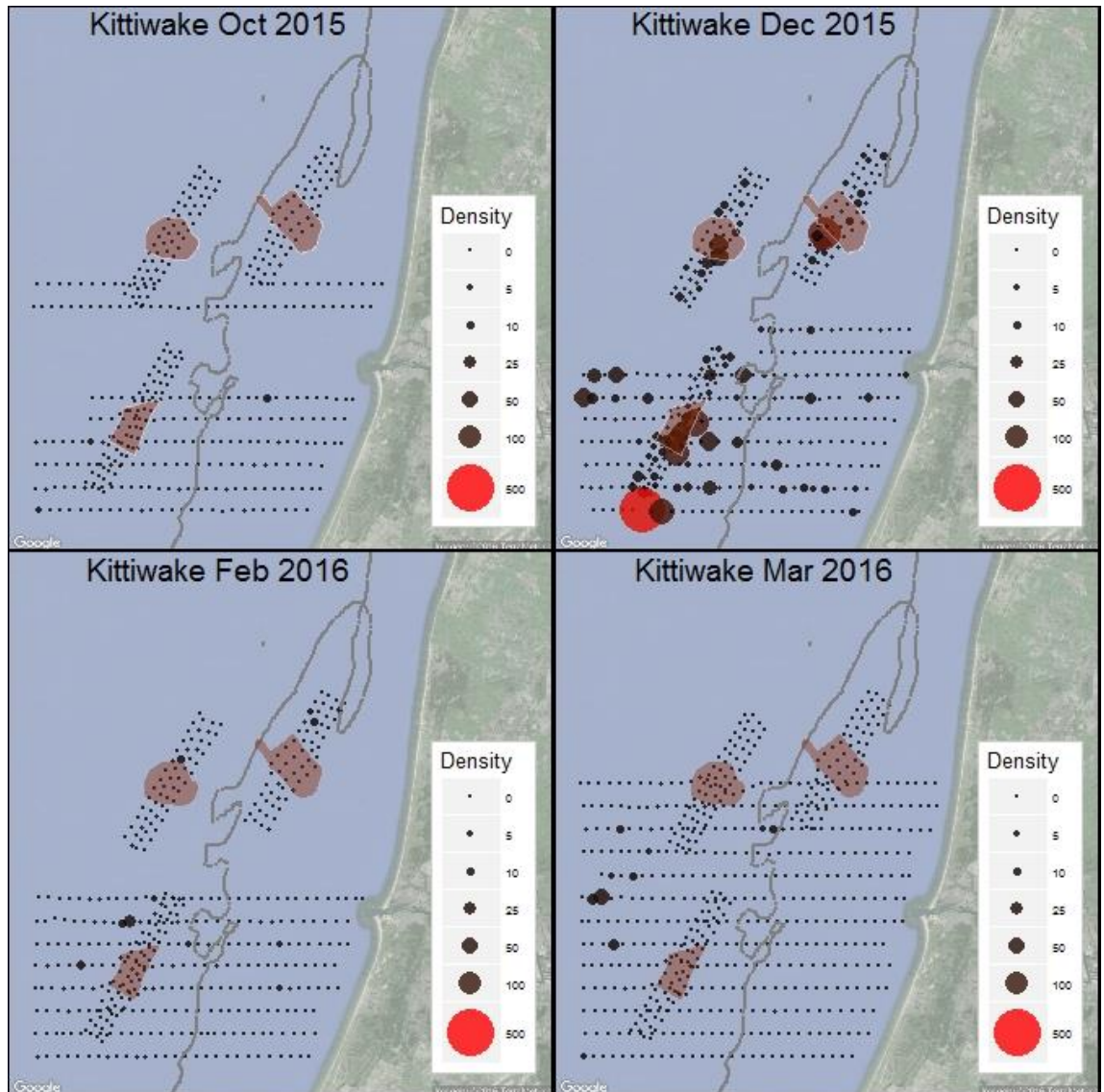


Figure 40. Observed density (birds/km²) of Black-legged Kittiwake during LUD T-1 surveys 2015-2016. Densities have been corrected for distance bias.

Kittiwake, 2002-2016

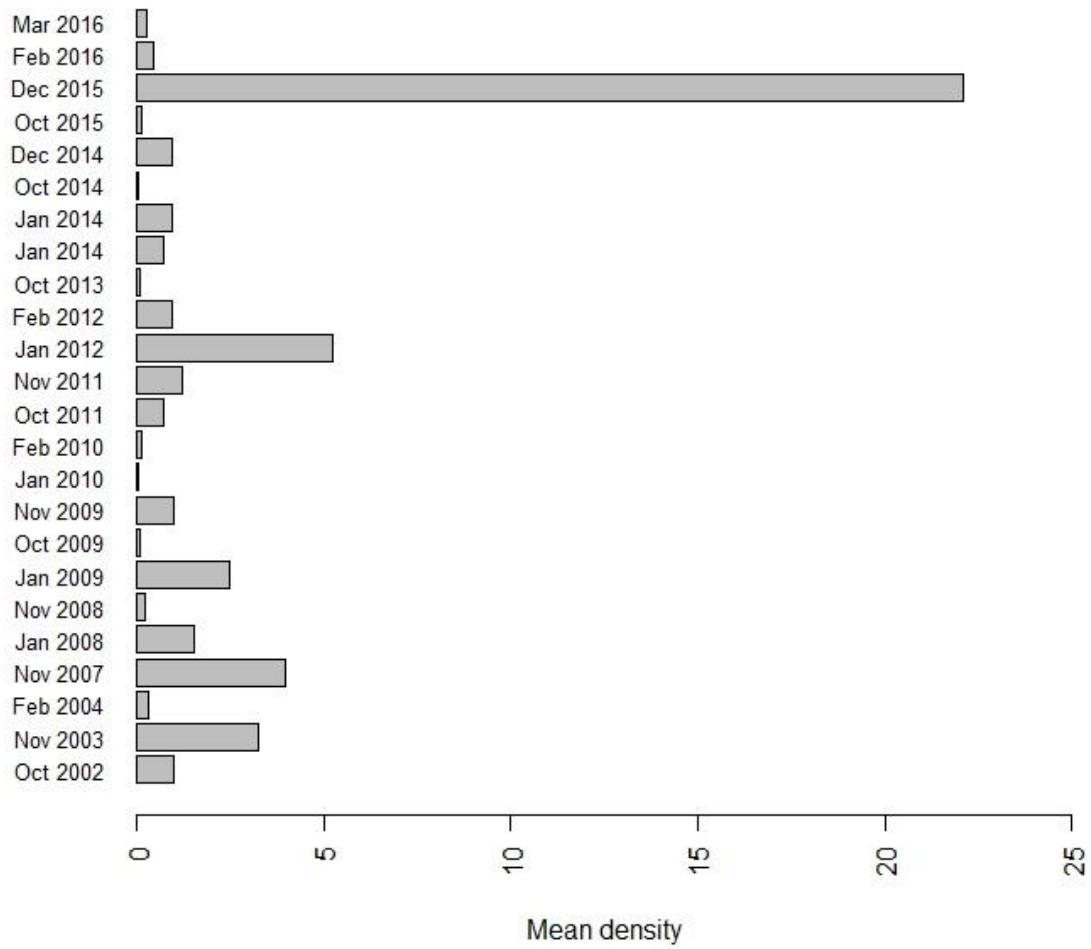


Figure 41. Mean observed density (birds/km²) of Black-legged Kittiwake during LUD pre- and post-construction surveys. Densities have been corrected for distance bias.

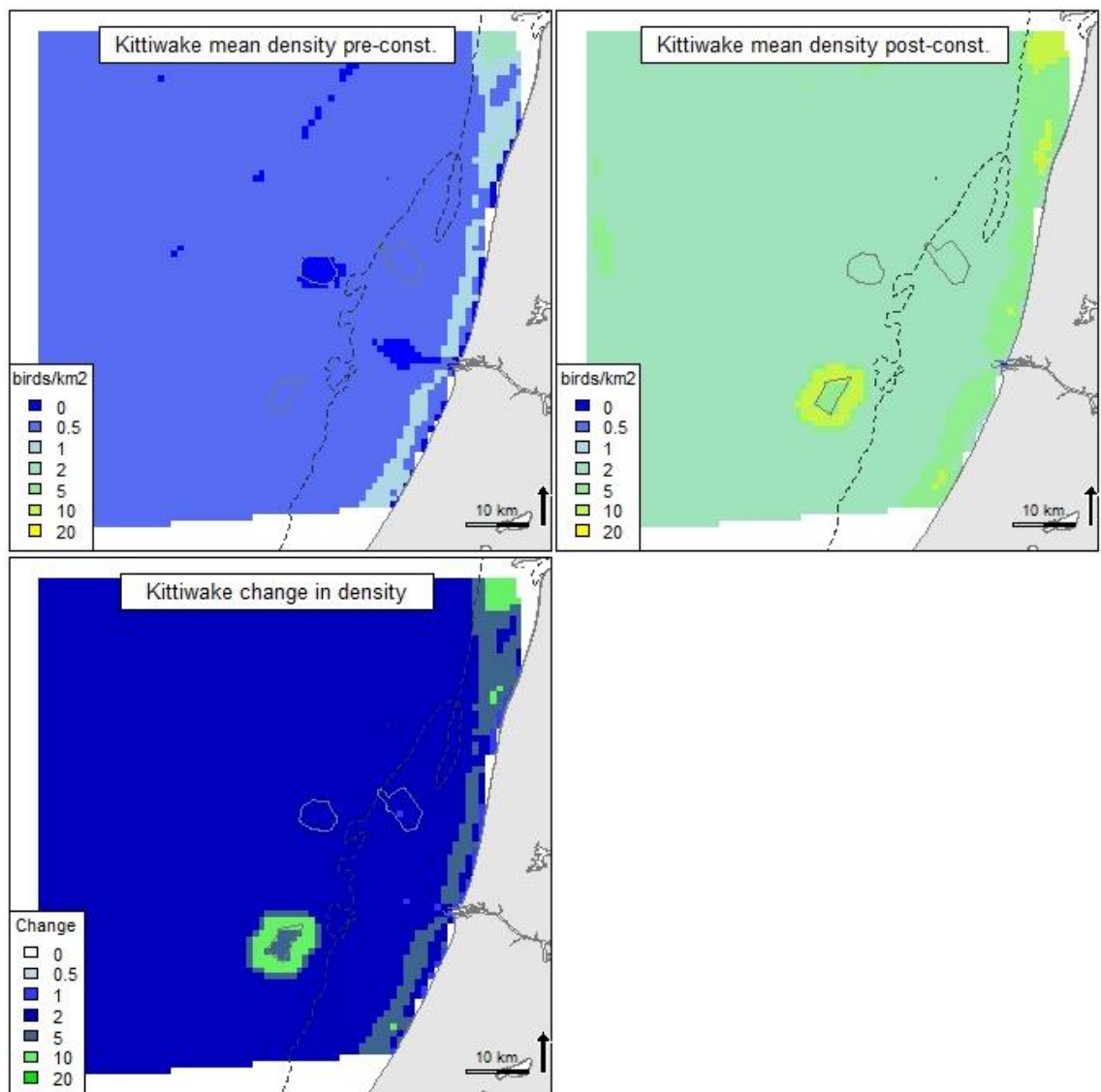


Figure 42. Predicted mean density (birds/km²) and distribution of wintering Black-legged Kittiwake during four LUD pre- and four LUD post-construction surveys, and the relative change in predicted density between the two periods. Note that all included surveys are OWEZ and PAWP post-construction surveys.

5.3.12 Common Guillemot *Uria aalge*

During the LUD-T1 surveys in 2015-2016 the densities of Common Guillemot varied with very high numbers observed in December 2015 and low numbers in March 2016 (Figure 43 and 44), and birds were seen in all three windfarms. The overall distribution reflected higher mean densities in the offshore parts of the study area, and lower densities close to the coast. A marked variation is apparent in the recorded densities of Common Guillemots between the 24 surveys of which 19 were included in the distribution analyses (Figure 44). Indication of a displacement of Common Guillemot from the LUD footprint is not very strong when just comparing mean densities within the windfarm and in buffers with increasing distance from the windfarm. According to the three pre-construction surveys, mean density of Common Guillemot in the windfarm was lower even before the windfarm was built in comparison to three 1.5 km buffers outside the windfarm. However, most importantly the variation in the data is huge according to the standard deviation (Figure 45). It is therefore evident that a modelling method able to account for the large variation in the data is needed to be able to define a displacement effect. Indications of a displacement seems stronger at PAWP where an increase in the buffers seems evident in comparison to the footprint

(Figure 46). Also at OWEZ the comparison of mean values indicates a displacement, but perhaps not as strongly as in PAWP which could be due to the more nearshore location (Figure 47).

Model results

According to the model the probability of presence increased with increasing salinity and current speeds and low shipping intensity. The distance variables to both PAWP and OWEZ were highly significant ($p < 0.01$) while the distance to LUD was significant on the 0.05 level. Hence, the model provided indications of avoidance of all three windfarms (Figure 48). Higher density was further explained by increasing water depth, both low and high current speeds and low shipping intensity. Distance to PAWP also indicated a significantly lower density (when present) of Common Guillemot whereas distance to OWEZ and LUD was not significant in the positive model part (Appendix A). The explanatory degree of the distribution model for the Common Guillemot was fair for both the presence-absence (26.4 %) and the positive part (16.7 %) of the model (Appendix A). The predictive accuracy was good according to the evaluation statistics with an AUC of 0.81 and a Spearman’s correlation between observed and predicted abundance of 0.52 when evaluated on 30% withheld data (Appendix A).

The empirical “power” analysis indicated that the distance to windfarm effect on Common Guillemots for PAWP was significant following 4 surveys post-construction, while a significant effect was found already with one post-construction survey for OWEZ (Figure 49).

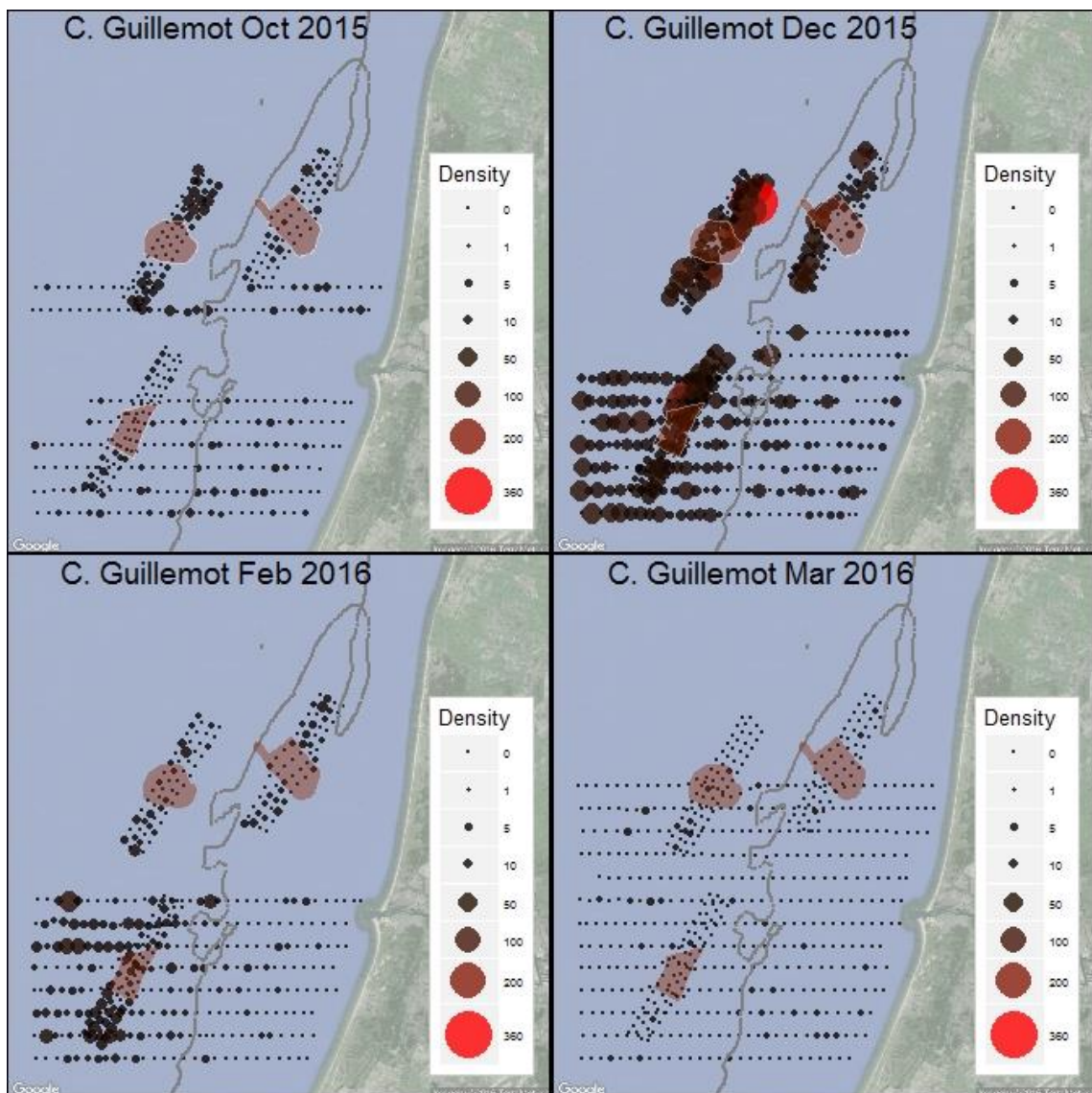


Figure 43. Observed density (birds/km²) of Common Guillemot during LUD T-1 surveys 2015-2016. Densities have been corrected for distance bias.

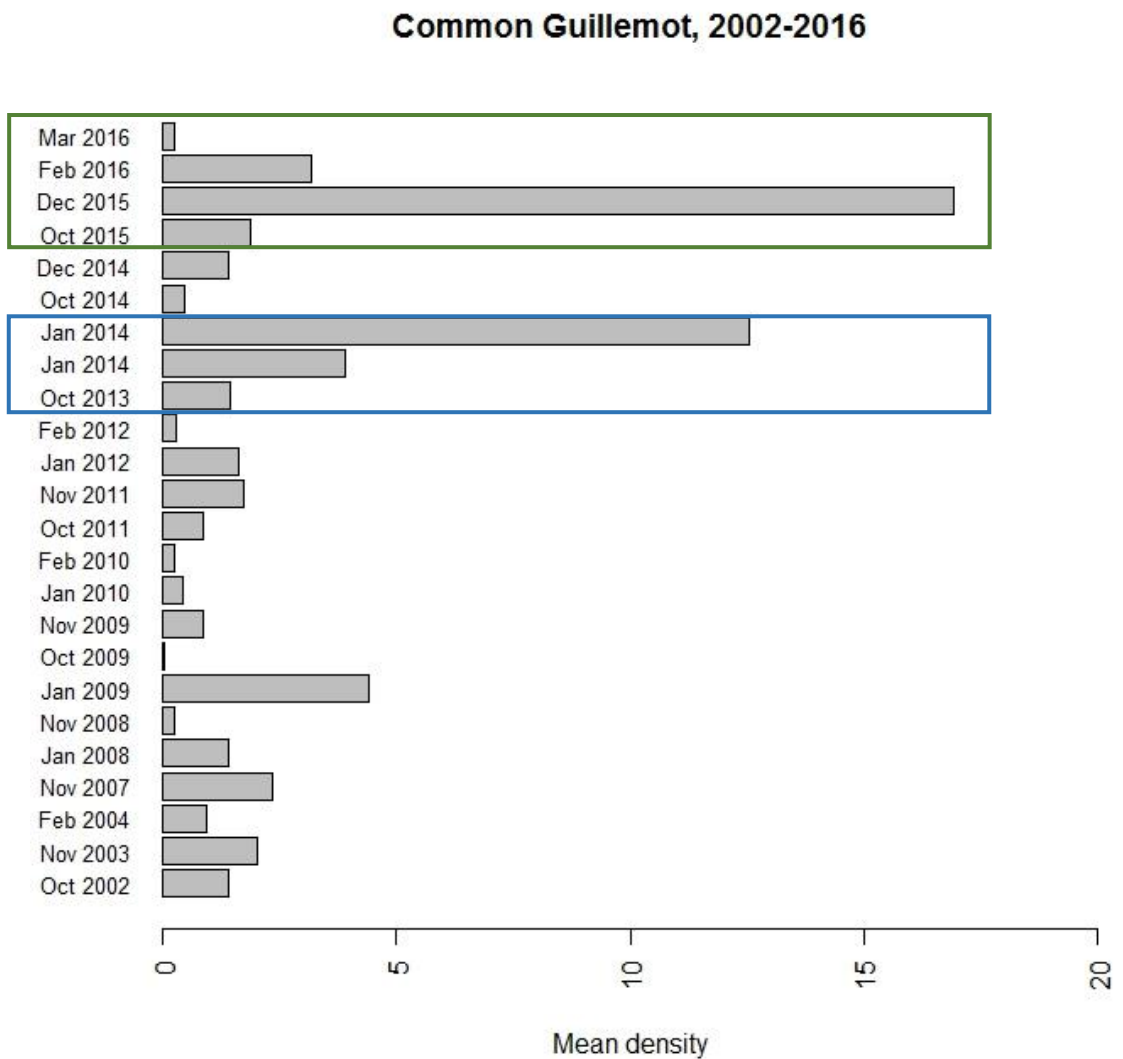


Figure 44. Mean observed density (birds/km²) of Common Guillemot during LUD pre-construction surveys (indicated by a blue rectangle) and post-construction surveys (green rectangle). Densities have been corrected for distance bias.

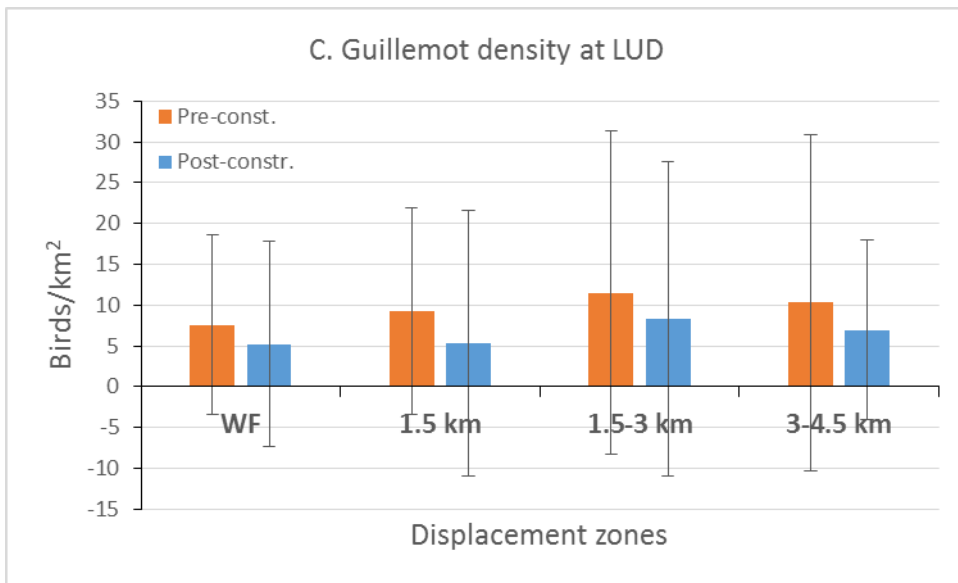


Figure 45. Mean density pre-construction and post-construction within the windfarm footprint and within three buffer zones around the windfarm, 1.5 km, 1.5 - 3 km and 3 - 4.5 km buffer.

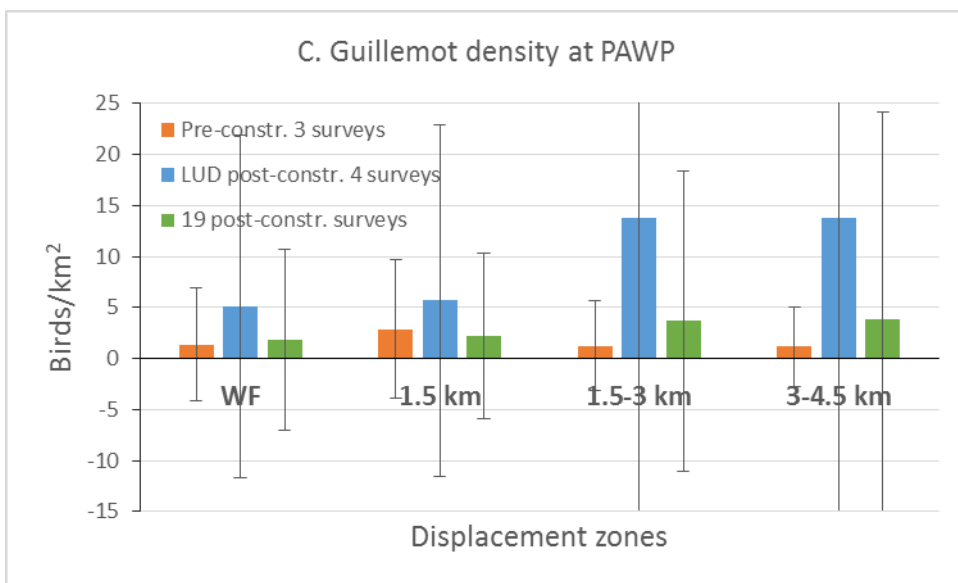


Figure 46. Mean density pre-construction and post-construction within the windfarm footprint and within three buffer zones around the windfarm, 1.5 km, 1.5 - 3 km and 3 - 4.5 km buffer.

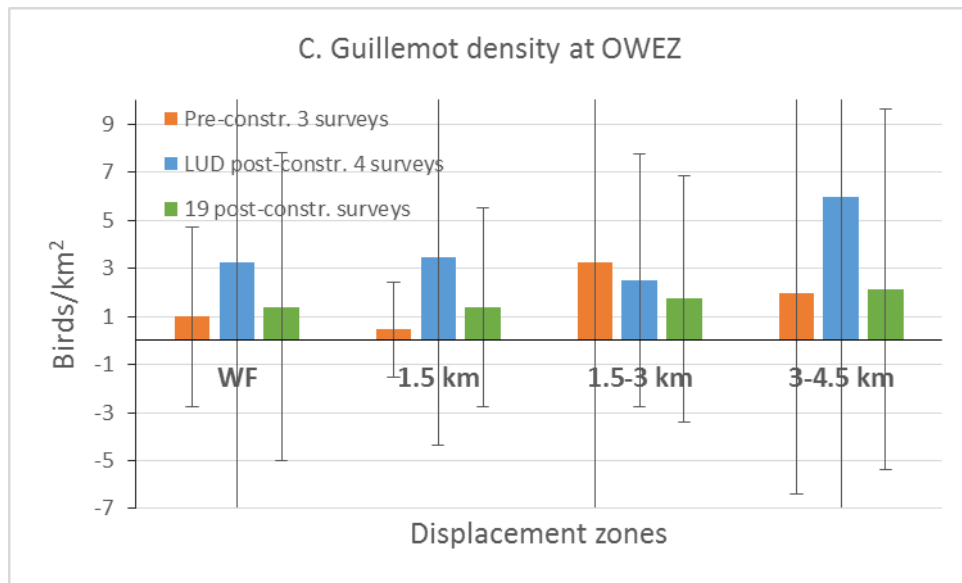


Figure 47. Mean density pre-construction and post-construction within the windfarm footprint and within three buffer zones around the windfarm, 1.5 km, 1.5 - 3 km and 3 - 4.5 km buffer.

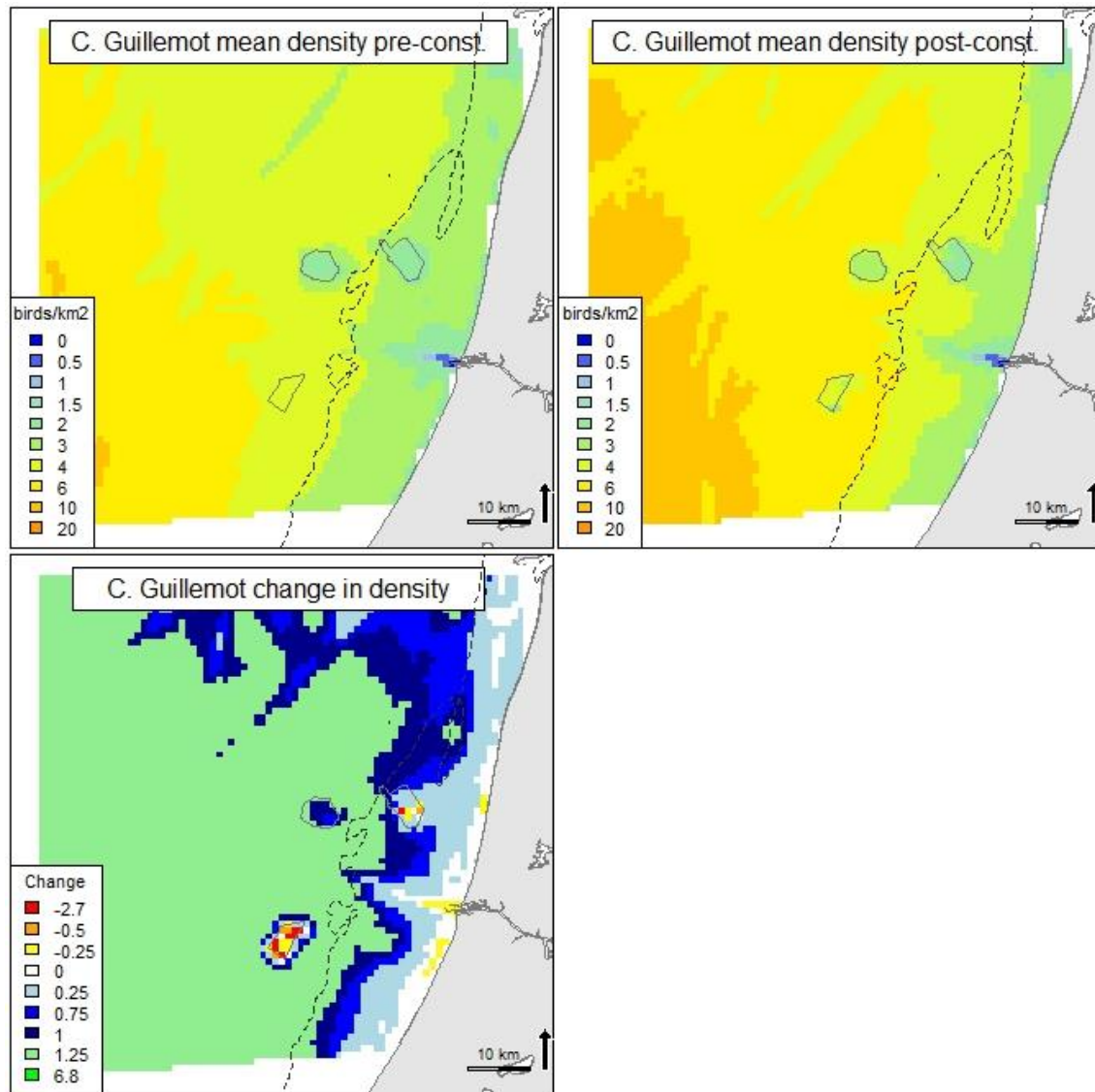


Figure 48. Predicted mean density (birds/km²) and distribution of wintering Common Guillemot during four LUD pre- and four LUD post-construction surveys, and the relative change in predicted density between the two periods. Note that all included surveys are OWEZ and PAWP post-construction surveys.

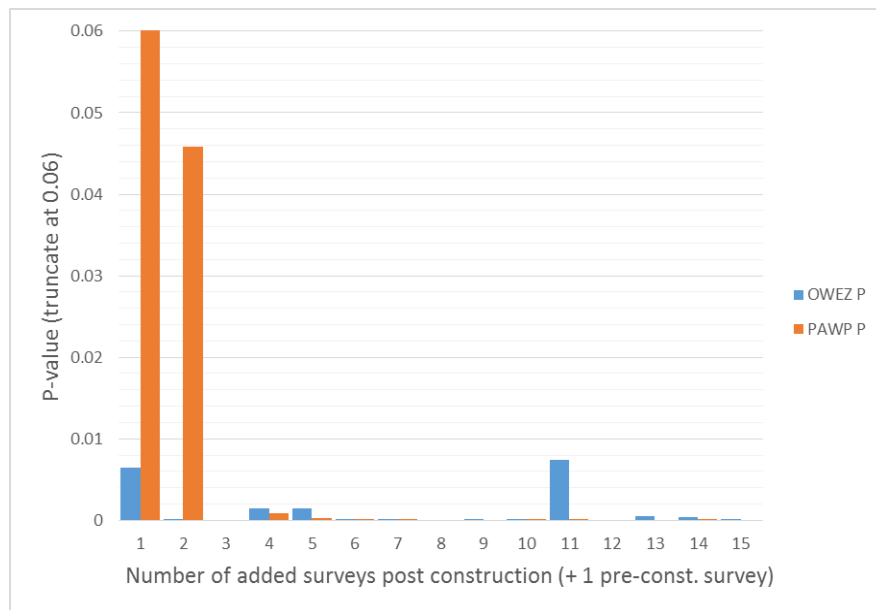


Figure 49. Significance (P-value) of effect parameter (distance from windfarm) for Common Guillemot in relation to the number of post-construction monitoring years at OWEZ and PAWP. The models with 3, 8 and 12 additional surveys did not converge. After four surveys the effect of both windfarms is significant for both windfarms, the p-value further decreases when more surveys are added.

Simulation “power” analysis

Simulations based on the relationships modelled using GAMM reported above were refitted and simulated on the existing post-construction survey conditions using GLMM (excluding the response from LUD). The power of detecting a decline of 10-90% in LUD was assessed using 100 simulations (of which generally around 80% converged, Table 10, Table 11). A high power (>80%) was achieved when 50% of both presence and density of Common Guillemot was reduced within windfarm + 4 km buffer (Table 10). When birds were displaced in the same manner only from within the windfarm a 75% displacement was required to achieve a reasonable power, >80% (Table 11). To further assess whether 8 surveys would be sufficient for detecting a 25% reduction with a high power, we used the 3 pre-construction survey and 1 construction survey as fictional post-construction surveys and thus simulated 100 times 8 fictional post-construction surveys with a 25 % displacement within the LUD windfarm. The results indicated that the power of detecting a 25% displacement of Common Guillemot following 8 surveys was rather low (Table 12). However, a 50% displacement had a power of 95.5% when 8 surveys were used (Table 12).

Table 10. The power of a presence/absence (PA) model part and positive density model part (POS, conditional on PA) including four post-construction surveys, with an artificial displacement of 10%, 25% and 50% from within the windfarm + 4 km buffer.

Displacement from WF + 4 km	PA	POS	N sim.
10%	0.012	0.062	81
25%	0.494	0.584	77
50%	1.000	1.000	85
75%	-	-	-

Table 11. The power of a presence/absence (PA) model part and positive density model part (POS, conditional on PA) including four post-construction surveys, with an artificial displacement of 25%, 50% and 75% from within the windfarm perimeter.

Displacement from WF	PA	POS	N sim.
10%	-	-	
25%	0.052	0.078	77
50%	0.709	0.430	79
75%	1.000	0.883	77

Table 12. The power of a presence/absence (PA) model part and positive density model part (POS, conditional on PA) including eight post-construction surveys, with an artificial 25% displacement from within the windfarm perimeter.

Displacement from WF	PA	POS	N sim.
25%	0.211	0.289	76
50%	1.000	0.955	88

5.3.13 Razorbill *Alca torda*

During the LUD-T1 surveys Razorbills were frequently observed in offshore waters, including in all three windfarms (Figure 50). The overall abundance of Razorbills wintering in the area during the 2015-2016 winter seems to be rather high compared to the mean density recorded between 2002 and 2014 (Figure 51).

Model results

Both the explanatory and predictive power of the Razorbill model was poor (Appendix A). Highest probability of presence was associated with areas with intermediate (10-20 m) water depth and high current speeds. The effect of the three windfarms on presence and abundance of Razorbills was insignificant. Although insignificant the response curves (Appendix A) indicate a lower probability of presence with decreasing distance to the windfarms, including LUD and therefore a reduction in the predicted density in LUD between pre- and post-construction can be seen (Figure 52).

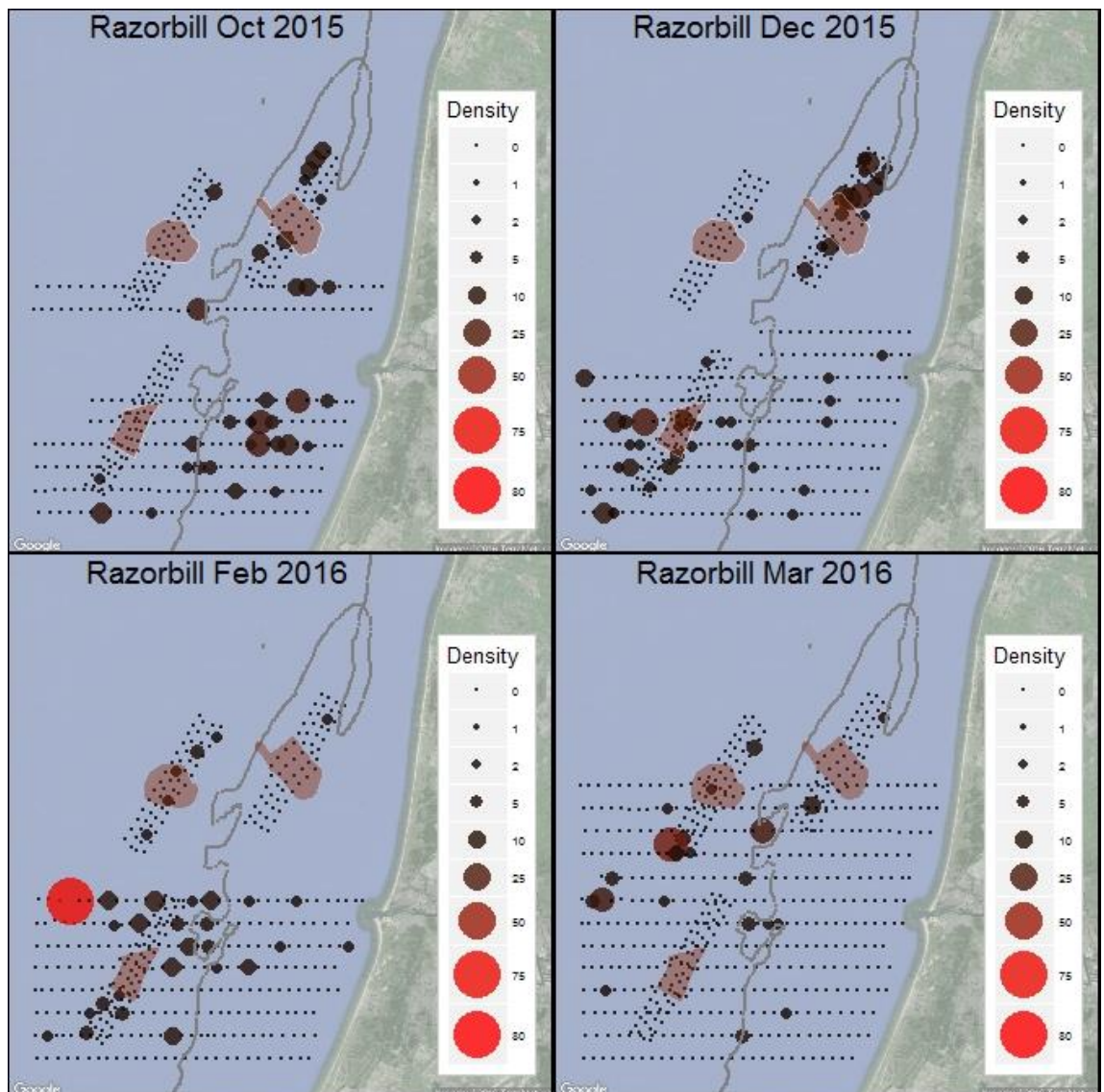


Figure 50. Observed density (birds/km²) of Razorbill during LUD T-1 surveys 2015-2016. Densities have been corrected for distance bias.

Razorbill, 2002-2016

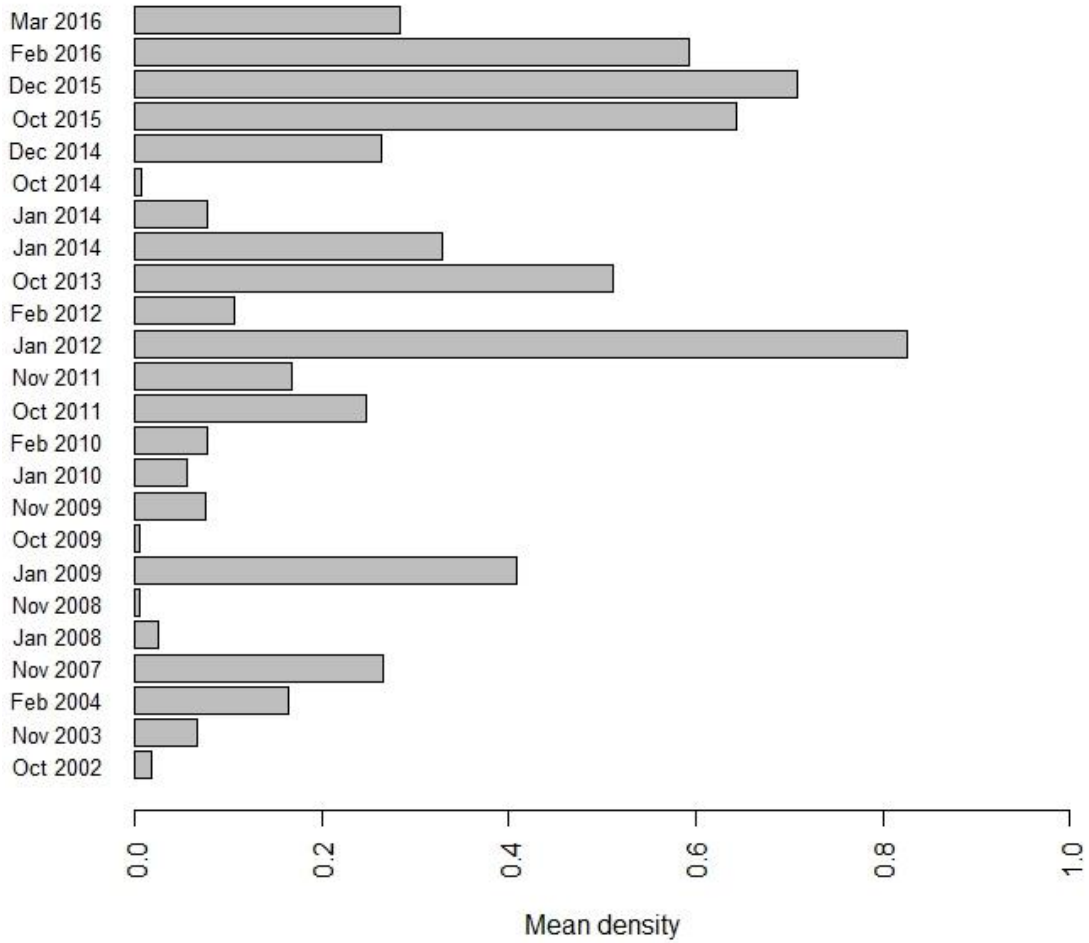


Figure 51. Mean observed density (birds/km²) of Razorbill during LUD pre- and post-construction surveys. Densities have been corrected for distance bias.

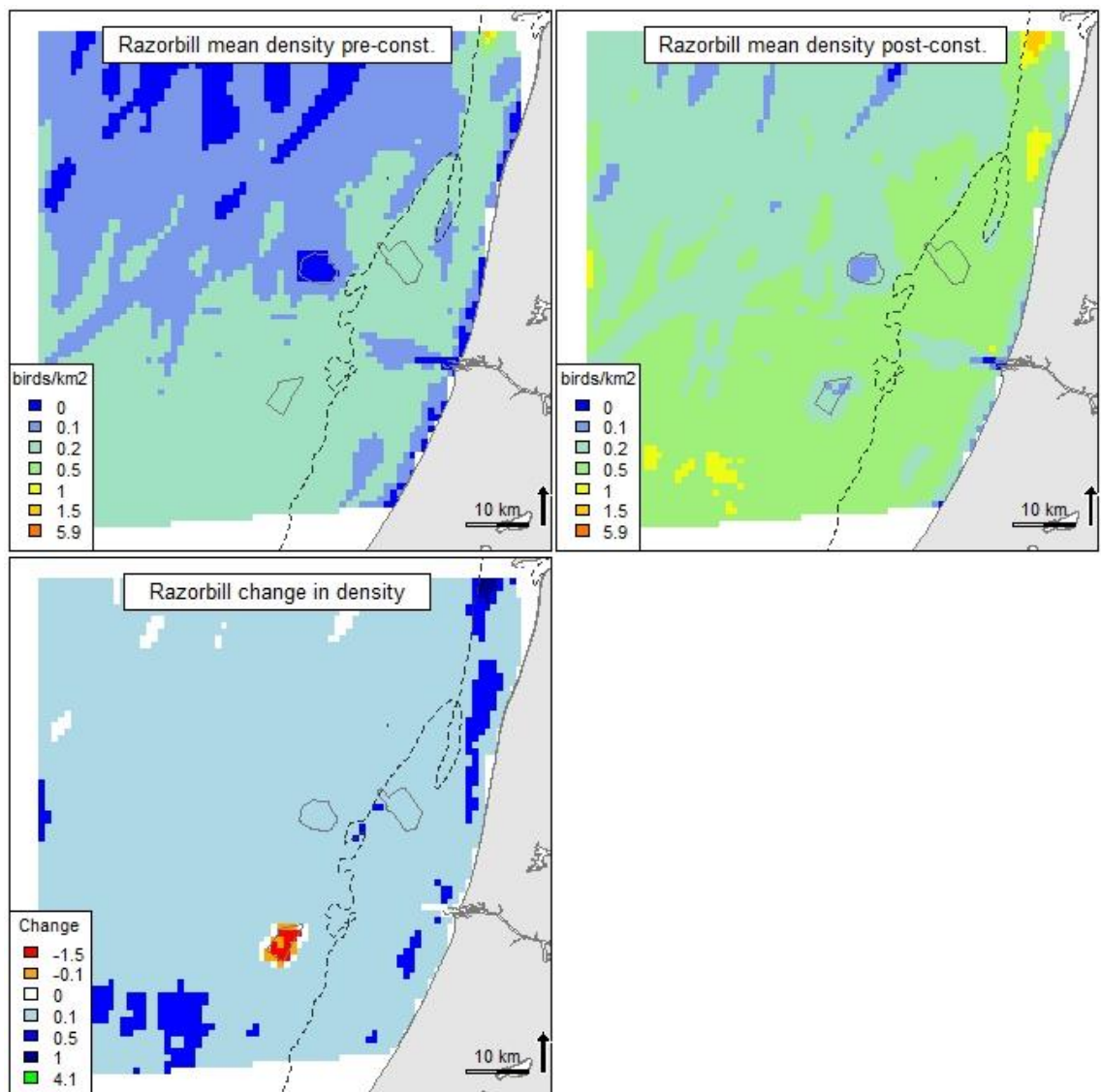


Figure 52. Predicted mean density (birds/km²) and distribution of wintering Razorbill during four LUD pre- and four LUD post-construction surveys, and the relative change in predicted density between the two periods. Note that all included surveys are OWEZ and PAWP post-construction surveys.

5.3.14 Marine mammal observations

Harbour Porpoise *Phocoena phocoena* was the most commonly observed marine mammal in the whole area. The tendency for most sightings in the southern part of the area, which was seen during T-0 and T-Constr was not so apparent during T-1 (Figure 53). The sightings included two observations in OWEZ, one in PAWP and one just at the periphery of LUD.

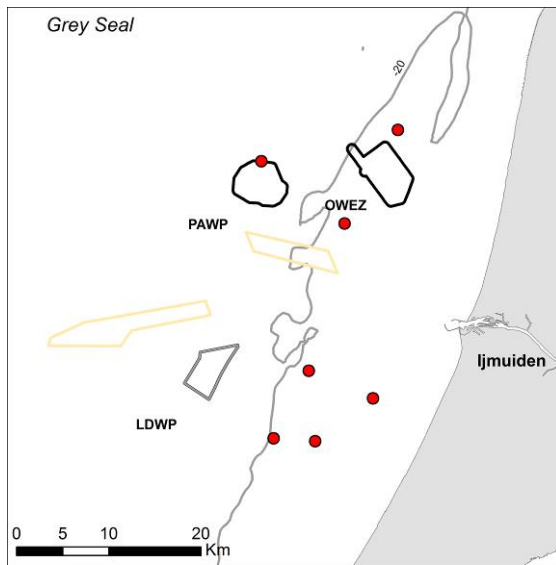
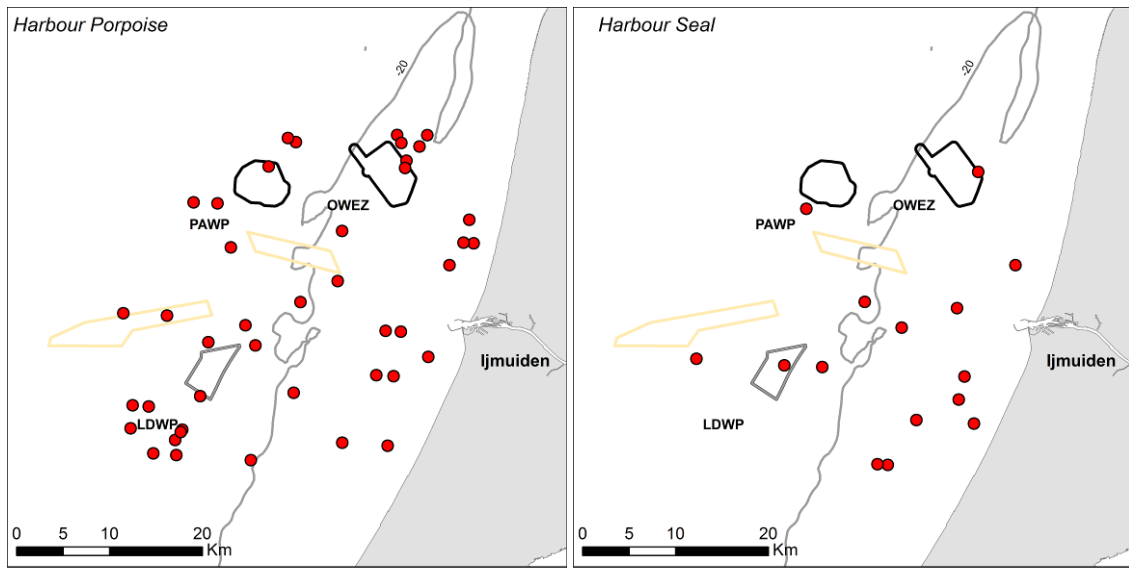


Figure 53. Observations of marine mammals during the LUD T-11 surveys 2015-2016. No corrections for possible double registrations have been made.

6 Discussion

The four LUD-T1 surveys provided knowledge about the distribution and abundance of seabirds during the first season following the construction of the Offshore Windfarm Eneco Luchterduinen. The abundance of the different species of seabirds largely follows the patterns from the LUD baseline and T-Constr periods with the overall impression that the waters around LUD are mainly characterised by high densities of Common Guillemot and low to moderate densities of other species of seabirds. However, during the December 2015 survey, high abundance of Northern Gannet was also recorded.

The T-1 results should be seen as the first step in the collection of evidence regarding potential displacement impacts of LUD on seabirds. Predicted changes in densities between LUD baseline and T-1 surveys were compared using the dynamic habitat modelling framework established during T-0 and using all available 19 surveys from 2007 to present. In addition, empirical analyses of OWEZ and PAWP data on the influence of the number of surveys on the power to detect displacement were undertaken to make an assessment of additional monitoring surveys required to detect displacement of Common Guillemots and Northern Gannets from LUD. These results were followed by simulations of the statistical power of the monitoring data to detect seabird displacement at LUD. As the modelling framework has been designed to include important habitat and pressure variables, the distance to the LUD, PAWP and OWEZ windfarms should represent the displacement effect.

The species specific-results are summarized in Table 13. The defined responses are generally in line with other studies when comparing to reviews done by for example Krijgsveld (2014) and Welcker & Nehls (2016). The LUD-T1 distribution models indicated negative responses of Northern Gannets (2 km avoidance) and Common Guillemot (2-4 km avoidance) to PAWP and OWEZ, as well as a positive response (attraction) of Great Cormorants to LUD, PAWP and OWEZ. This was the case, even if displacement of Gannets and Guillemots was not complete, and both species were observed in the windfarms. Due to the short scale of the displacement no cumulative displacement effects due to OWEZ and PAWP were found. The empirical analyses of the power of OWEZ and PAWP data to detect displacement effects on Northern Gannet and Common Guillemot indicated that displacement of both species could be determined following four surveys post-construction (one survey at PAWP for the Guillemot). However, simulations based on the existing post-construction survey conditions indicated, that following four surveys a reasonable power (>80%) for both species could only be achieved in situations with at least 75% displacement from LUD. If a displacement buffer of 4 km was added a power above 80% could be achieved with 50% displacement. Simulating the power to detect 25% and 50% displacement from LUD without a 4 km buffer and following eight surveys indicated that high power would not be achieved for Northern Gannet under these conditions within this number of surveys. Based on these simulations it seems most unlikely given the oceanographic variability, mobile behaviour and hence variability of abundance of Northern Gannet at LUD that it will be possible to detect reductions of 50% of this species from this windfarm after T2. It is therefore recommended to finalise all surveys as planned under T2, and re-assess the power of the collected data as scheduled before deciding on execution of T3.

The distribution models for Northern Gannet and Common Guillemot were fair, judged from their explanatory power, and the predictive accuracy was good for the Common Guillemot model. As documented by the available surveys included in the models, the abundance of both species in the studied region off the Dutch coast varies between years. This is especially the case with respect to Northern Gannet, which is closely associated with the North Sea water mass. As the distribution models have been specifically designed to account for the oceanographic variability it is reasonable to judge the results of both the empirical and the simulation based power tests as relatively reliable.

Table 13. Summary of species-specific responses to the LUD, PAWP and OWEZ windfarms, significant displacement/attraction or no detected impact. Significance of both model parts are given for each windfarm (presence-absence/positive model part). In the last column the results of a review of displacement patterns from several windfarms presented in Welcker & Nehls 2016 are given for comparison with other studies.

Species	LUD	PAWP	OWEZ	Description	General review (Welcker & Nehls 2016)
Divers	-	<0.001/-	<0.05/ns	Avoidance	10/10 avoidance
Great Crested Grebe	-	-	<0.001/ns	Avoidance	?
Northern Gannet	ns/ns	<0.001/ns	<0.001/ns	Avoidance	8/10 avoidance
Great Cormorant	<0.001/ns	<0.001/<0.01	<0.001/<0.001	Attraction	?
Little Gull	<0.001/ns	<0.05/ns	ns/ns	Avoidance	5/8 avoidance
Black-headed Gull	ns/-	ns/ns	ns/ns	No detected impact	
Common Gull	ns/ns	ns/ns	ns/ns	No detected impact	5/6 no displacement
Lesser Black-backed Gull	ns/ns	ns/ns	ns/ns	No detected impact	5/8 no displacement
Herring Gull	ns/ns	ns/ns	ns/ns	No detected impact	6/8 no displacement
Greater Black-backed Gull	ns/ns	<0.01/ns	<0.05/<0.001	Attraction to periphery of WF	5/7 no displacement, 2 attractions
Black-legged Kittiwake	ns/<0.05	ns/ns	ns/ns	Higher density just outside LUD	5/7 no displacement
Common Guillemot	<0.05/ns	<0.001/<0.01	<0.001/ns	Avoidance,	9/11 avoidance (Alcids pooled)
Razorbill	ns/ns	<0.05/ns	ns/ns	Avoidance	9/11 avoidance (Alcids pooled)

7 References

- Buckland, S.T., Anderson, D.R., Burnham, K.P., Laake, J.L., Borchers, D.L., and Thomas, L. 2001. Introduction to distance sampling - Estimating abundance of biological populations. Oxford University Press, Oxford. Burnham, K.P., and Anderson, D.R. 2002. Model Selection and Multimodel Inference: A Practical Information-Theoretic Approach, 2nd ed. Springer-Verlag. ISBN 0-387-95364-7. Camphuysen, C.J. & Garthe, S. 2004. Recording foraging seabirds at sea: standardised recording and coding of foraging behaviour and multi-species foraging associations. *Atlantic Seabirds* 5: 1-23.
- Camphuysen CJ, Fox TJ, Leopold MF & Petersen IK, 2004. Towards standardised seabirds at sea census techniques in connection with environmental impact assessments for offshore wind farms in the U.K. - A comparison of ship and aerial sampling methods for marine birds, and their applicability to offshore wind farm assessments. NIOZ Report to Cowrie / The Crown Estate.
- Hastie, T. & Tibshirani, R. 1990. Generalized Additive Models. Chapman & Hall, London. Leopold M.F., Camphuysen C.J., ter Braak C.J.F., Dijkman E.M., Kersting K. & van Lieshout S.M.J. 2004. Baseline studies North Sea wind farms: Lot 5 marine birds in and around the future sites Nearshore Windfarm (NSW) and Q7. Alterra-rapport 1048.
- Krijgsveld, K.L. 2014. Avoidance behaviour of birds around offshore wind farms. Overview of knowledge including effects of configuration. Bureau Waardenburg, Rijkswaterstaat Report no. 13-268.
- Leopold, M.F., van Bemmelen, R.S.A. & Zuur, A.F. 2013. Responses of Local Birds to the Offshore Wind Farms PAWP and OWEZ off the Dutch mainland coast. Report number C151/12. Imares Report.
- Maclean, I.M.D., Rehfish, M. M., Skov, H. & Thaxter, C. B. 2013. Evaluating the statistical power of detecting changes in the abundance of seabirds at sea. *Ibis*: 113-126.
- Pérez-Lapeña, B. K. Wijnberg, M., Hulscher, S. J. M. H & Stein, A. 2010. Environmental impact assessment of offshore wind farms: a simulation-based approach. *Journal of Applied Ecology* 47: 1110–1118.
- Petersen I.K., Christensen T.K., Kahlert J., Desholm M. & Fox A.D. 2006. Final results of bird studies at the offshore wind farms at Nysted and Horns Rev, Denmark. NERI Report, commissioned by DONG energy and Vattenfall A/S.
- Skov, H., Leonhard, S.B., Heinänen, S., Zydalis, R., Jensen, N.E., Durinck, J., Johansen, T.W., Jensen, B.P., Hansen, B.L., Piper, W., Grøn, P.N. 2012. Horns Rev 2 Monitoring 2010-2012. Migrating Birds. Orbicon, DHI, Marine Observers and Biola. Report commissioned by DONG Energy.
- Skov, H., Heinänen, S., Nyborg, L. & Lazcny, M. 2015. Offshore Wind Farm Eneco Luchterduinen Ecological monitoring of seabirds. T0 report. Commissioned by Eneco. DHI.
- Tasker M.L., Jones P.H., Dixon T.J. & Blake B.F. 1984. Counting seabirds at sea from ships: a review of methods employed and a suggestion for a standardized approach. *Auk* 101: 567-577.
- Vanermen, N., Onkelinx, T. Verschelde, P., Courtens, W., Van de walle, M., Verstraete, H. & Stienen, E. W. M. 2015. Assessing seabird displacement at offshore windfarms: power ranges of a monitoring and data handling protocol. *Hydrobiologia*, 756:155-167.
- Welcker, J. & Nehls, G. 2016. Displacement of seabirds by an offshore wind farm in the North Sea. *Mar Ecol Prog Ser*, 554: 173-182.

APPENDICES

APPENDIX A – Detailed results of species distribution models for the T-1 surveys

Red-throated and Black-throated Divers

Table A.1. Smooth terms, adjusted R-squared and evaluation statistics for the Red-throated and Black-throated Diver distribution models. F statistics and the approximate significance for the smooth terms and t-statistic and the significance for the parametric terms are shown. Variables not included in either the presence/absence or positive model part are indicated with a dash. The results of the evaluation test show AUC for presence/absence and the Spearman's correlation for the density predictions. The evaluation test is based on a model fitted on 70% and tested on 30% of withheld data. 'n.s.' indicates terms with p-values > 0.05. The significant effect of the windfarms are marked in bold.

Smooth terms	Presence/absence		Positive density	
	F	p	F	p
LUD (max 4 km) not included	-	-	-	-
PAWP (max 4 km) parametric	10.814	<0.001	-	-
OWEZ (max 4 km) parametric	2.125	<0.05	0.796	n.s.
Depth	-	-	-	-
Salinity	45.137	<0.001	-	-
Shipping intensity (AIS)	-	-	-	-
Current speed	12.902	<0.001	39.121	<0.001
Eddy potential (vorticity)	5.015	<0.05	-	-
Current gradient	-	-	-	-
Parametric terms	t	p	t	p
AIS (if parametric)	-	-	-	-
Survey 5	4.83	<0.001	0.34	n.s.
Survey 6	-0.964	n.s.	-3.886	<0.001
Survey 7	0.088	n.s.	0.108	n.s.
Survey 8	4.716	<0.001	0.648	n.s.
Survey 9	5.449	<0.001	0.601	n.s.
Survey 10	5.663	<0.001	2.047	<0.05
Survey 11	0.709	n.s.	-2.734	<0.01
Survey 12	0.502	n.s.	-2.07	<0.05
Survey 13	3.645	<0.001	-1.518	n.s.
Survey 14	5.766	<0.001	-0.776	n.s.
Survey 15	6.71	<0.001	0.269	n.s.
Survey 16	2.298	<0.05	0.722	n.s.
Survey 17	-0.091	n.s.	-0.172	n.s.
Survey 18	-1.781	n.s.	-0.162	n.s.
Survey 21	-	-	-	-
Survey 22	0.407	n.s.	-0.547	n.s.
Survey 23	0.84	n.s.	0.341	n.s.
Survey 24	-1.606	n.s.	-0.43	n.s.
Sample size (n)	7655		335	
Adjusted R ²	20.20%		14.00%	
AUC	0.84			
Spearman's corr.	0.37			

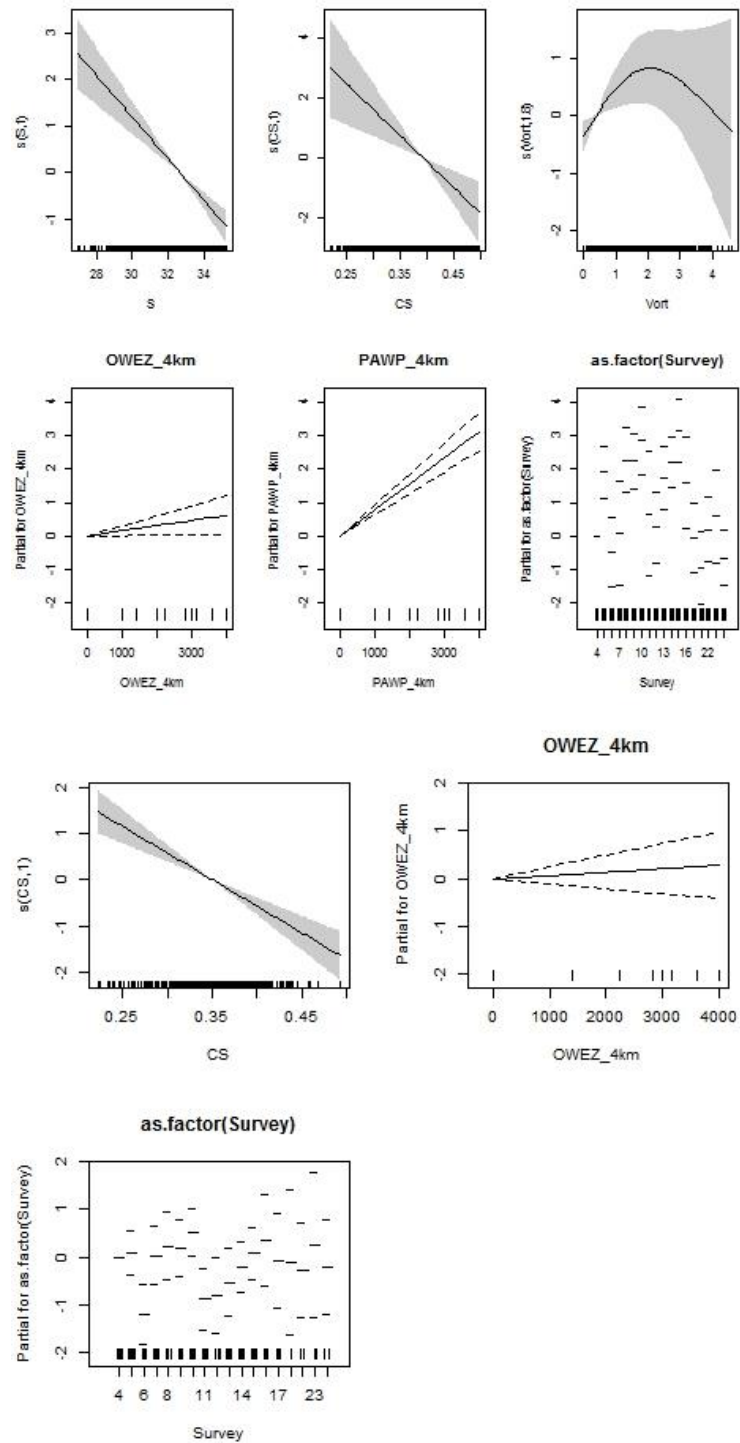


Figure A.1. Partial GAM plots for the Red-throated and Black-throated Diver distribution model – presence-absence (upper panel) and positive density (lower panel) parts. The values of the environmental variables are shown on the X-axis and the probability on the Y-axis in the scale of the linear predictor. The grey shaded areas and the dotted lines (for factors) show the 95% Bayesian confidence intervals. The degree of smoothing is indicated in the legend of the Y-axis.

Great Crested Grebe

Table A.2. Smooth terms, adjusted R-squared and evaluation statistics for the Great Crested Grebe distribution models. F statistics and the approximate significance for the smooth terms and t-statistic and the significance for the parametric terms are shown. Variables not included in either the presence/absence or positive model part are indicated with a dash. The results of the evaluation test show AUC for presence/absence and the Spearman's correlation for the density predictions. The evaluation test is based on a model fitted on 70% and tested on 30% of withheld data. 'n.s.' indicates terms with p-values > 0.05. The significant effect of the windfarms are marked in bold.

Smooth terms	Presence/absence		Positive density	
	F	p	F	p
LUD (max 4 km) not included	-	-	-	-
PAWP (max 4 km) not included	-	-	-	-
OWEZ (max 4 km) parametric	13.236	<0.001	0.048	n.s
Depth	108.035	<0.001	5.49	<0.01
Salinity	133.407	<0.001	4.195	<0.05
Shipping intensity (AIS)	-	-	-	-
Current speed	-	-	-	-
Eddy potential (vorticity)	-	-	-	-
Current gradient	-	-	-	-
Parametric terms	t	p	t	p
AIS (if parametric)	-	-	-	-
Survey 5	12.621	<0.001	6.18	<0.001
Survey 6	5.731	<0.001	0.02	n.s.
Survey 7	10.684	<0.001	6.048	<0.001
Survey 8	-	-	-	-
Survey 9	11.587	<0.001	1.74	n.s.
Survey 10	22.7	<0.001	3.777	<0.001
Survey 11	17.214	<0.001	3.995	<0.001
Survey 12	-	-	-	-
Survey 13	5.652	<0.001	1.872	n.s.
Survey 14	10.944	<0.001	2.955	<0.01
Survey 15	7.674	<0.001	3.044	<0.01
Survey 16	-	-	-	-
Survey 17	11.379	<0.001	4.148	<0.001
Survey 18	18.096	<0.001	3.074	<0.01
Survey 21	-	-	-	-
Survey 22	6.578	<0.001	2.673	<0.01
Survey 23	9.201	<0.001	1.307	n.s.
Survey 24	-	-	-	-
Sample size (n)	5718		184	
Adjusted R ²	23.80%		3.60%	
AUC	0.93			
Spearman's corr.	0.44			

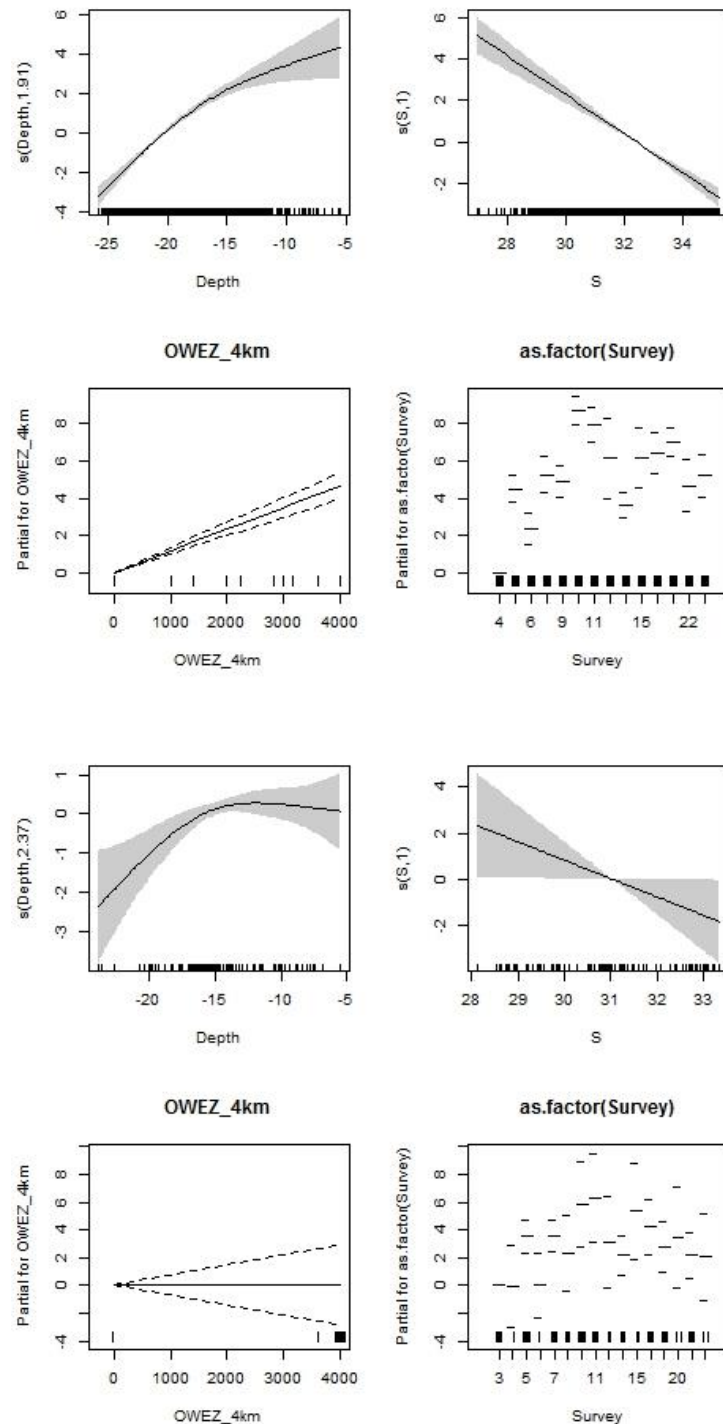


Figure A.2. Partial GAM plots for the Great Crested Grebe distribution model – presence-absence (upper panel) and positive density (lower panel) parts. The values of the environmental variables are shown on the X-axis and the probability on the Y-axis in the scale of the linear predictor. The grey shaded areas and the dotted lines (for factors) show the 95% Bayesian confidence intervals. The degree of smoothing is indicated in the legend of the Y-axis.

Northern Gannet

Table A.3. Smooth terms, adjusted R-squared and evaluation statistics for the Northern Gannet distribution models. F statistics and the approximate significance for the smooth terms and t-statistic and the significance for the parametric terms are shown. Variables not included in either the presence/absence or positive model part are indicated with a dash. The results of the evaluation test show AUC for presence/absence and the Spearman's correlation for the density predictions. The evaluation test is based on a model fitted on 70% and tested on 30% of withheld data. 'n.s.' indicates terms with p-values > 0.05. The significant effect of the windfarms are marked in bold.

Smooth terms	Presence/absence		Positive density	
	F	p	F	p
LUD (max 4 km)	0.856	n.s	0.572	n.s
PAWP (max 4 km)	27.947	<0.001	2.122	n.s
OWEZ (max 4 km)	39.472	<0.001	0.039	n.s
Depth	14.957	<0.001	5.797	<0.05
Salinity	15.015	<0.001	21.951	<0.001
Shipping intensity (AIS)	-		2.417	n.s.
Current speed	18.561	<0.001	-	
Eddy potential (vorticity)	-		-	
Current gradient	-		-	
Parametric terms	t	p	t	p
AIS (if parametric)	-2.12	<0.05	-	
Survey 5	-8.028	<0.001	-3.382	<0.001
Survey 6	-1.608	n.s.	-2.217	<0.05
Survey 7	-2.906	<0.01	2.011	<0.05
Survey 8	-4.436	<0.001	-4.673	<0.001
Survey 9	-0.943	n.s.	-1.796	n.s.
Survey 10	-4.509	<0.001	-3.693	<0.001
Survey 11	-2.785	<0.01	-3.341	<0.001
Survey 12	-2.44	<0.05	-2.63	<0.01
Survey 13	-3.699	<0.001	-4.679	<0.001
Survey 14	-4.93	<0.001	-2.912	<0.01
Survey 15	-6.752	<0.001	-3.031	<0.01
Survey 16	-2.432	<0.05	-4.692	<0.001
Survey 17	-15.815	<0.001	-1.747	n.s.
Survey 18	-12.97	<0.001	-2.794	<0.01
Survey 21	-6.115	<0.001	-4.643	<0.001
Survey 22	-1.471	n.s.	-1.078	n.s.
Survey 23	-2.073	<0.05	-3.276	<0.001
Survey 24	-12.575	<0.001	-3.572	<0.001
Sample size (n)	8081		1145	
Adjusted R ²	11.60%		4.60%	
AUC	0.78			
Spearman's corr.	0.20			

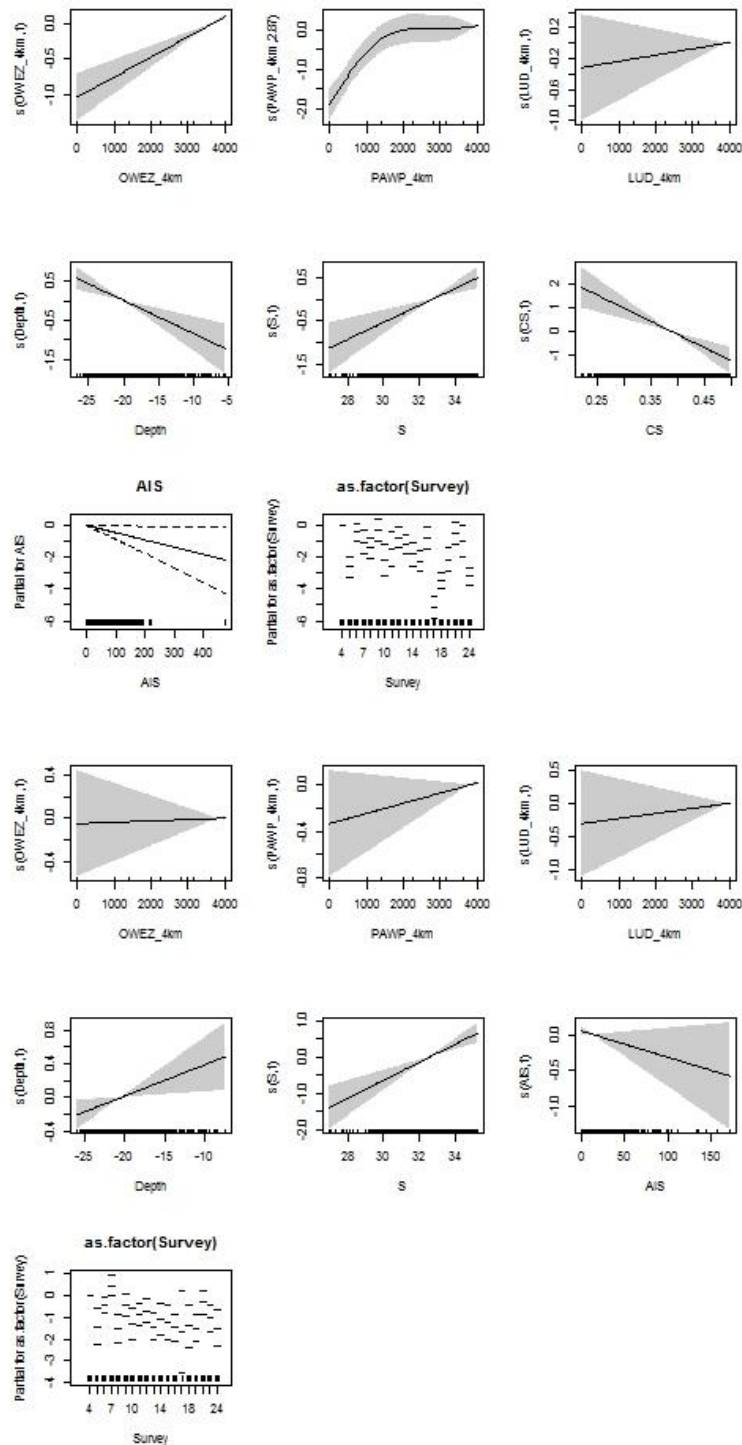


Figure A.3. Partial GAM plots for the Northern Gannet distribution model – presence-absence (upper panel) and positive density (lower panel) parts. The values of the environmental variables are shown on the X-axis and the probability on the Y-axis in the scale of the linear predictor. The grey shaded areas and the dotted lines (for factors) show the 95% Bayesian confidence intervals. The degree of smoothing is indicated in the legend of the Y-axis.

Great Cormorant

Table A.4. Smooth terms, adjusted R-squared and evaluation statistics for the Great Cormorant distribution models. F statistics and the approximate significance for the smooth terms and t-statistic and the significance for the parametric terms are shown. Variables not included in either the presence/absence or positive model part are indicated with a dash. The results of the evaluation test show AUC for presence/absence and the Spearman's correlation for the density predictions. The evaluation test is based on a model fitted on 70% and tested on 30% of withheld data. 'n.s.' indicates terms with p-values > 0.05. The significant effect of the windfarms are marked in bold.

Smooth terms	Presence/absence		Positive density	
	F	p	F	p
LUD (max 4 km)	39.656	<0.001	0.378	n.s.
PAWP (max 4 km)	63.683	<0.001	8.715	<0.01
OWEZ (max 4 km)	34.19	<0.001	40.742	<0.001
Depth	16.181	<0.001	-	
Salinity	2.665	n.s.	1.12	n.s.
Shipping intensity (AIS)	30.487	<0.001	-	
Current speed	5.112	<0.01	-	
Eddy potential (vorticity)	-		18.984	<0.001
Current gradient	-		-	
Parametric terms	T	p	t	p
AIS (if parametric)	-		-	
Survey 5	0.211	n.s.	-1.849	n.s.
Survey 6	-1.578	n.s.	3.484	<0.001
Survey 7	-1.747	n.s.	1.01	n.s.
Survey 8	4.058	<0.001	0.057	n.s.
Survey 9	2.528	<0.05	-0.667	n.s.
Survey 10	1.041	n.s.	-1.217	n.s.
Survey 11	-0.673	n.s.	-0.26	n.s.
Survey 12	-0.453	n.s.	-0.542	n.s.
Survey 13	1.166	n.s.	-0.249	n.s.
Survey 14	1.267	n.s.	-1.153	n.s.
Survey 15	-0.047	n.s.	0.167	n.s.
Survey 16	-0.398	n.s.	-2.132	<0.05
Survey 17	-3.215	<0.001	-0.676	n.s.
Survey 18	-2.812	<0.01	-0.688	n.s.
Survey 21	-1.486	n.s.	-0.148	n.s.
Survey 22	-0.14	n.s.	-0.447	n.s.
Survey 23	0.379	n.s.	-1.285	n.s.
Survey 24	-1.439	n.s.	0.073	n.s.
Sample size (n)	8081		439	
Adjusted R ²	15.10%		0%	
AUC	0.87			
Spearman's corr.	0.15			

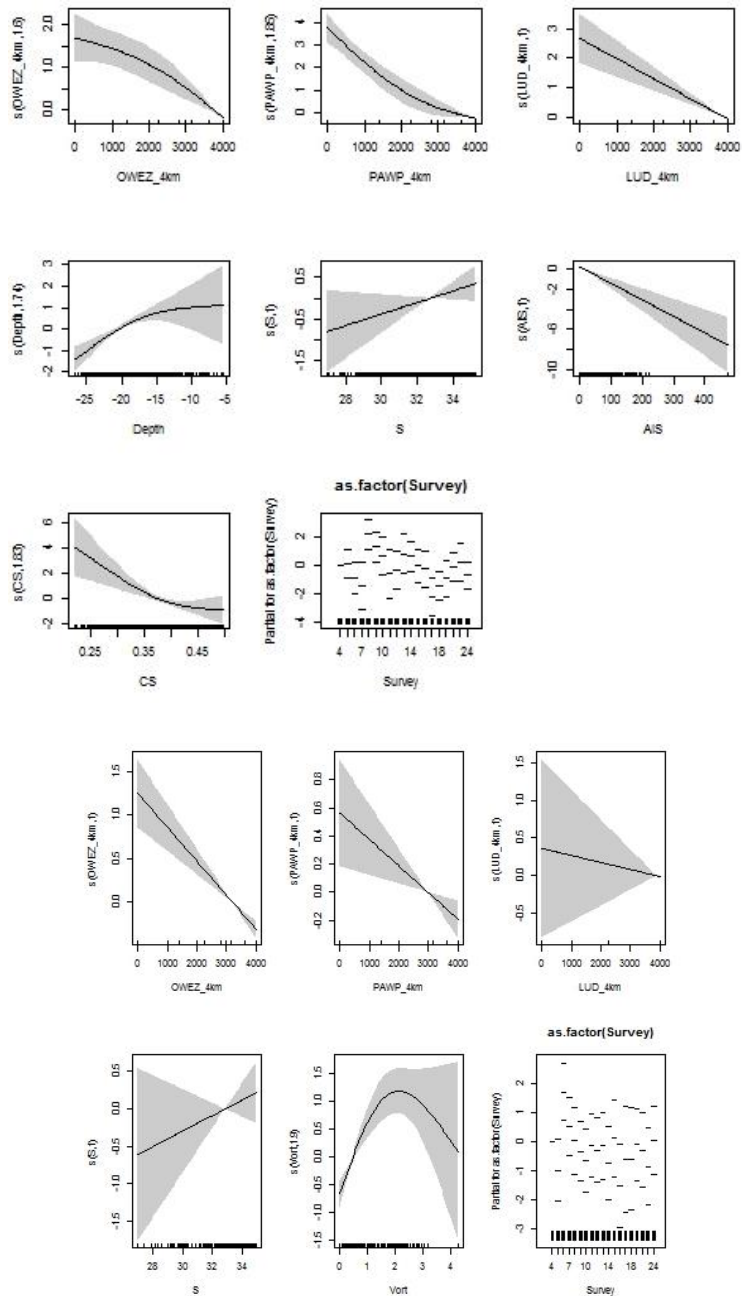


Figure A.4. Partial GAM plots for the Great Cormorant distribution model – presence-absence (upper panel) and positive density (lower panel) parts. The values of the environmental variables are shown on the X-axis and the probability on the Y-axis in the scale of the linear predictor. The grey shaded areas and the dotted lines (for factors) show the 95% Bayesian confidence intervals. The degree of smoothing is indicated in the legend of the Y-axis.

Little Gull

Table A.5. Smooth terms, adjusted R-squared and evaluation statistics for the Little Gull distribution models. F statistics and the approximate significance for the smooth terms and t-statistic and the significance for the parametric terms are shown. Variables not included in either the presence/absence or positive model part are indicated with a dash. The evaluation test did not converge due to too low sample size. 'n.s.' indicates terms with p-values > 0.05. The significant effect of the windfarms are marked in bold.

Smooth terms	Presence/absence		Positive density	
	F	p	F	p
LUD (max 4 km)	40.861	<0.001	0.401	n.s.
PAWP (max 4 km)	6.35	<0.05	0.077	n.s.
OWEZ (max 4 km)	0.712	n.s.	0.028	n.s.
Depth	1.454		-	
Salinity	5.722	<0.05	-	
Shipping intensity (AIS)	-		-	
Current speed	1.08	n.s.	-	
Eddy potential (vorticity)	-		-	
Current gradient	1.684	n.s.	-	
Parametric terms	T	p	t	p
AIS (if parametric)	-3.338	<0.001	-	
Survey 5	2.157	<0.05	-2.386	<0.05
Survey 6	1.413	n.s.	-2.181	<0.05
Survey 7	-0.79	n.s.	-0.868	n.s.
Survey 8	-		-	
Survey 9	4.479	<0.001	-0.131	n.s.
Survey 10	0.103	n.s.	-1.628	n.s.
Survey 11	3.079	<0.01	-0.32	n.s.
Survey 12	0.553	n.s.	-1.112	n.s.
Survey 13	-0.075	n.s.	-0.55	n.s.
Survey 14	3.637	<0.001	-1.177	n.s.
Survey 15	1.322	n.s.	-0.849	n.s.
Survey 16	3.234	<0.001	0.658	n.s.
Survey 17	2.548	<0.05	-1.789	n.s.
Survey 18	2.768	<0.01	-1.065	n.s.
Survey 21	0.965	n.s.	0.05	n.s.
Survey 22	0.467	n.s.	-1.058	n.s.
Survey 23	-0.414	n.s.	0.703	n.s.
Survey 24	3.863	<0.001	0.812	n.s.
Sample size (n)	7607		258	
Adjusted R ²	4.20%		0.00%	
AUC	-			
Spearman's corr.	-			

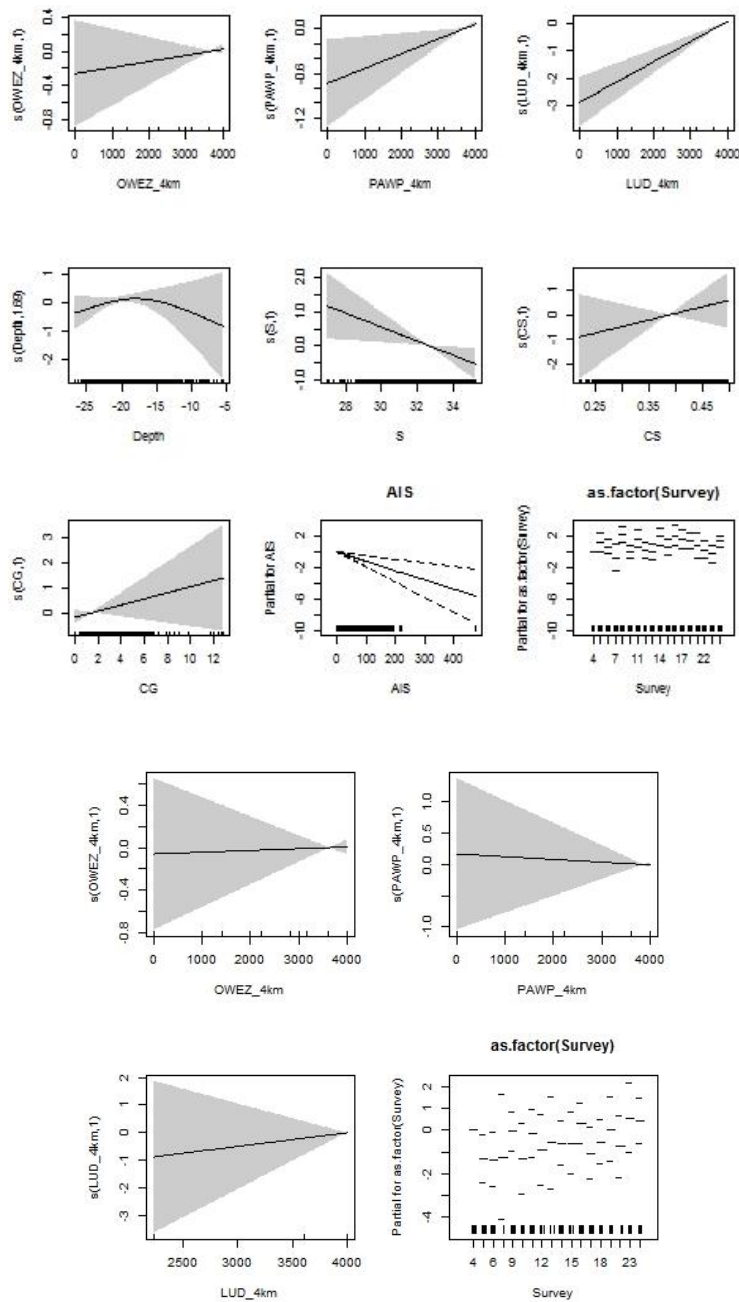


Figure A.5. Partial GAM plots for the Little Gull distribution model – presence-absence (upper panel) and positive density (lower panel) parts. The values of the environmental variables are shown on the X-axis and the probability on the Y-axis in the scale of the linear predictor. The grey shaded areas and the dotted lines (for factors) show the 95% Bayesian confidence intervals. The degree of smoothing is indicated in the legend of the Y-axis.

Black-headed Gull

Table A.6. Smooth terms, adjusted R-squared and evaluation statistics for the Black-headed Gull distribution models. F statistics and the approximate significance for the smooth terms and t-statistic and the significance for the parametric terms are shown. Variables not included in either the presence/absence or positive model part are indicated with a dash. The evaluation test did not converge due to too low sample size. 'n.s.' indicates terms with p-values > 0.05. The significant effect of the windfarms are marked in bold.

Smooth terms	Presence/absence		Positive density	
	F	p	F	p
LUD (max 4 km)	1.669	n.s	-	-
PAWP (max 4 km)	0.122	n.s	3.852	n.s
OWEZ (max 4 km)	0.339	n.s	1.534	n.s
Depth	53.626	<0.001	-	-
Salinity	-	-	-	-
Shipping intensity (AIS)	-	-	-	-
Current speed	-	-	-	-
Eddy potential (vorticity)	-	-	-	-
Current gradient	-	-	-	-
Parametric terms	T	p	t	p
AIS (if parametric)	-	-	-	-
Survey 5	-0.775	n.s.	0.121	n.s.
Survey 6	-0.128	n.s.	-1.214	n.s.
Survey 7	-1.559	n.s.	0.224	n.s.
Survey 8	1.09	n.s.	1.242	n.s.
Survey 9	-1.48	n.s.	0.223	n.s.
Survey 10	-	-	-	-
Survey 11	-1.856	n.s.	0.648	n.s.
Survey 12	-2.383	<0.05	-0.001	n.s.
Survey 13	1.06	n.s.	-0.259	n.s.
Survey 14	-1.87	n.s.	-1.061	n.s.
Survey 15	-3.86	<0.001	-0.429	n.s.
Survey 16	1.216	n.s.	0.855	n.s.
Survey 17	-5.902	<0.001	0.185	n.s.
Survey 18	-1.636	n.s.	4.478	<0.001
Survey 21	0.666	n.s.	-0.015	n.s.
Survey 22	1.713	n.s.	-0.824	n.s.
Survey 23	-3.134	<0.01	-0.905	n.s.
Survey 24	-1.855	n.s.	0.787	n.s.
Sample size (n)	7663		174	
Adjusted R ²	3.30%		1.30%	
AUC	-		-	
Spearman's corr.	-		-	

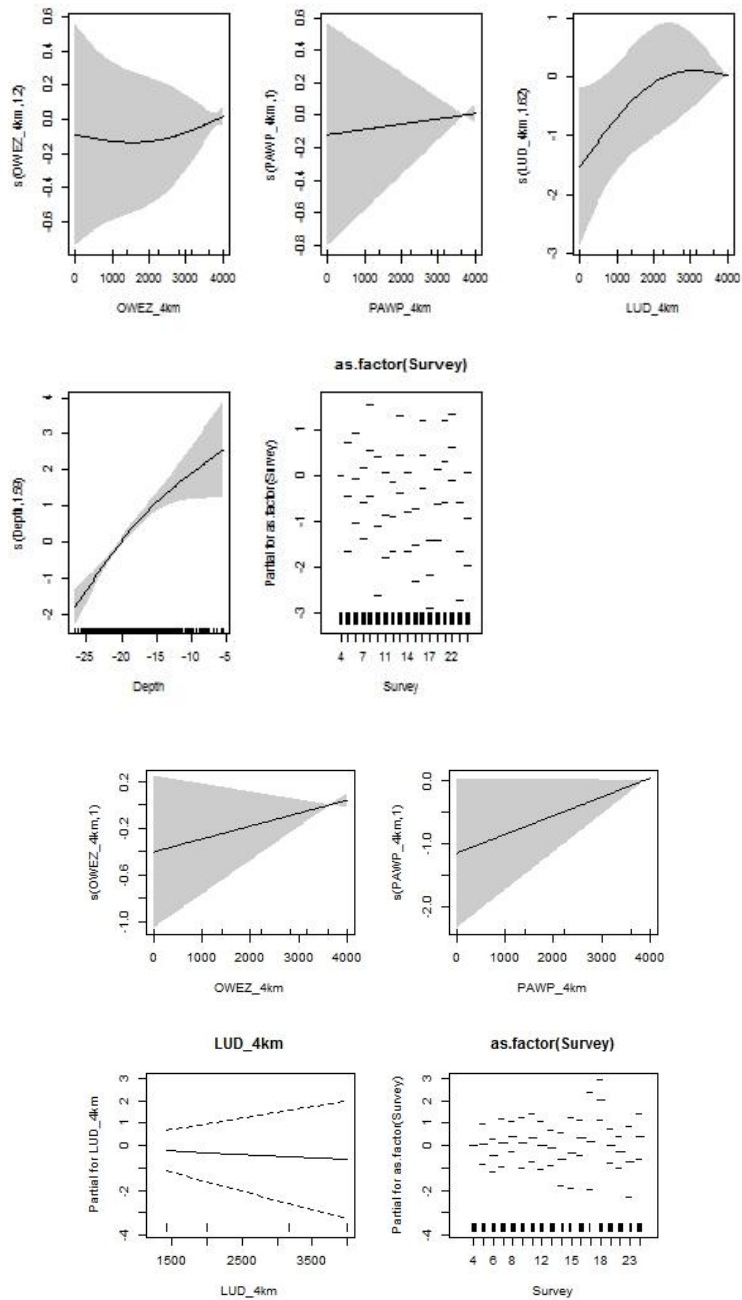


Figure A.6. Partial GAM plots for the Black-headed Gull distribution model – presence-absence (upper panel) and positive density (lower panel) parts. The values of the environmental variables are shown on the X-axis and the probability on the Y-axis in the scale of the linear predictor. The grey shaded areas and the dotted lines (for factors) show the 95% Bayesian confidence intervals. The degree of smoothing is indicated in the legend of the Y-axis.

Common Gull

Table A.7. Smooth terms, adjusted R-squared and evaluation statistics for the Common Gull distribution models. F statistics and the approximate significance for the smooth terms and t-statistic and the significance for the parametric terms are shown. Variables not included in either the presence/absence or positive model part are indicated with a dash. The evaluation test did not converge due to too low sample size. 'n.s.' indicates terms with p-values > 0.05.

Smooth terms	Presence/absence		Positive density	
	F	P	F	p
LUD (max 4 km)	0.75	n.s	2.331	n.s
PAWP (max 4 km)	0.094	n.s	0.204	n.s
OWEZ (max 4 km)	2.473	n.s	1.315	n.s
Depth	45.115	<0.001	1.473	n.s.
Salinity	-		2.744	n.s.
Shipping intensity (AIS)	-		-	
Current speed	-		14.527	<0.001
Eddy potential (vorticity)	-		-	
Current gradient	8.556	<0.01	0.337	n.s.
Parametric terms	t	P	t	p
AIS (if parametric)	-		-	
Survey 5	2.094	<0.05	-2.259	<0.05
Survey 6	7.345	<0.001	-3.785	<0.001
Survey 7	4.65	<0.001	-1.726	n.s.
Survey 8	-1.701	n.s.	-0.835	n.s.
Survey 9	-2.484	<0.05	-0.178	n.s.
Survey 10	6.33	<0.001	-0.577	n.s.
Survey 11	1.275	n.s.	-4.252	<0.001
Survey 12	-3.045	<0.01	-3.38	<0.001
Survey 13	0.931	n.s.	-1.278	n.s.
Survey 14	1.589	n.s.	-0.326	n.s.
Survey 15	2.131	<0.05	-1.528	n.s.
Survey 16	-4.585	<0.001	-0.475	n.s.
Survey 17	-6.185	<0.001	-3.231	<0.001
Survey 18	-3.389	<0.001	1.722	n.s.
Survey 21	0.985	n.s.	-2.576	<0.01
Survey 22	-1.521	n.s.	1.911	n.s.
Survey 23	-0.142	n.s.	2.218	<0.05
Survey 24	-2.177	<0.05	-1.421	n.s.
Sample size (n)	8081		1583	
Adjusted R ²	13.30%		4.00%	
AUC	-			
Spearman's corr.	-			

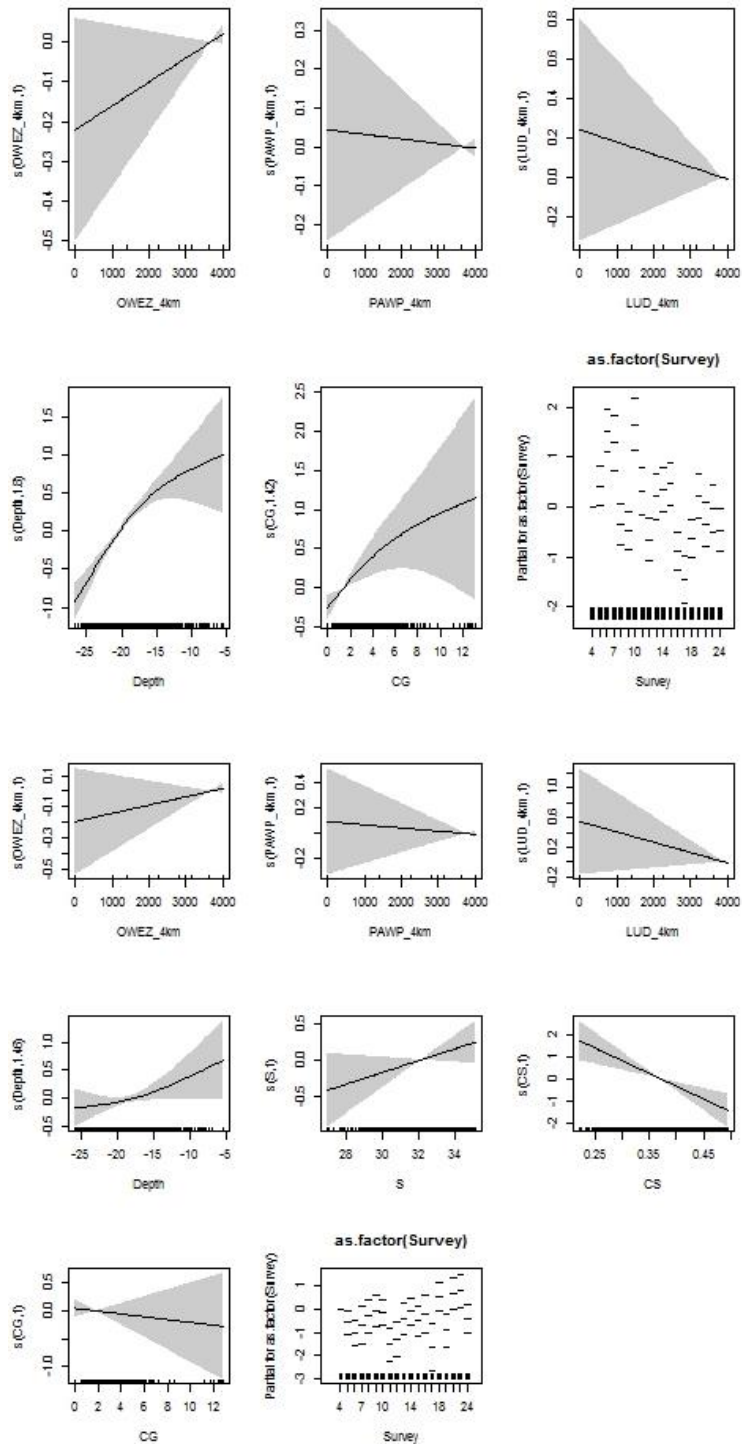


Figure A.7. Partial GAM plots for the Common Gull distribution model – presence-absence (upper panel) and positive density (lower panel) parts. The values of the environmental variables are shown on the X-axis and the probability on the Y-axis in the scale of the linear predictor. The grey shaded areas and the dotted lines (for factors) show the 95% Bayesian confidence intervals. The degree of smoothing is indicated in the legend of the Y-axis.

Lesser Black-backed Gull

Table A.8. Smooth terms, adjusted R-squared and evaluation statistics for the Lesser Black-backed Gull distribution models. F statistics and the approximate significance for the smooth terms and t-statistic and the significance for the parametric terms are shown. Variables not included in either the presence/absence or positive model part are indicated with a dash. The evaluation test did not converge due to too low sample size. 'n.s.' indicates terms with p-values > 0.05.

Smooth terms	Presence/absence		Positive density	
	F	p	F	p
LUD (max 4 km)	0.021	n.s	1.811	n.s
PAWP (max 4 km)	0	n.s	2.09	n.s
OWEZ (max 4 km)	2.848	n.s	0	n.s
Depth	7.327	<0.01	8.324	<0.001
Salinity	7.551	<0.01	-	
Shipping intensity (AIS)	-		-	
Current speed	6.134	<0.05	-	
Eddy potential (vorticity)	-		-	
Current gradient	-		-	
Parametric terms	t	p	t	p
AIS (if parametric)	-		-	
Survey 5	-1.552	n.s.	-0.608	n.s.
Survey 6	2.836	<0.01	-0.552	n.s.
Survey 7	-5.157	<0.001	-0.161	n.s.
Survey 8	5.547	<0.001	0.59	n.s.
Survey 9	3.118	<0.01	-0.223	n.s.
Survey 10	-		-	
Survey 11	1.88	n.s.	-0.532	n.s.
Survey 12	4.761	<0.001	0.405	n.s.
Survey 13	1.742	n.s.	0.14	n.s.
Survey 14	1.01	n.s.	0.011	n.s.
Survey 15	5.459	<0.001	-0.011	n.s.
Survey 16	6.2	<0.001	0.685	n.s.
Survey 17	-5.212	<0.001	0.063	n.s.
Survey 18	-2.752	<0.01	0.705	n.s.
Survey 21	6.315	<0.001	0.706	n.s.
Survey 22	2.839	<0.01	0.289	n.s.
Survey 23	3.686	<0.001	0.518	n.s.
Survey 24	7.42	<0.001	2.001	<0.05
Sample size (n)	7663		610	
Adjusted R ²	8.40%		0.70%	
AUC	-			
Spearman's corr.	-			

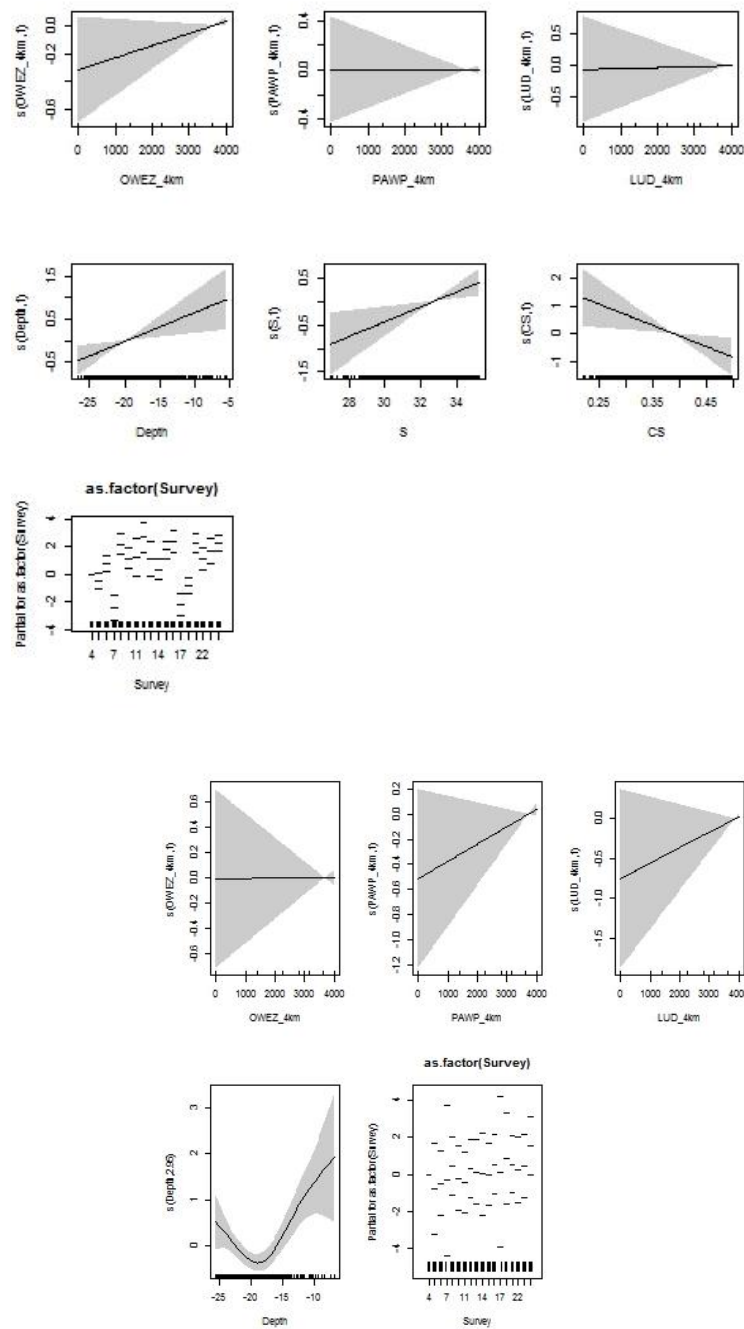


Figure A.8. Partial GAM plots for the Lesser Black-backed Gull distribution model – presence-absence (upper panel) and positive density (lower panel) parts. The values of the environmental variables are shown on the X-axis and the probability on the Y-axis in the scale of the linear predictor. The grey shaded areas and the dotted lines (for factors) show the 95% Bayesian confidence intervals. The degree of smoothing is indicated in the legend of the Y-axis.

Herring Gull

Table A.9. Smooth terms, adjusted R-squared and evaluation statistics for the Herring Gull distribution models. F statistics and the approximate significance for the smooth terms and t-statistic and the significance for the parametric terms are shown. Variables not included in either the presence/absence or positive model part are indicated with a dash. The results of the evaluation test show AUC for presence/absence and the Spearman's correlation for the density predictions. The evaluation test is based on a model fitted on 70% and tested on 30% of withheld data. 'n.s.' indicates terms with p-values > 0.05.

Smooth terms	Presence/absence		Positive density	
	F	p	F	p
LUD (max 4 km)	1.009	n.s	0.768	n.s
PAWP (max 4 km)	0.579	n.s	0.038	n.s
OWEZ (max 4 km)	0.249	n.s	0.038	n.s
Depth	20.758	<0.001	-	
Salinity	-		15.397	<0.001
Shipping intensity (AIS)	-		-	
Current speed	-		14.748	<0.001
Eddy potential (vorticity)	-		-	
Current gradient	5.287	<0.01	3.782	<0.05
Parametric terms	t	p	t	p
AIS (if parametric)	-		-	
Survey 5	3.893	<0.001	-3.694	<0.001
Survey 6	1.457	n.s.	-3.552	<0.001
Survey 7	4.387	<0.001	-2.956	<0.01
Survey 8	-0.613	n.s.	-1.316	n.s.
Survey 9	-2.328	<0.05	-0.962	n.s.
Survey 10	-1.186	n.s.	-2.764	<0.01
Survey 11	-1.519	n.s.	-4.688	<0.001
Survey 12	0.055	n.s.	-4.382	<0.001
Survey 13	-3.288	<0.001	-0.82	n.s.
Survey 14	-2.915	<0.01	-1.757	n.s.
Survey 15	-1.366	n.s.	-2.287	<0.05
Survey 16	-5.092	<0.001	0.561	n.s.
Survey 17	-2.257	<0.05	-2.652	<0.01
Survey 18	-0.412	n.s.	0.272	n.s.
Survey 21	0.022	n.s.	-4.463	<0.001
Survey 22	1.426	n.s.	1.669	n.s.
Survey 23	-2.708	<0.01	0.951	n.s.
Survey 24	-3.324	<0.001	-1.404	n.s.
Sample size (n)	8081		804	
Adjusted R ²	13.10%		7.10%	
AUC	0.76			
Spearman's corr.	0.15			

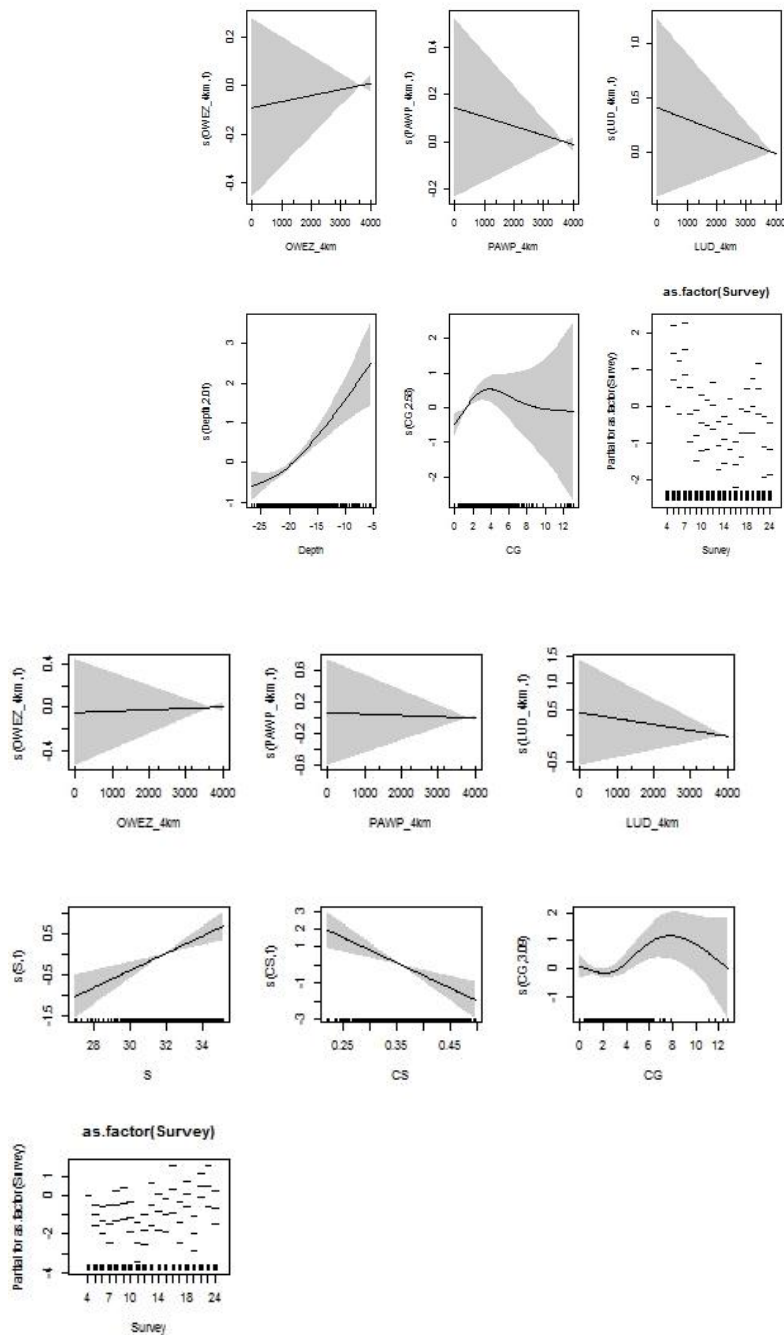


Figure A.9. Partial GAM plots for the Herring Gull distribution model – presence-absence (upper panel) and positive density (lower panel) parts. The values of the environmental variables are shown on the X-axis and the probability on the Y-axis in the scale of the linear predictor. The grey shaded areas and the dotted lines (for factors) show the 95% Bayesian confidence intervals. The degree of smoothing is indicated in the legend of the Y-axis.

Great Black-backed Gull

Table A.10. Smooth terms, adjusted R-squared and evaluation statistics for the Great Black-backed Gull distribution models. F statistics and the approximate significance for the smooth terms and t-statistic and the significance for the parametric terms are shown. Variables not included in either the presence/absence or positive model part are indicated with a dash. The results of the evaluation test show AUC for presence/absence and the Spearman's correlation for the density predictions. The evaluation test is based on a model fitted on 70% and tested on 30% of withheld data. 'n.s.' indicates terms with p-values > 0.05. The significant effect of the windfarms are marked in bold.

Smooth terms	Presence/absence		Positive density	
	F	p	F	p
LUD (max 4 km)	0.017	n.s	0.081	n.s
PAWP (max 4 km)	7.85	<0.01	1.574	n.s
OWEZ (max 4 km)	6.207	<0.05	5.987	<0.001
Depth	20.323	<0.001	6.674	<0.001
Salinity	14.269	<0.001	5.638	<0.05
Shipping intensity (AIS)	-	-	-	-
Current speed	-	-	-	-
Eddy potential (vorticity)	-	-	-	-
Current gradient	5.201	<0.05	10.2	<0.001
Parametric terms	T	p	t	p
AIS (if parametric)	-	-	-	-
Survey 5	-0.092	n.s.	-2.436	<0.05
Survey 6	2.313	<0.05	-0.072	n.s.
Survey 7	-0.952	n.s.	2.42	<0.05
Survey 8	-1.868	n.s.	-1.729	n.s.
Survey 9	-3.598	<0.001	-1.299	n.s.
Survey 10	-4.463	<0.001	-1.9	n.s.
Survey 11	-4.337	<0.001	-2.676	<0.01
Survey 12	-1.325	n.s.	-0.774	n.s.
Survey 13	-2.554	<0.05	-0.333	n.s.
Survey 14	-3.006	<0.01	-2.03	<0.05
Survey 15	-6.275	<0.001	-1.714	n.s.
Survey 16	-6.028	<0.001	-1.061	n.s.
Survey 17	-8.76	<0.001	-1.209	n.s.
Survey 18	-10.494	<0.001	0.606	n.s.
Survey 21	-5.02	<0.001	-1.261	n.s.
Survey 22	-4.467	<0.001	1.475	n.s.
Survey 23	-4.765	<0.001	1.219	n.s.
Survey 24	-6.818	<0.001	-0.894	n.s.
Sample size (n)	8081		1548	
Adjusted R ²	10.40%		1.10%	
AUC	0.73			
Spearman's corr.	0.18			

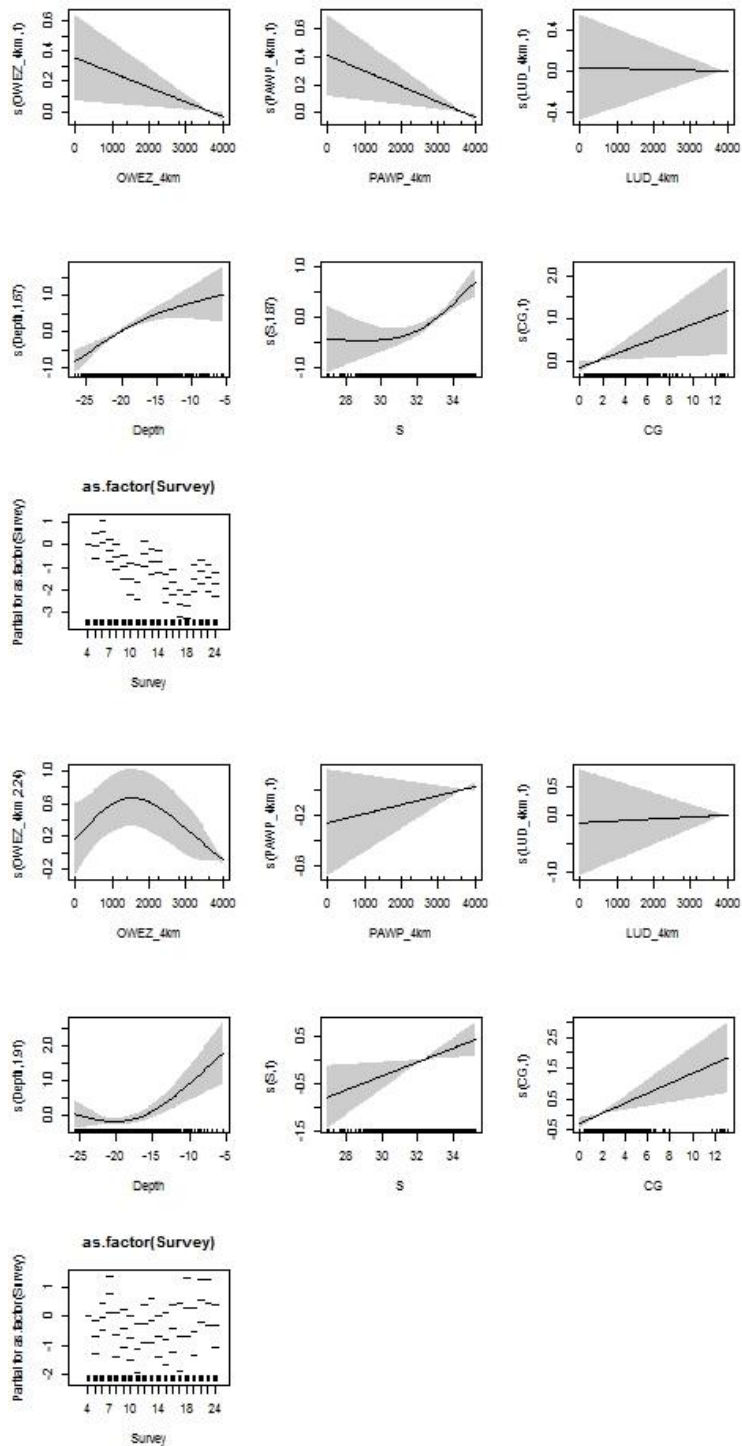


Figure A.10. Partial GAM plots for the Great Black-backed Gull distribution model – presence-absence (upper panel) and positive density (lower panel) parts. The values of the environmental variables are shown on the X-axis and the probability on the Y-axis in the scale of the linear predictor. The grey shaded areas and the dotted lines (for factors) show the 95% Bayesian confidence intervals. The degree of smoothing is indicated in the legend of the Y-axis.

Black-legged Kittiwake

Table A.11. Smooth terms, adjusted R-squared and evaluation statistics for the Black-legged distribution models. F statistics and the approximate significance for the smooth terms and t-statistic and the significance for the parametric terms are shown. Variables not included in either the presence/absence or positive model part are indicated with a dash. The evaluation test did not converge due to low sample size. 'n.s.' indicates terms with p-values > 0.05. The significant effect of the windfarms are marked in bold.

Smooth terms	Presence/absence		Positive density	
	F	p	F	p
LUD (max 4 km)	3.847	n.s	5.965	<0.05
PAWP (max 4 km)	0.005	n.s	0.799	n.s
OWEZ (max 4 km)	2.983	n.s	0.416	n.s
Depth	2.13	n.s.	0.164	n.s.
Salinity	-		0.962	n.s.
Shipping intensity (AIS)	-		-	
Current speed	2.526	n.s.	0.342	n.s.
Eddy potential (vorticity)	7.349	<0.01	-	
Current gradient	-		4.063	<0.05
Parametric terms	t	p	t	p
AIS (if parametric)	-1.332		-	
Survey 5	-0.946	n.s.	-2.286	<0.05
Survey 6	-4.282	<0.001	-2.706	<0.01
Survey 7	0.413	n.s.	-0.866	n.s.
Survey 8	-10.432	<0.001	-1.697	n.s.
Survey 9	-4.652	<0.001	-0.97	n.s.
Survey 10	-11.547	<0.001	-1.601	n.s.
Survey 11	-8.316	<0.001	-0.829	n.s.
Survey 12	-3.976	<0.001	-1.708	n.s.
Survey 13	-3.16	<0.01	-1.614	n.s.
Survey 14	0.01	n.s.	1.18	n.s.
Survey 15	-2.513	<0.05	-2.27	<0.05
Survey 16	-10.206	<0.001	-0.884	n.s.
Survey 17	-3.892	<0.001	-1.744	n.s.
Survey 18	-5.832	<0.001	-1.394	n.s.
Survey 21	-7.874	<0.001	-2.151	<0.05
Survey 22	-2.094	<0.05	5.081	<0.001
Survey 23	-5.508	<0.001	-1.063	n.s.
Survey 24	-9.976	<0.001	-0.096	n.s.
Sample size (n)	8081		1693	
Dev. Exp.	19.20%		3.00%	
Adjusted R ²	-			
Spearman's corr.	-			

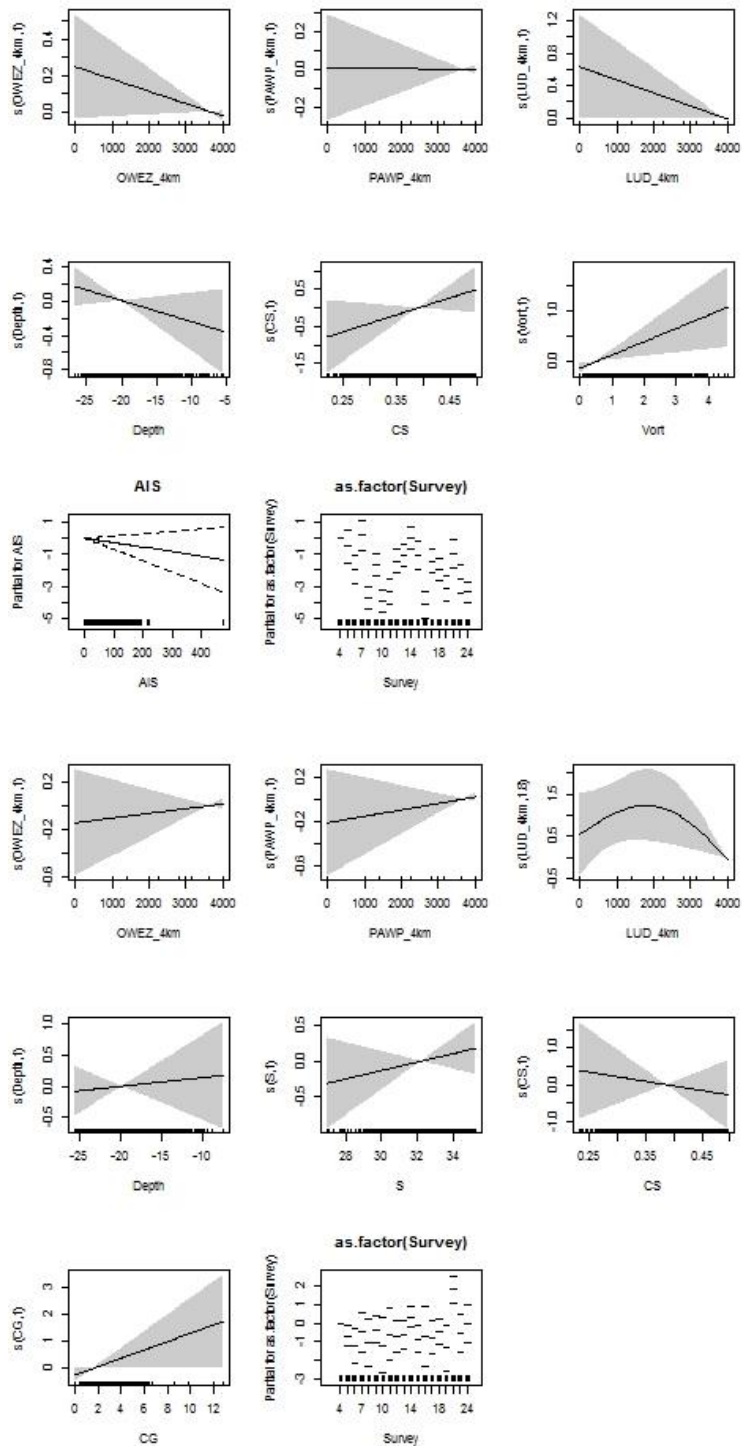


Figure A.11. Partial GAM plots for the Kittiwake distribution model – presence-absence (upper panel) and positive density (lower panel) parts. The values of the environmental variables are shown on the X-axis and the probability on the Y-axis in the scale of the linear predictor. The grey shaded areas and the dotted lines (for factors) show the 95% Bayesian confidence intervals. The degree of smoothing is indicated in the legend of the Y-axis.

Common Guillemot

Table A.12. Smooth terms, adjusted R-squared and evaluation statistics for the Common Guillemot distribution models. F statistics and the approximate significance for the smooth terms and t-statistic and the significance for the parametric terms are shown. Variables not included in either the presence/absence or positive model part are indicated with a dash. The results of the evaluation test show AUC for presence/absence and the Spearman's correlation for the density predictions. The evaluation test is based on a model fitted on 70% and tested on 30% of withheld data. 'n.s.' indicates terms with p-values < 0.05. The significant effect of the windfarms are marked in bold.

Smooth terms	Presence/absence		Positive density	
	F	p	F	p
LUD (max 4 km)	4.553	<0.05	0.99	n.s
PAWP (max 4 km)	27.581	<0.001	8.585	<0.01
OWEZ (max 4 km)	10.888	<0.001	1.804	n.s
Depth	-		5.86	<0.05
Salinity	17.191	<0.001	-	
Shipping intensity (AIS)	-		-	
Current speed	11.903	<0.001	4.5	<0.05
Eddy potential (vorticity)	-		-	
Current gradient	-		-	
Parametric terms	t	p	t	p
AIS (if parametric)	-1.955	n.s.	-1.582	n.s.
Survey 5	-0.923	n.s.	-2.899	<0.01
Survey 6	-4.822	<0.001	-3.989	<0.001
Survey 7	2.064	<0.05	-1.294	n.s.
Survey 8	-18.596	<0.001	-3.319	<0.001
Survey 9	-6.521	<0.001	-4.448	<0.001
Survey 10	-6.435	<0.001	-4.346	<0.001
Survey 11	-8.734	<0.001	-2.156	<0.05
Survey 12	-3.493	<0.001	-2.956	<0.01
Survey 13	0.464	n.s.	-3.635	<0.001
Survey 14	-0.973	n.s.	-3.343	<0.001
Survey 15	-8.395	<0.001	-5.223	<0.001
Survey 16	-6.169	<0.001	-3.233	<0.001
Survey 17	1.596	n.s.	-1.087	n.s.
Survey 18	7.466	<0.001	3.016	<0.01
Survey 21	-0.972	n.s.	-2.335	<0.05
Survey 22	3.208	<0.001	4.694	<0.001
Survey 23	-2.964	<0.01	-2.377	<0.05
Survey 24	-9.296	<0.001	-3.776	<0.001
Sample size (n)	8081		2255	
Adjusted R ²	26.40%		16.70%	
AUC	0.81			
Spearman's corr.	0.52			

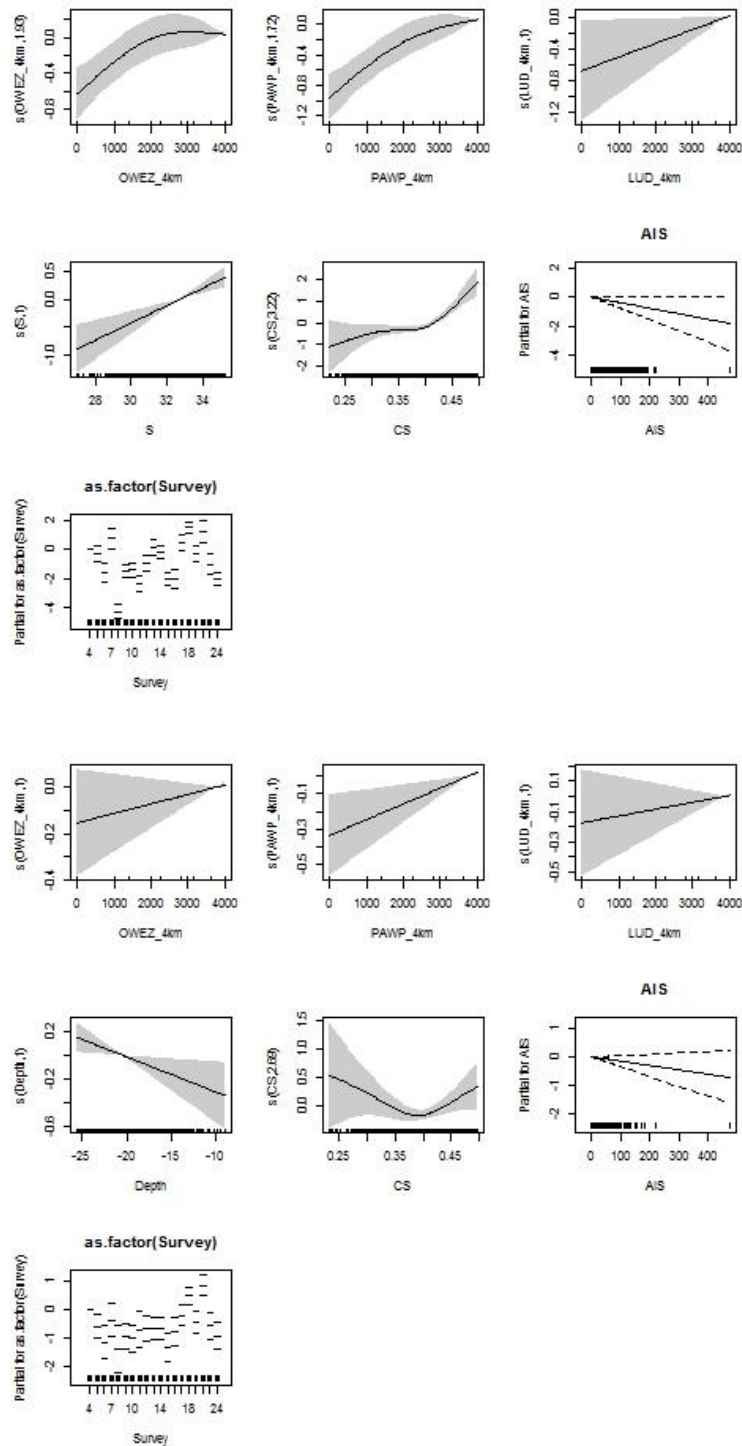


Figure A.12. Partial GAM plots for the Common Guillemot distribution model – presence-absence (upper panel) and positive (lower panel) parts. The values of the environmental variables are shown on the X-axis and the probability on the Y-axis in the scale of the linear predictor. The grey shaded areas and the dotted lines (for factors) show the 95% Bayesian confidence intervals. The degree of smoothing is indicated in the legend of the Y-axis.

Razorbill

Table A.13. Smooth terms, adjusted R-squared and evaluation statistics for the Razorbill distribution models. F statistics and the approximate significance for the smooth terms and t-statistic and the significance for the parametric terms are shown. Variables not included in either the presence/absence or positive model part are indicated with a dash. The evaluation test did not converge due to low sample size. 'n.s.' indicates terms with p-values < 0.05. The significant effect of the windfarms are marked in bold.

Smooth terms	Presence/absence		Positive density	
	F	p	F	p
LUD (max 4 km)	3.38	n.s	0.036	n.s
PAWP (max 4 km)	5.411	<0.05	2.42	n.s
OWEZ (max 4 km)	0.508	n.s	2.117	n.s
Depth	11.467	<0.01	1.036	
Salinity	-		2.732	
Shipping intensity (AIS)	-		4.185	<0.05
Current speed	9.379	<0.01	-	
Eddy potential (vorticity)	-		5.863	<0.05
Current gradient	-		-	
Parametric terms	t	p	t	p
AIS (if parametric)	-		-	
Survey 5	-2.45	<0.05	-1.61	
Survey 6	-2.77	<0.01	-1.381	
Survey 7	3.727	<0.001	-0.873	
Survey 8	-8.397	<0.001	-1.664	
Survey 9	-4.757	<0.001	-0.652	
Survey 10	-1.359		-2.647	<0.01
Survey 11	-0.31		-0.211	
Survey 12	1.982	<0.05	-1.308	
Survey 13	1.534		-2.566	<0.05
Survey 14	3.849	<0.001	-2.68	<0.01
Survey 15	0.223		-3.341	<0.001
Survey 16	-0.242		-0.299	
Survey 17	2.344	<0.05	-0.228	
Survey 18	-2.722	<0.01	-1.956	
Survey 21	4.676	<0.001	-0.582	
Survey 22	1.676		-1.159	
Survey 23	0.349		-0.507	
Survey 24	0.905		-0.777	
Adjusted R ²	8081		321	
Dev. Exp.	4.50%		4.60%	
AUC	-			
Spearman's corr.	-			

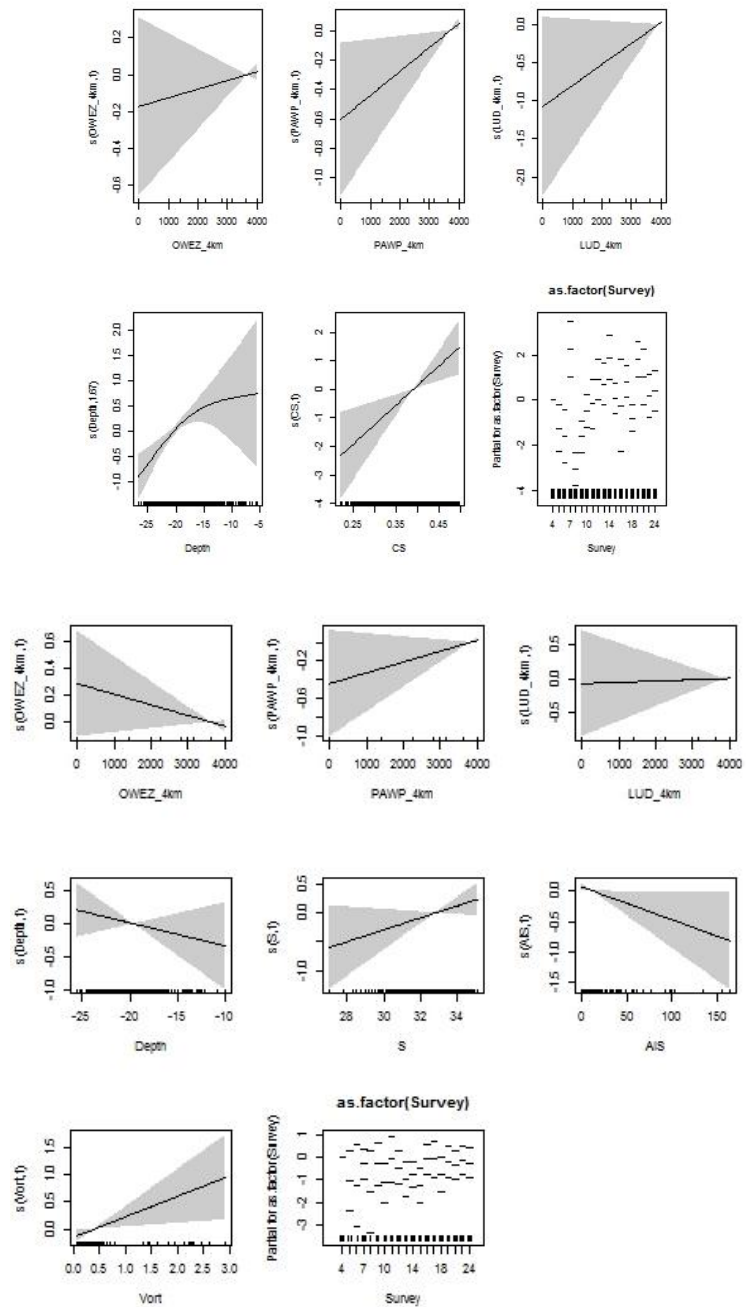


Figure A13. Partial GAM plots for the Razorbill distribution model – presence-absence (upper panel) and positive density (lower panel) parts. The values of the environmental variables are shown on the X-axis and the probability on the Y-axis in the scale of the linear predictor. The grey shaded areas and the dotted lines (for factors) show the 95% Bayesian confidence intervals. The degree of smoothing is indicated in the legend of the Y-axis.

APPENDIX B – Overview of the environmental variables in the “greater” study area during surveys between February 2012 and March 2016

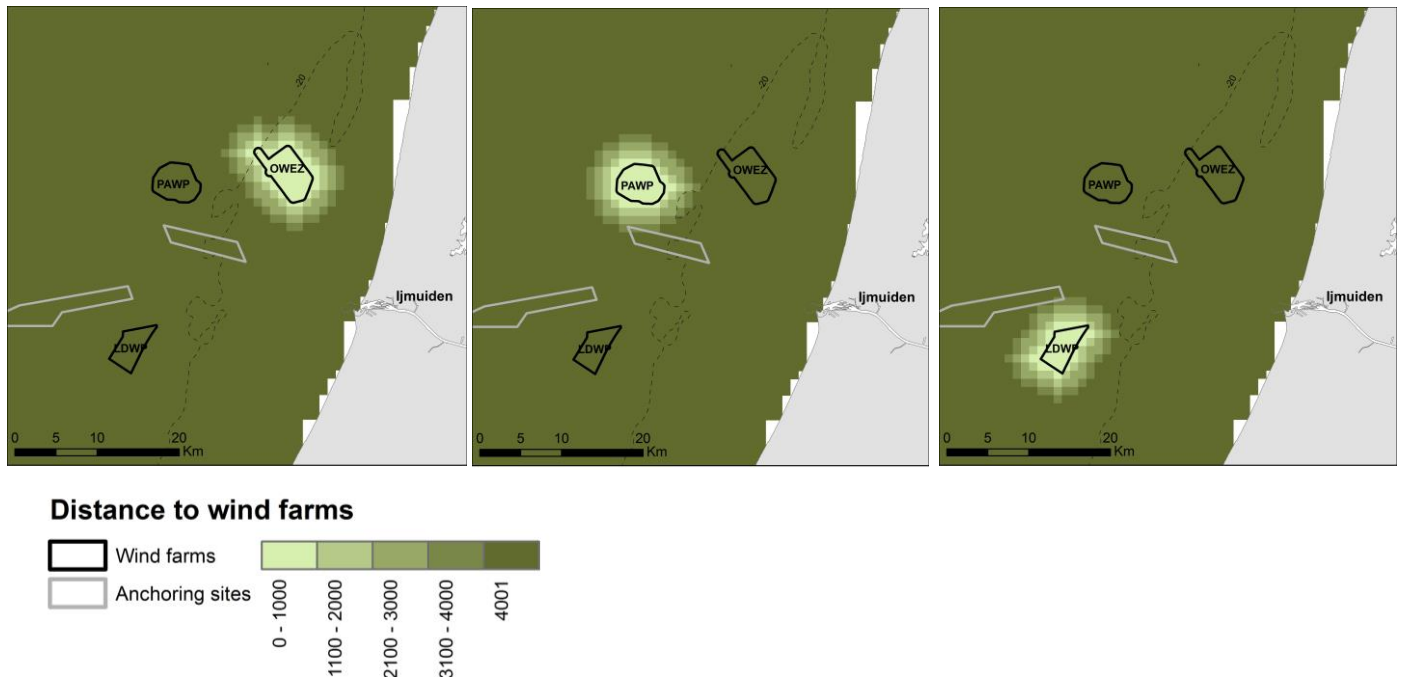


Figure B.1 Distance to windfarms [m]. Distances > 4000 m are all equal to 4001 m.

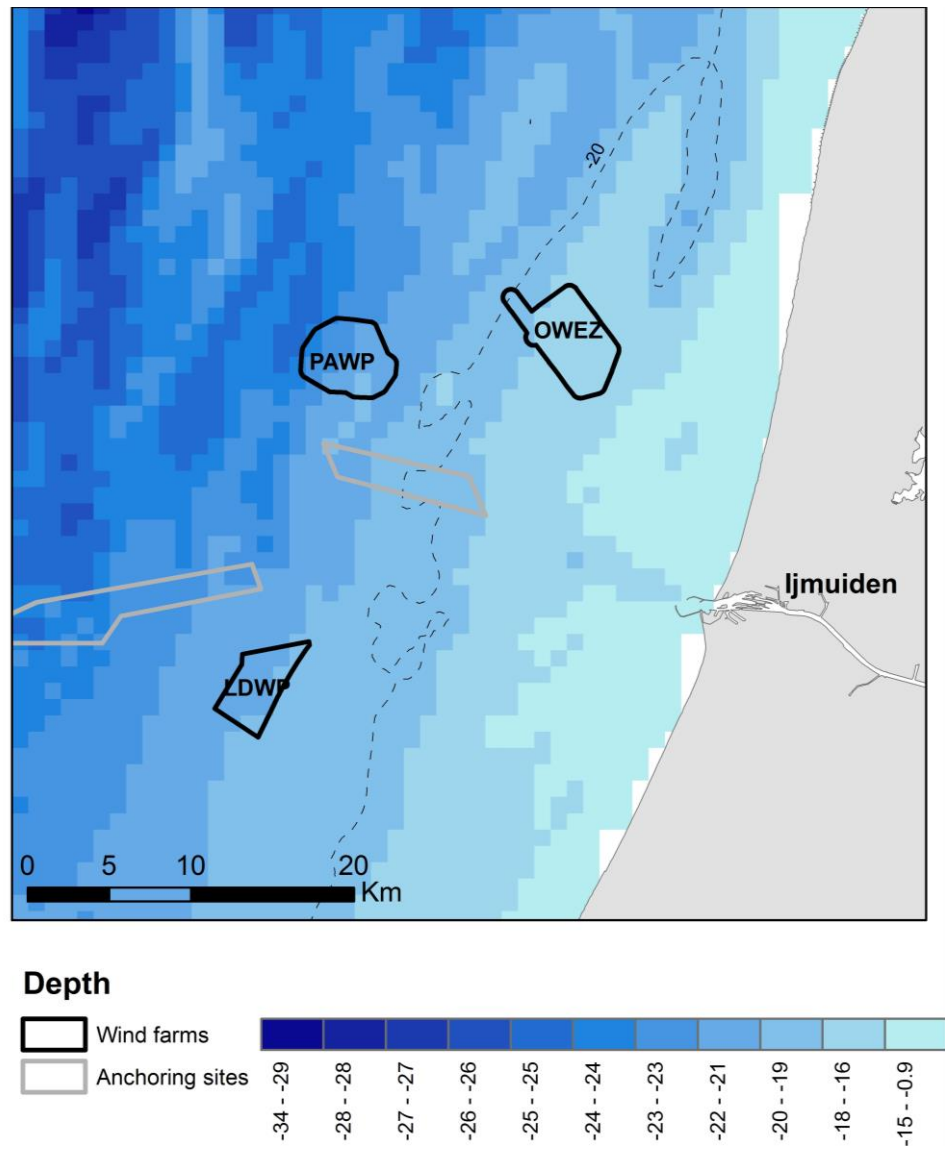


Figure B.2 Bathymetry of the greater study area [m].

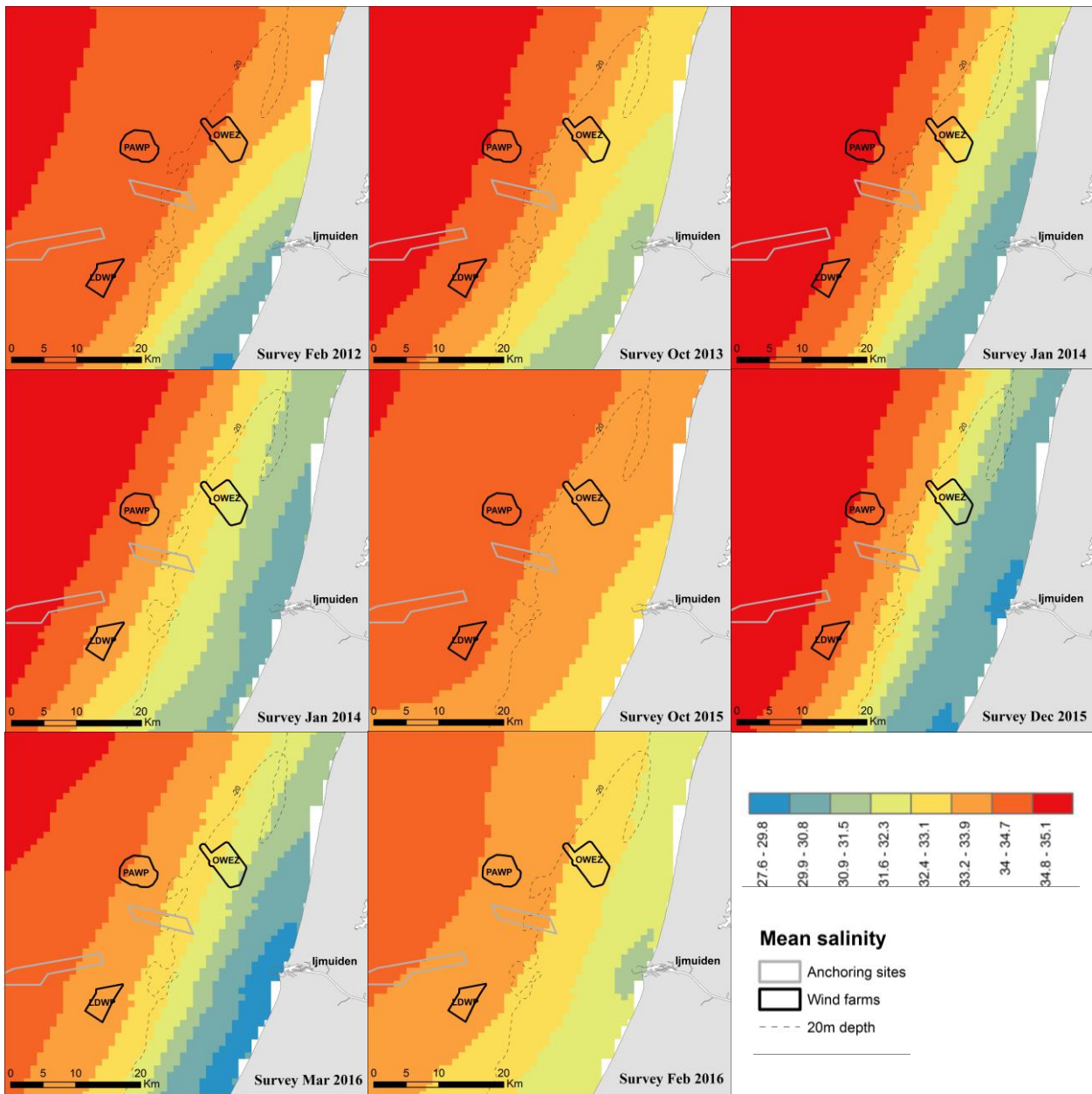


Figure B.3 Mean modelled salinity [PSU] during each survey period between February 2012 and March 2016.

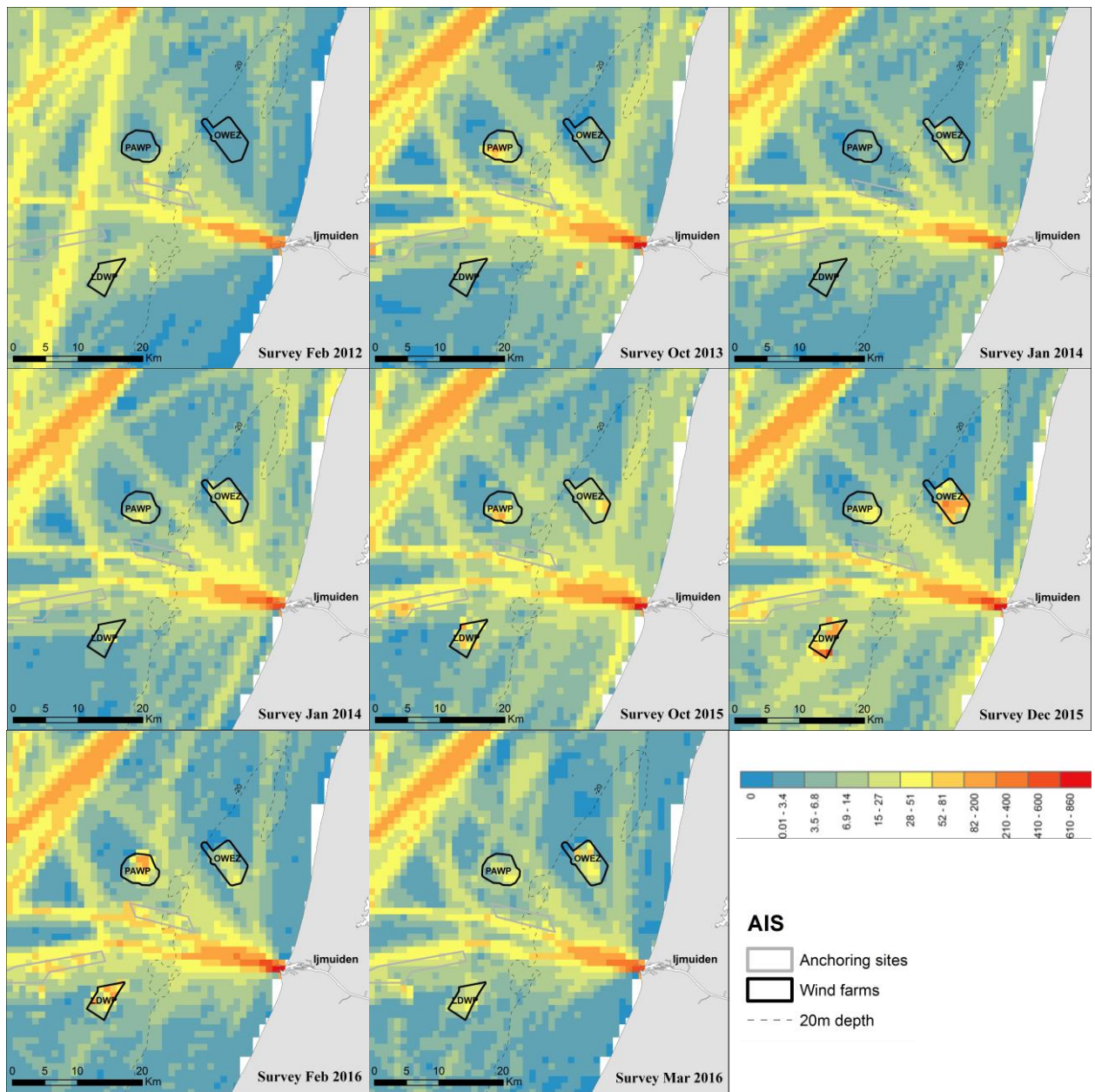


Figure B.4 Relative shipping intensity (AIS) during surveys between February 2012 and March 2016

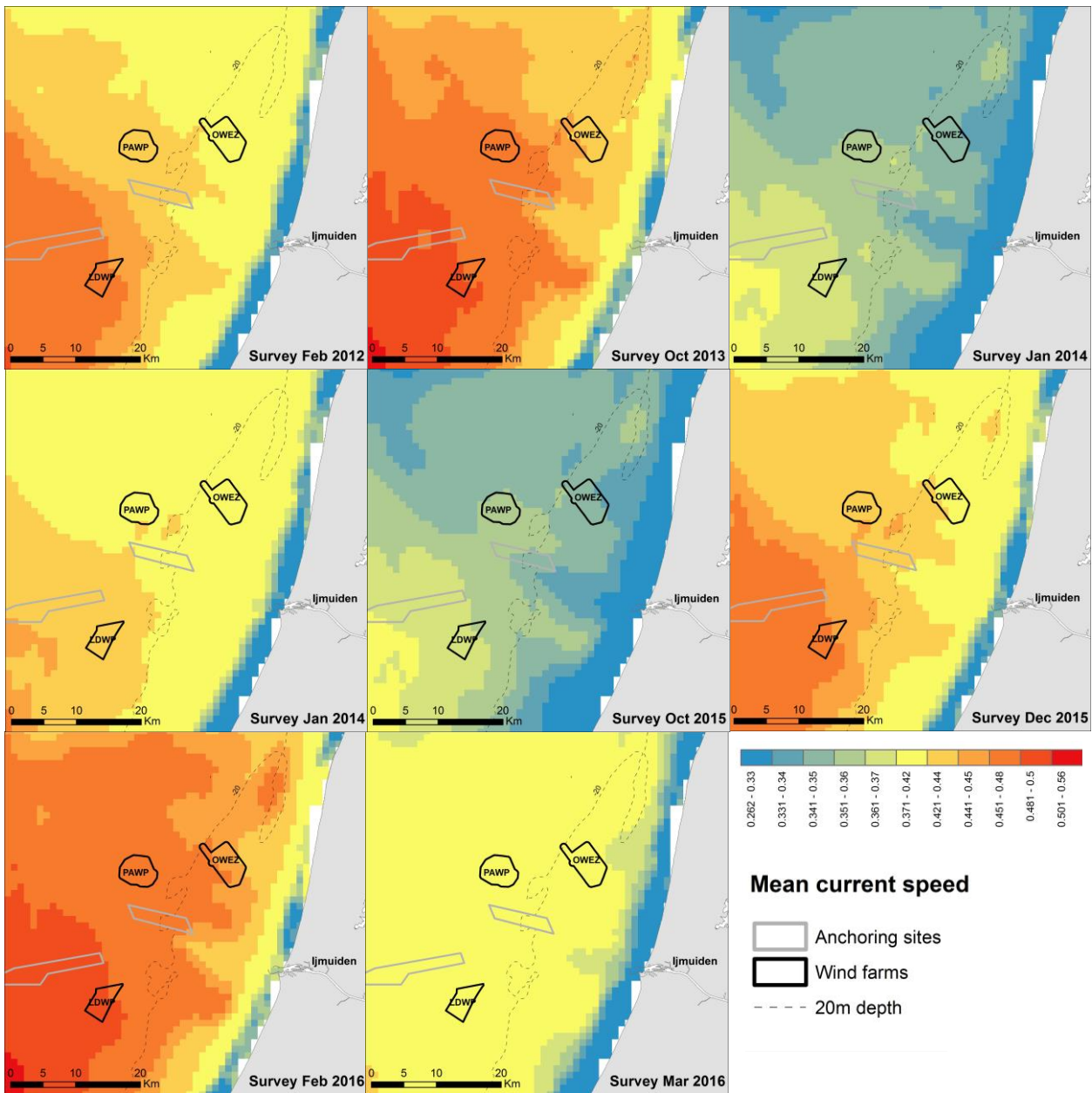


Figure B.5 Mean modelled current speed [m s^{-1}] during each survey period between February 2012 and March 2016.

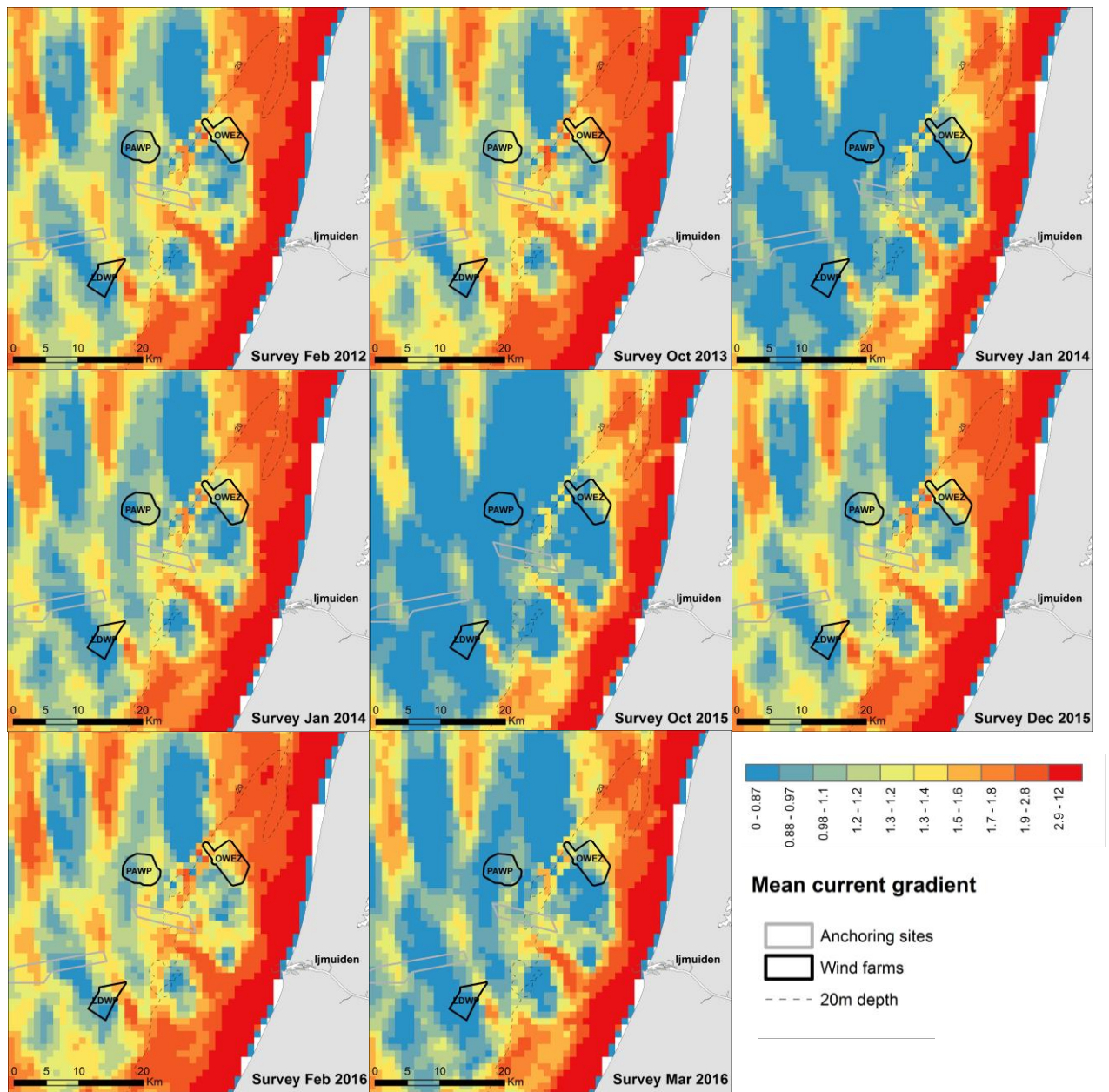


Figure B.6 Mean modelled current gradient during each survey period between February 2012 and March 2016.

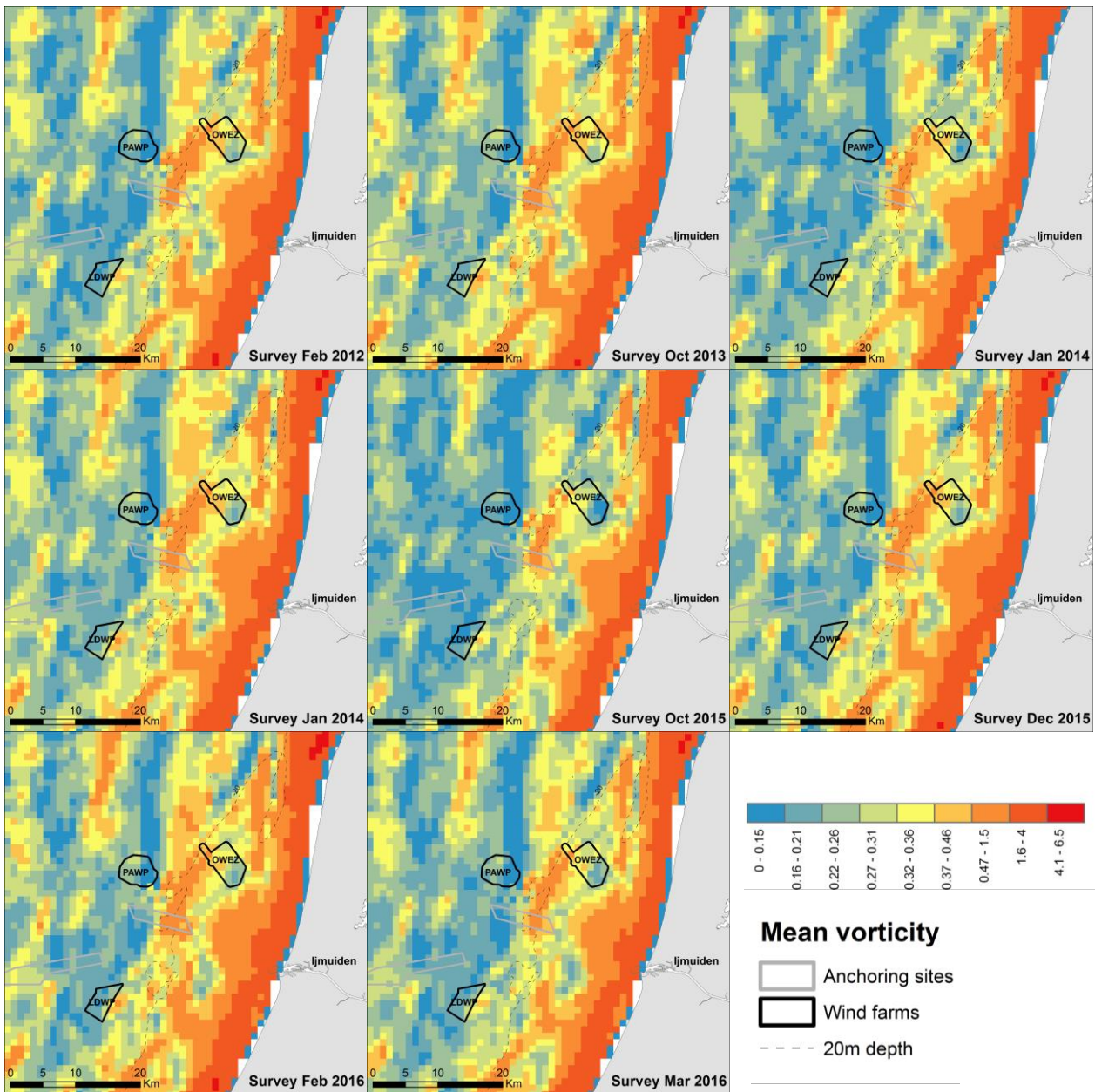


Figure B.7 Mean modelled eddy potential (vorticity) during each survey period between February 2012 and March 2016.

APPENDIX C – Example of simulation for “power” calculation of significant impact of LUD

Simulation based on modelled environmental relationships with Common Guillemot observations

Below, one simulation (out of 100 per displacement scenario) is illustrated together with the true aggregated observations and the modelled GAMM responses. The same simulation is used for illustration. In the “true” simulations different simulations are run for each displacement scenario (i.e. the example illustrated is not part of the real analyses, but the method is the same). Also only one survey is visualized although all the models are run on all surveys, both pre-construction (15 surveys) and post-construction (4 surveys). The analyses steps are:

- 1) The final GAMM model based on the real survey data (Figure C.1) is mimicked by a GLMM, however excluding the response to LUD windfarm
- 2) The GLMM model is simulated on the same environmental conditions as in the actual data 100 times. One survey from one simulation is visualised in (Figure C.2). Assuming no impact from LUD.
- 3) Different artificial displacement scenarios are implemented by randomly reducing the occurrences by for example 50% (Figure C.3 upper) and 75% (Figure C.4 upper).
- 4) The same GAMM models as in step 1 (including distance to LUD) is fitted on each simulation and the p-value from the “distance to LUD” is extracted (Figure C.3 and Figure C.4 lower). Note that the responses are the same or similar to the GAMM in step 1 (Figure C.1), which the data are simulated based on.
- 5) The power is calculated as the proportion of models with a significant ($p < 0.01$) response of LUD

All four Common Guillemot post-construction surveys are mapped in Figure C.5 to visualize the high variability in density and distribution between surveys.

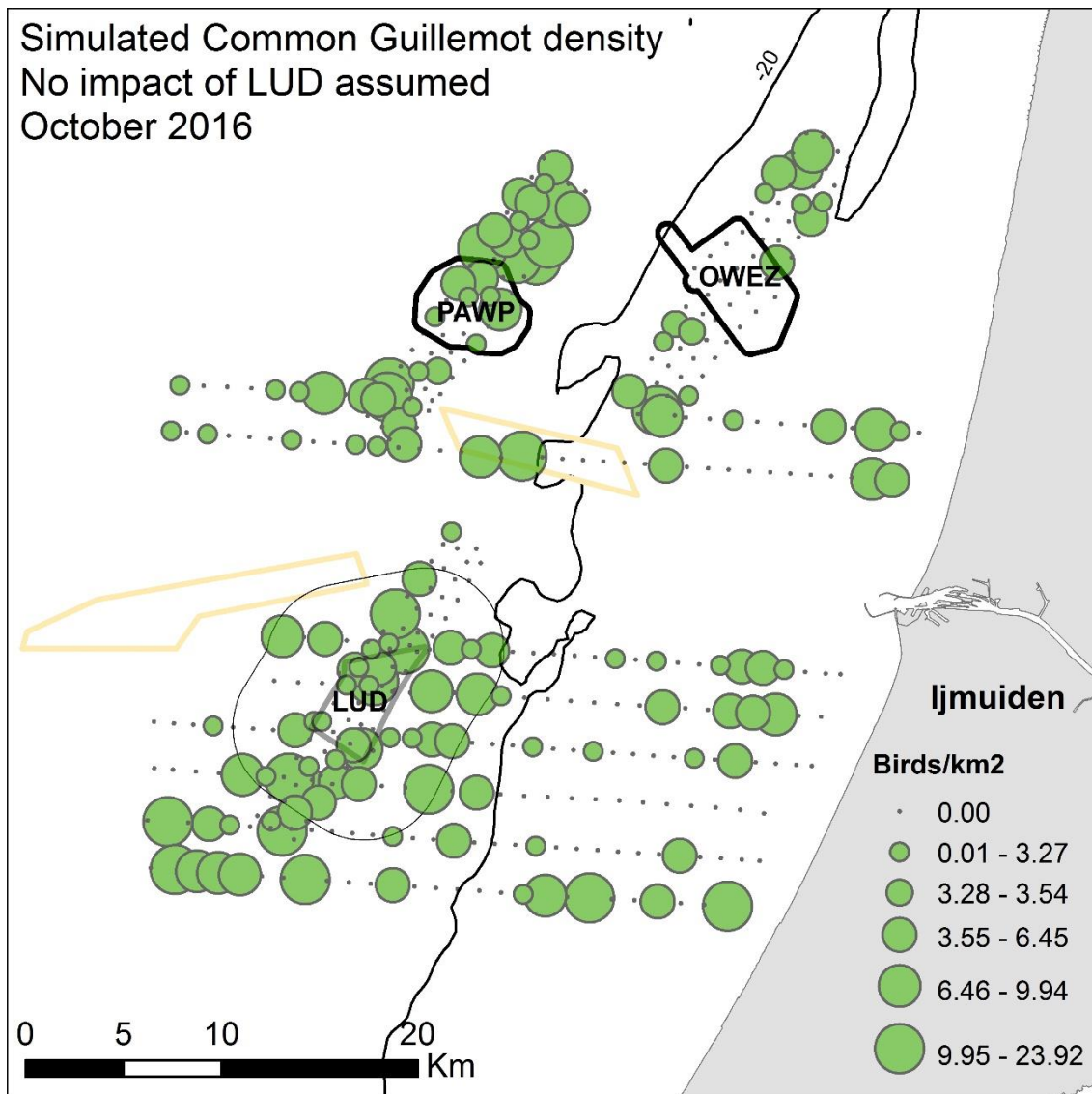


Figure C.2. A Simulated bird distribution based on the GLMM mimicking the GAMM model in figure (Figure C.1) but excluding LUD impact.

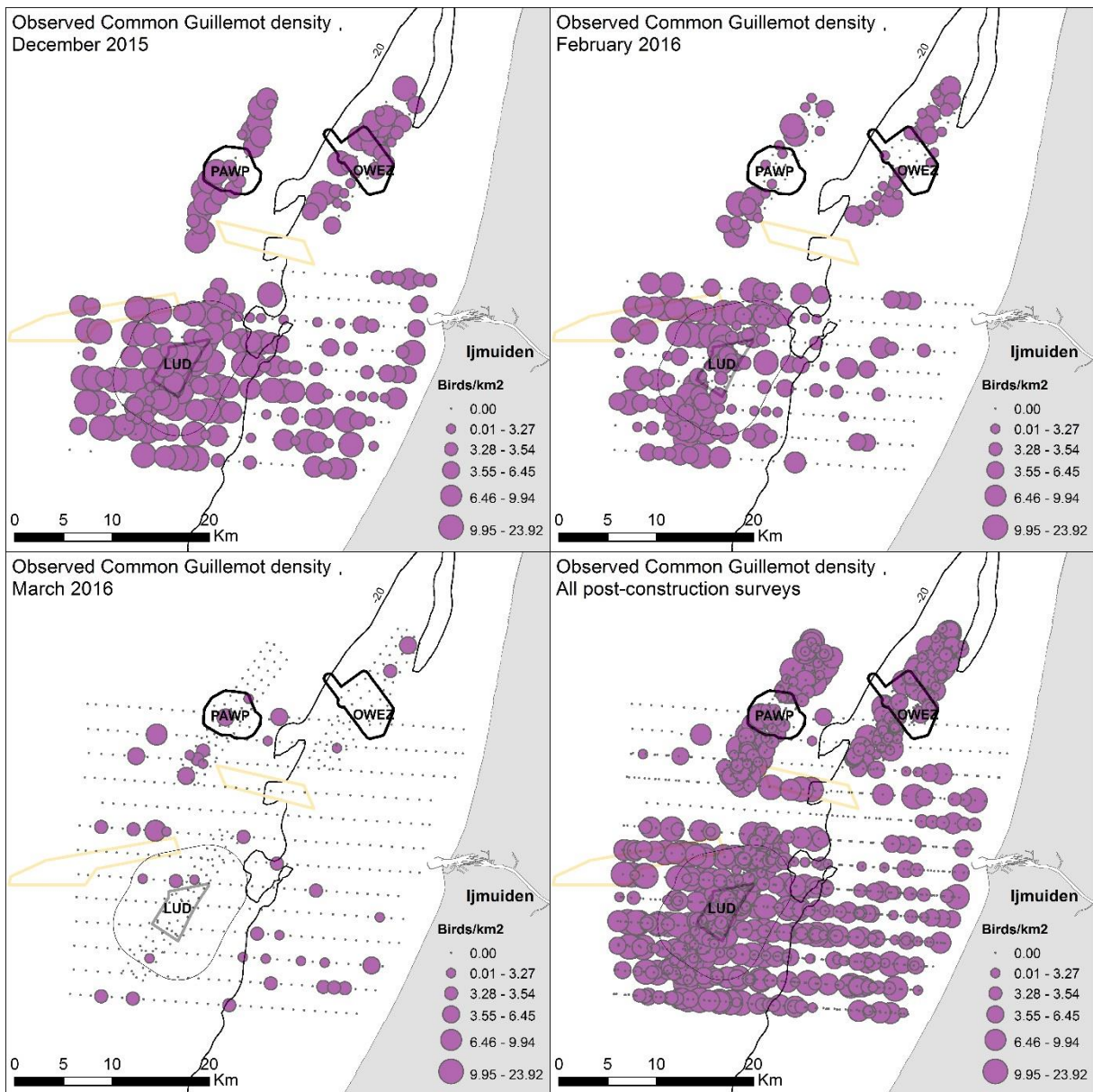


Figure C.5. The three other post-construction surveys (in addition to October 2015 visualised in Figure C1). The combined distribution (all post-construction surveys plotted in the same figure) is visualised in the lower right figure.